December 2016

The Economy of Preventive Maintenance of Concrete Bridges Due to Corrosion

Haotian Zhang
Syracuse University

Recommended Citation

Zhang, Haotian, "The Economy of Preventive Maintenance of Concrete Bridges Due to Corrosion" (2016). *Dissertations - ALL*. 603.
https://surface.syr.edu/etd/603

ABSTRACT

The current practice for physical evaluation and delayed maintenance of deteriorated concrete bridge is fundamentally wrong. This research presents a new approach for the evaluation of the condition states of steel reinforced concrete bridge members, which is based on their chemical conditions instead of the physical deficiencies such as cracks and delamination. Using the proposed chemical based inspection approach, a more effective and economic preventive maintenance plan could be achieved. The available non-destructive evaluation (NDE) methods and preventive maintenance measure are identified. Since the chloride induced corrosion is the major factor that dictates the service life of the steel reinforced bridge element, a refined equation for estimation of the diffusion coefficient of chloride ions into concrete is proposed.

A Finite Element Analysis (FEA) model that accounts for time-dependent and temperature-dependent diffusion coefficient was developed and verified against experimental data produced by several researchers. The results of the numerical analysis showed good agreement with experimental data. After validation against experimental data, the FEA model was used to evaluate the effectiveness of the preventive maintenance measures, such as surface sealers and overlays. The chloride profiles derived from the FEA model was then used as an indicator to select appropriate preventive maintenance measures at the right time based on the chloride concentration at the surface of the steel. A simplified concrete bridge deck element is selected to compare the life-cycle cost of a bridge deck with different concrete mix design and different maintenance strategies under various exposure conditions.

For cost-effective management of concrete highway bridges, the following measures should be taken, depending on the exposure conditions:

1. For **severe exposure** conditions, such as coastal area or cold regions that require a large amount of deicing salt, carbon steel reinforced bridge decks have a short service life. Therefore, a well-planned preventive maintenance strategy needs to be implemented in order to postpone or eliminate the needs of major rehabilitation and replacement. In such case, the use of stainless steel could be the most economical solution for the long run. In addition, the use of integrated overlay made of high performance concrete or cathodic protection systems may reduce the life-cycle cost based on a 75-year expected service life.
2. For **moderate exposures**, the use of overlays and surface sealers has been deemed cost-effective. However, the life-cycle cost is very sensitive for sealer application since it needs to be reapplied frequently. Thus, the effectiveness of the sealer should be closely monitored by the Non-destructive Evaluation (NDE) methods.
3. For **mild exposures**, the corrosion may not be the most critical deterioration mechanism for the bridge deck element. The riding surface of the bridge deck needs to be replaced periodically due to other deterioration mechanisms such as erosion, fatigue cracks, etc.

In conclusion, this research shows that it is not only economical, but also necessary to allocate more funds to perform in-depth, chemical oriented non-destructive tests and active preventive maintenance.

THE ECONOMY OF PREVENTIVE MAINTENANCE OF CONCRETE BRIDGES DUE TO CORROSION

by

Haotian Zhang

BS., Tianjin University, China, 2010
MS., Syracuse University, 2013

Dissertation
Submitted in partial fulfillment of the requirements for the degree of
Doctor of Philosophy in Civil Engineering.

Syracuse University
December 2016

ACKNOWLEDGMENTS

I wish to express my truthful gratitude towards my advisor, Professor Riyad S. Aboutaha. Prof. Aboutaha is the most knowledgeable, kind and sincere professor I have ever worked with. He has walked me through all the stages of the research. His willingness to give me his time so generously has been much appreciated. Without his consistent guidance, instructions, and friendly encouragement, this dissertation would have never reached its present form.

My sincere thanks should also go to my dissertation committee members, Professors: Utpal Roy, Eric M. Lui, Dawit Negussey, Hossein Ataei and Baris Salman.

I would also love to express my gratitude to my parents and my wife for all the support, understanding, encouragement and love throughout this research.

TABLE OF CONTENTS

LIST OF TABLES

LIST OF FIGURES

1. INTRODUCTION

1.1. Background

The unique combination of steel and concrete has made reinforced concrete one of the most popular construction material systems in the world. However, the lack of understanding of the long-term performance of concrete and the severity of the exposure condition has caused serious problems. Existing concrete bridges are serving shorter service life than designed service life due to higher deterioration rate caused by various deterioration mechanisms, such as corrosion, freezing and thawing actions, carbonation and alkali-silica reaction. These problems have reduced the service life of the structures or have forced extensive maintenance, which both come at great economic costs. As a result, conditions of bridges needs to be evaluated periodically. The root cause of the deterioration should be determined and followed by proper maintenance treatments. However, the existing inspection manuals primarily focus on detecting physical damage in concrete bridge elements, such as cracks, delamination, spalls, efflorescence, etc. If no physical damage is detected, very minimal maintenance actions are taken. Due to the lack of awareness of ongoing chemical deterioration reactions, preventive maintenance measures are applied commonly on a cyclical base without understanding of the performance and effectiveness of the preventive maintenance measures. Chemical non-destructive tests, on the other hand, give the opportunity for evaluators to determine the chemical conditions of the concrete bridge elements. The data could be used not only to estimate the remaining service life of the bridge elements based on the deterioration model, but also to evaluate the performance and the effectiveness of the preventive maintenance measures. Therefore, a chemical based inspection method should be incorporated into the current inspection manuals for routine inspection.

1.2. Objectives

The primary objective of this study is to demonstrate the economy of preventive maintenance that is based on the chemical condition assessment of concrete bridges. This study involves investigations for better understanding of the deterioration of concrete bridges under combined effects of harmful compounds and environmental exposure, and to develop a new mathematical model for corrosion initiation estimation. The proposed model is validated comparing the published experimental/field data and further calibrated using finite element analysis. The new developed model will be used in the life cycle cost analysis to optimize the preventive maintenance activities, which would result in better inspection and preventive maintenance scheduling for concrete bridges in the U.S.

1.3. Research Plan

The main tasks of this research is shown as follows:

1. Review of literature on effect of different concrete deterioration mechanisms, especially chloride induced corrosion;
2. Review of the numerical models for expression of chloride concentration threshold (Cth), chloride diffusion coefficient (Dc) and the surface concentration of chloride (Cs);
3. Propose a refined model to estimate those factors by linking parameters that represent the durability of the concrete, such as moisture content, permeability, porosity,

cracks, binder capacity, binder type, compressive strength, density, presence of the cracks, freeze-thaw effect;

4. Perform finite element analysis (FEA) for chloride diffusion process to analyze the impact of different factors. Rule out the factors that not have a significant impact on the Cth, Dc, Cs;
5. Perform cost analysis for preventive maintenance measures. The unit cost, service life and the effectiveness will be analyzed.
6. For different exposure conditions, conduct life cycle analyses for a typical bridge deck element under current maintenance practices as well as the proposed preventive maintenance measures.
7. Develop a guideline for inspection and preventive maintenance based on the numerical threshold values for chemical compounds obtained from NDT tests.

1.4. Outline of the Dissertation

Chapter 1 presents an introduction to the research. The background of the research, objectives and the scope of the dissertation is illustrated.

Chapter 2 provides a brief overview of the current inspection and maintenance practice and an introduction on deterioration mechanisms for reinforced concrete bridge members. In addition, it provides a more detailed literature review on deterioration caused by chloride induced corrosion.

Chapter 3 presents the development of the refined analytical model for predicting chloride diffusion coefficients. The experimental data that were obtained by other researchers are used to validate the model.

In Chapter 4, finite element analysis is performed to analyze the impact of different variables: material properties, exposure conditions, and the application of preventive maintenance activities. Also the effectiveness of preventive maintenance measures such as overlays and surface sealers are evaluated. The simulated chloride profiles are also compared with the experimental data in order to validate the model.

Chapter 5 discusses the cost analysis of a typical concrete bridge deck element under different maintenance strategies while facing different exposure conditions over a 75-year expected service life.

Chapter 6 provides brief recommendations on future inspection and maintenance programs. A chemical based NDE inspection method is proposed to better evaluate the chemical conditions of the concrete bridge elements. Using this approach, more economical maintenance strategies involving active preventive maintenance could be achieved for a longer service life and a lower life-cycle cost.

Chapter 7 presents the summary and conclusion, as well as recommendations for future studies.

2. LITERATURE REVIEW

2.1. Introduction

A cost-effective bridge is a bridge whose maintenance is based on its chemical condition over its entire service life. If deterioration mechanisms are prevented, a bridge would cost considerably less to maintain and it would safely serve its full design service life, if not longer. The practice of physical evaluation and delayed maintenance of deteriorated concrete bridges has resulted in large number of bridges in need of repair. The current inspection manuals are primarily focused on detecting physical damage in concrete bridge elements. If no physical damage is detected, very minimal maintenance actions are taken. This is the main reason why the number of US bridges that are classified as structurally deficient is on the rise. Given the need for future expansion of the US transportation network and increase in number of new bridges, there is a need for cost-effective maintenance process that prevents deterioration mechanism from start, or at least stops it at a very early stage.

The most economical approach to maintain existing concrete bridges is by adopting an active preventive maintenance approach. An in-depth investigation of the combined deterioration effects of various deterioration mechanisms is needed to establish sound thresholds for harmful chemicals in concrete bridge elements. Such established thresholds are critical for cost-effective maintenance decision making, in a timely fashion, before any deterioration starts.

2.2. Current Inspection and Maintenance Practices

2.2.1 Current Inspection Practices

The manual for bridge element inspection (AASHTO, 2013) illustrates the condition assessment philosophy as multipath and defect concepts. The condition of the elements is described by using multipath distress language within the defined condition state. The multipath distress language provides the means to fully incorporate all possible defects within the overall condition assessment of the element. The overall condition of an element can be utilized in an aggregate form, or broken down into specific defects present as desired by the agency for bridge maintenance system use. There are four condition states represented by 1 to 4 scale where the element state is good, fair, poor or severe respectively. The condition is evaluated by the defects on the element, which are generally delamination, spall, cracks and exposed rebar for concrete components. An example of the condition description for a typical reinforced concrete deck element is shown in Table 2-1.

It can be seen that the current condition rating system mostly depends on the physical defects, such as cracks, scaling, spalling, delamination, exposed rebar, which can only reflect the condition of the concrete bridge element after it experienced a certain degree of deterioration. Although, this condition rating system gives straightforward condition assessment for the concrete bridge structures, it does not reveal the ongoing chemical reactions within the components. Therefore, it is hard for the inspectors to determine the actual chemical condition of the concrete and it is also difficult for the inspectors to predict the future deterioration if the element is still in a good or fair condition.

Table 2-1 Condition State Definitions for Reinforced Concrete Deck (AASHTO, 2013)

Defects	**Condition States**			
	1	**2**	**3**	**4**
	Good	**Fair**	**Poor**	**Severe**
Delamination/ Spall/ Patched Area	None.	Delaminated. Spall 1 in. or less deep or 6 in. or less in diameter. Patched area that is sound.	Spall greater than 1 in. deep or greater than 6 in. diameter. Patched area that is unsound or showing distress. Does not warrant structural review.	The condition warrants a structural review to determine the effect on strength or serviceability of the element or bridge; OR a structural review has been completed and the defects impact strength or serviceability of the element or bridge.
Exposed Rebar	None.	Present without measurable section loss.	Present with measurable section loss but does not warrant structural review.	
Efflorescence/ Rust Staining	None.	Surface white without build-up or leaching without rust staining.	Heavy build-up with rust staining.	
Cracking	Width less than 0.012 in. or spacing greater than 3.0 ft.	Width 0.012-0.05 in. or spacing of 1.0-3.0 ft.	Width greater than 0.05 in. or spacing of less than 1 ft.	
Abrasion/ Wear	No abrasion or wearing.	Abrasion or wearing has exposed coarse aggregate but the aggregate remains secure in the concrete	Coarse aggregate is loose or has popped out of the concrete matrix due to abrasion or wear.	
Damage	Not applicable.	The element has impact damage. The specific damage caused by the impact has been captured in Condition State 2 under the appropriate material defect entry.	The element has impact damage. The specific damage caused by the impact has been captured in Condition State 3 under the appropriate material defect entry.	The element has impact damage. The specific damage caused by the impact has been captured in Condition State 4 under the appropriate material defect entry.

Guided by the inspection manuals published by AASHTO, FHWA and state DOTs, the current inspection practices mainly require routine inspection with a fixed interval. The visual inspection and sounding inspection based on the bridge elements' physical condition are still predominant. (Figure 2-1) The current inspection manuals also do not pay much attention to the components that appear to be in good condition, as these members might be on the verge of physical deterioration.

Figure 2-1 Chain drag and hammer testing (SHRP2, 2015)

Although Visual inspection is a powerful assessment method, it is not fully reliable since it can be affected by a myriad of factors, such as subjective factors, physical and environmental factors, task factors and organizational factors, as presented in (Moore, 2001). Based on the distribution of the condition ratings and observations made during the study conducted by Moore (2001), routine inspections are completed with significant variability from the routine inspection tasks. This variability is most prominent in the assignment of condition ratings, but is also present in inspection documentation. Therefore, visual inspection may lead to inconsistent ratings as they depend on the engineering judgement of the inspector. Furthermore, it is obvious that some components are hard to access for inspectors to give visual inspection or physical condition assessment due to their location or geometric restraints.

In addition, visual inspection may not be capable of obtaining the full information needed to evaluate the potential of future deterioration for bridge elements. For example, crack width and depth are two essential parameters used to estimate chloride penetration into the concrete. Unlike crack width, the crack depth is often not recorded by the inspectors since it is hard to determine the actual crack depth by visual inspection alone. However, the crack depth, in some cases, dictates the remaining service life of the element since the external contamination can reach the surface of the reinforcing steel directly if the crack is deep enough. In this case, a non-destructive test such as Surface Wave Transmission can be selected to complement the visual inspection.

Despite the fact that advanced inspection methods are widely adopted by states DOTs in their bridge inspection practices, these methods are only recommended and granted under restricted circumstances:

1. Alternative methods to get inspection done while it is hard to get access for routine inspection including visual and conventional physical inspection methods.
2. Complimentary methods to get accurate condition assessment while routine inspection cannot give conclusion about the deterioration condition about area, severity and progressing status.
3. Helping to make decisions regarding major rehabilitation, repair or replacement of deteriorated bridge components.

However, the NDT methods should not be limited as a complementary method or a decision making tool for major rehabilitation works, although they performed well on those tasks. The NDT tests are capable of giving the inspector full range of parameters that describes the reinforced concrete, such as the compressive strength, porosity, permeability, density, elastic modulus, diffusion coefficient, chloride concentration, carbonation depth, etc. By adopting these parameters, a scientific deterioration model could be derived. The model could be used to predict the future deterioration level for a bridge if enough data are collected. Therefore, the advanced NDT methods, including Chemical NDTs, should not be limited as in-depth inspection methods. It needs to be regulated into the routine inspection process in order to achieve a more cost-effective bridge life-cycle management strategy.

2.2.2 **Current Maintenance Practices**

Bridge maintenance can generally be classified into four stages: Active preventive, passive, delayed, and ignored. The type of maintenance strategy an agency employs is largely related to the assets and capabilities of said agency. As described in detail in NCHRP 14-20 “Consequences of Delayed Maintenance,” a balance must be reached between cost, desired service level, delay/catch-up periods, discount rates, and other factors. The typical outcomes for different maintenance types are listed along with the concrete condition, structure safety and the cost for the retrofit measures as shown in Figure 2-2. It can be seen that if the small defects cannot be rehabilitated on time, they will become a threat for the overall safety of the structure and the maintenance cost will increase dramatically as the degradation continues.

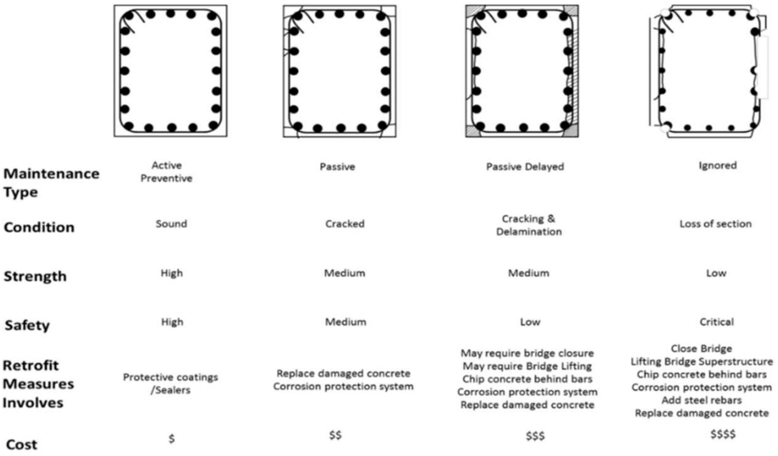

Maintenance Type	Active Preventive	Passive	Passive Delayed	Ignored
Condition	Sound	Cracked	Cracking & Delamination	Loss of section
Strength	High	Medium	Medium	Low
Safety	High	Medium	Low	Critical
Retrofit Measures Involves	Protective coatings /Sealers	Replace damaged concrete Corrosion protection system	May require bridge closure May require Bridge Lifting Chip concrete behind bars Corrosion protection system Replace damaged concrete	Close Bridge Lifting Bridge Superstructure Chip concrete behind bars Corrosion protection system Add steel rebars Replace damaged concrete
Cost	$	$$	$$$	$$$$

Figure 2-2 Qualitative cost of maintenance versus type of maintenance method (Aboutaha, 2004)

2.2.2.1 Different Maintenance Activities for various Bridge Elements

Due to the different locations, functions, and the exposure conditions of the structure elements, the maintenances activities may vary for different bridge components. The typical types of maintenance measures are summarized in Table 2-2.

Table 2-2 Typical types of Maintenance for Various Concrete Bridge Elements

Typical types of maintenance for various concrete bridge elements				
Bridge element	Preventive	Active	Reactive	Delayed
Concrete structural Deck	Annual or biennial washing; seal deck on a scheduled basis	Seal fine cracks as they appear	Remove concrete around spalled areas and patch; perform full-depth repairs; possible overlay entire deck if necessary	Do nothing until entire deck (or portions thereof) needs complete replacement.
Bearings	Clean and paint (where applicable) as needed	Realign bearings if necessary	Replace frozen or otherwise deteriorated bearings	Take no action until bearing failure.
Superstructure/substructure concrete	Annual or biennial washing; seal elements on a scheduled basis	Seal fine cracks as they appear	Patch spalled areas	Wait until serious deterioration has occurred where significant levels of replacement or rehabilitation are necessary.

Typical types of maintenance for various concrete bridge elements (Cont.)				
Bridge element	Preventive	Active	Reactive	Delayed
Deck joints	Clean and remove debris on annual basis (or as needed)	N.A.	N.A.	Wait until serious deterioration has occurred where significant levels of replacement or rehabilitation are necessary.
Deck drains	Clean and remove debris on annual basis (or as needed)	N.A.	N.A.	Wait until serious failure has occurred where significant levels of replacement or rehabilitation are necessary.

Most state agencies follow AASHTO's recommendations for preventive maintenance. Also most DOTs stress the importance of annual cleaning of exposed bridge elements at the end of the salting season, as well as the importance of sealing concrete at intervals where economy and effectiveness would be maximized (within the effective lifespan of the sealers). However, cyclical maintenance is generally just that: cyclic. Little or no attention is paid to actual need. In state bridge maintenance manuals, as well as AASHTO's maintenance manual, maintenance is assumed to be needed on a cyclic basis, but no attention is paid to effectiveness of these measures at individual sites or whether or not preventive maintenance measures should be performed more or less frequently in different environments and conditions.

On the other hand, preventive maintenance actions need to be applied based on the actual chemical condition of the elements. It needs not only the advanced inspection techniques or structure monitoring systems to detect the potential threats to the concrete bridge, but also an innovative mathematical model to anticipate the deterioration states of the structure that accounts for different variables.

2.3. Deterioration of Steel Reinforced Concrete Members

The unique combination of steel and concrete has made reinforced concrete one of the most popular construction materials in the world. However, the lack of understanding of the long-term performance of concrete and the severity of environmental impacts has caused serious problems. Existing concrete structures are experiencing higher deterioration rates and lasting for shorter service life due to different causes of deterioration of reinforced concrete structures such as corrosion, freezing and thawing action, carbonation and alkali-silica reaction. Durability issues are greatly ignored in design, construction, and maintenance during the service life of structures. These problems have reduced the service life of the structures or have forced extensive repairs, which both come with great economic costs. As a result, a basic understanding of the deterioration mechanisms for concrete subjected to chemical attacks by the surrounding environment is essential to conduct meaningful evaluation and selecting a successful maintenance strategy.

2.3.1 **Corrosion of Reinforcing Steel Bars in Concrete**

Corrosion, in the context of steel reinforcement in concrete, is a self-generated electrochemical activity. It requires the simultaneous presence of moisture and oxygen and resulting from differences in potentials.

An electrochemical cell is formed when an anode and a cathode are connected within a conductor. In the case of steel, the anodic reaction occurs as following:

$$Fe \leftrightarrow Fe^{2+} + 2e^{-} \tag{2.1}$$

As this process occurs, a cathodic reaction is needed to consume the free electrons released form the anodic reaction, and this reaction is typically:

$$O_2 + 2H_2O + 4e^{-} \leftrightarrow 4OH^{-} \tag{2.2}$$

The concrete serves as the electrolyte for the corrosion of steel as it conducts the current by means of ionic diffusion. The process is illustrated in the Figure 2-3.

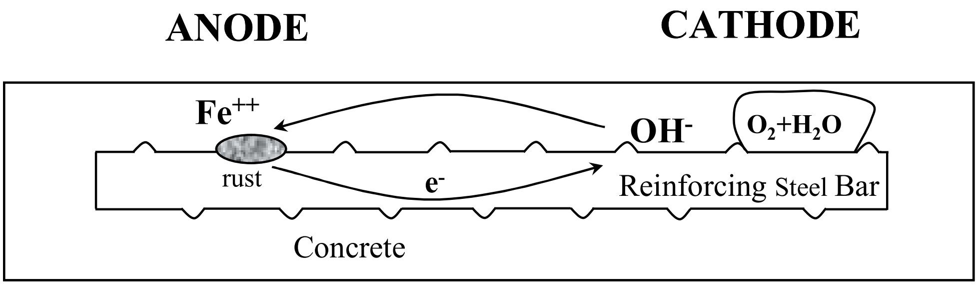

Figure 2-3 Corrosion cell in reinforced concrete member (Hime & Erlin, 1987)

However, in some special case, the cathodic reaction may be in the form of hydrogen evolution. This might occur in two cases:

1. At a very negative potential or a very high cathodic current density;

2. In a carbonated concrete in which the pH value of the pore solution has become very low.

The intermediate corrosion product, Fe^{2+}, could be further transformed into $Fe^{3+}$and be accumulated at the surface of steel reinforcement. (Song, 1998)

Normally, the pore solution is rich in oxygen with a high pH value. So Fe^{2+} can stay in the form of $Fe(OH)_2$ or $Fe(OH)_3$, forming a thin passive film on the steel surface, which consequently retards the corrosion reaction. However, under some conditions the protective film may not be formed or the formed passive film would break down. This may be caused by the invasion of carbon dioxide ions, chloride ions, and other chemical elements. Once the alkalinity of the concrete drops down, the corrosion rate of the steel increases dramatically.

2.3.2 Carbonation of Concrete

The carbonation of cementitious materials is a neutralization reaction of the basic compounds of hydrated cement (essentially $\mathrm{Ca(OH)_2}$and C – S – H) by carbonic acid. CO_2, present in non-polluted air at 0.035% by volume, is dissolved in the aqueous pore solution and forms carbonic acid. (Houst, 2002)

The pore solution of hardened cementitious materials like mortar or concrete contains essentially sodium and potassium hydroxides. Indeed, the solubility of $\mathrm{Ca(OH)_2}$strongly decreases when the concentration of hydroxyl ions increases. Carbonation reactions can be written as follows:

$$\mathrm{2NaOH + CO_2 \rightarrow Na_2CO_3 + H_2O} \tag{2.3}$$

$$\mathrm{Na_2CO_3 + Ca(OH)_2 \rightarrow CaCO_3 + 2NaOH} \tag{2.4}$$

$$3Na_2CO_3 + 3CaO \cdot SiO_2 \cdot 4H_{O2} \rightarrow 3CaCO_3 + 2SiO_2 + 6NaOH + H_2O \qquad (2.5)$$

This process continues as long as $Ca(OH)_2$and C – S – H are present, and the pH of the pore solution keeps dropping as a result.

2.3.3 **Deterioration of Concrete Due to Freeze-and-thaw effect**

There are two types of Freeze-thaw damages: surface scaling and internal cracking. The former may occur on both horizontal and vertical surfaces, but mainly where water or snow can naturally deposit and the surface remains wet for long periods. The susceptibility to surface scaling will increase significantly in the presence of de-icing chemicals (Jana, 2007). Internal cracking under field conditions is less commonly observed or recognized. Sampling for structural analyses by plane sections or thin sections will provide valuable information for the identification and elimination of other causes. The phenomenon may be observed on parts of structures in direct contact with free water and subjected to capillary suction, such as the lower parts of supporting walls and dam structures above the water surface. It is also believed that freeze-thaw cracking may combine with or start after deterioration initiated by other detrimental mechanisms, such as alkali aggregate reactions. (Ronning, 2001)

2.3.4 **Deterioration of Concrete Due to Alkali-silica Reaction**

The Alkali-silica Reaction in concrete is a chemical reaction between reactive forms of silica present in the aggregates and the high alkaline pore solution. Two main mechanisms constitute the ASR. Firstly, silica is dissolved from the aggregates, whereby a gel is formed and secondly, the swelling of the gel by imbibition of water, which results in the expansion and deterioration of the affected concrete. (Bangert, 2004)

The reaction begins with an attack of the alkaline hydroxides present in the cement on the reactive silica particles in the aggregate. When poorly crystalline hydrous silica is exposed to a highly alkaline solution, there is an acid-base reaction between the OH^{-}ions in solution and the $\mathrm{Si}-\mathrm{OH}$ groups:

$$\equiv \mathrm{Si}-\mathrm{OH}+OH^{-} \rightarrow\equiv \mathrm{Si}-\mathrm{O}^{-}+H_2O \tag{2.6}$$

As additional OH^- ions penetrate into the structure, some of the siloxane (Si-O-Si) linkages are also attacked, following the equations shown below (Dent-Glasser, 1981):

$$\equiv \mathrm{Si}-\mathrm{OH}-\mathrm{Si}\equiv +2OH^{-} \rightarrow\equiv 2(\mathrm{Si}-\mathrm{O}^{-})+H_2O \tag{2.7}$$

To maintain charge equilibrium, positive ions (Na^+ and K^+) diffuse into the structure to balance the negative charges present on the terminal oxygen atoms. The disruption of the siloxane linkages ultimately weakens the structure. Provided that sufficient amounts of alkali-hydroxides are available, this process continues, producing an alkaline-silicate solution.

Due to the absorption of water, the gel may have a volume significantly larger than the silica particles originally attacked or consumed. In saturated concrete, the amount of water available in the reaction is abundant. Therefore, the rate of gel growth depends on the rate of the alkali-silica reaction. However, in the case of an unsaturated member, the rate of expansion or growth of the gel does not occur simultaneously with the reaction. It is prolonged over a longer period of time since the expansion rate is dependent on the ability of water vapor to diffuse through the surface of the concrete (Hobbs, 1988).

2.3.5 **Combined Effect of Different Deterioration Mechanisms**

As discussed above, the deterioration mechanism of concrete bridge components subjected to chemical attacks may include but are not limited to: corrosion of reinforcing bars in concrete, freezing and thawing cycles, carbonation of concrete, and alkali-silica reaction.

In many cases, the root cause of a deterioration problem is the corrosion of the concrete structures. The corrosion process is an electrochemical mechanism in which metal is reduced to a lesser state of energy, that being its natural ore. Various causes exist; the most predominate being chlorides, carbonization, and oxygen. Aside from the previously mentioned elements, there are other chemicals known to cause a reduction in the pH of concrete.

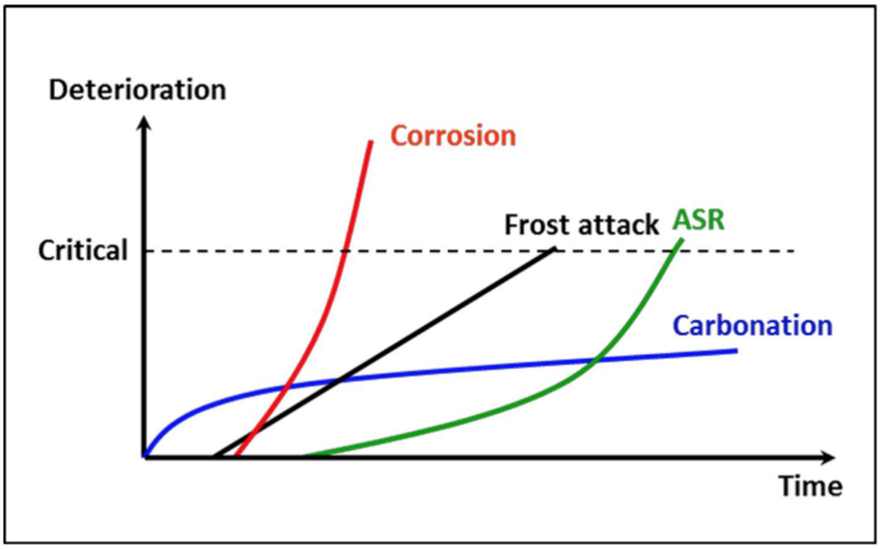

Figure 2-4 Simplifies deterioration mechanism, (Aboutaha, 2004)

Figure above shows simplified deterioration mechanism in severe environments. The combined effects of these mechanisms are more damaging, which may start at time zero and increasing with a greater slope. The carbonation process will affect the pH value of the pore solution in the concrete, which may lead to the depassivation of the steel. However, on the other hand, it may also change the binding capacity of the concrete as well as slow the chloride ingress velocity. So the overall impact may be controversial and depends highly on the engineering judgment and the experimental work. The impact on corrosion caused by ASR and freeze-and-thaw effect is also hard to evaluate. The fine cracks caused by these deterioration mechanisms may dramatically affect the chloride diffusion coefficient, and the surface cracks will lead to a higher chloride concentration at the crack tips.

2.4. Chloride Diffusion

2.4.1 Background Information

Chloride ions and other aggressive particles penetrate through concrete via different mechanisms depending on the driving force involved. The most well-known chloride transport mechanisms are diffusion, permeability and absorption. Other phenomena such as chloride binding can also influence chloride ingress.

The moisture content of concrete and the surrounding environment determine the driving force and the mechanisms by which chloride penetrates into concrete. In saturated concrete, chloride transport occurs by diffusion through the pore solution. However, under unsaturated condition, which is a common state for concrete with exposed surfaces, the movement of chloride ions is largely controlled by absorption through the capillary pore system and diffusion of chlorides through pore solution.

In bridges, concrete experiences wet and dry circles due to rain or condensation. Liquid in the pores evaporates progressively from the surface. Under this circumstance, the chloride will most likely enter the concrete surface initially by absorption and then diffuse into inner portions. A reservoir will be generated and topped up by periodic absorption events. If the concrete dries out to a greater depth, subsequent wettings carry the chlorides deeper into the concrete. Thus it would appear that absorption and diffusion are important transport mechanism associated with chloride ingress in bridges. (Hong, 1999)

Since the chloride diffusion is the most dominating mechanism for chloride ingression into the concrete and it is suitable for long-term modeling, the chloride diffusion is the only transportation mechanism that we adopt in our model.

2.4.2 **Derivation of the Ion Diffusion Equation**

When concrete is saturated such as in submerged conditions, diffusion is the dominant mechanism for chloride transportation. Also, it is suitable for long-term performance evaluation. For non-steady-state conditions, the concentration gradient changes with time, the flux can be simply described according to Fick's second law:

$$\mathrm{D}\frac{\partial^2 \mathrm{C}}{\partial \mathrm{x}^2} = \frac{\partial \mathrm{C}}{\partial \mathrm{t}} \tag{2.8}$$

Where,

C= Chloride concentration

D= Diffusion coefficient

t= Time

x= Depth

Assuming constant *D*, the equation can be solved by applying the error function solution:

$$\mathrm{C}_{(\mathrm{x,t})} = \mathrm{C}_0 + (\mathrm{C}_\mathrm{s} - \mathrm{C}_0)(1 - \mathrm{erf}\frac{\mathrm{x}}{2\sqrt{\mathrm{Dt}}}) \tag{2.9}$$

Where,

C_0= Initial chloride content in concrete

C_s= Surface Chloride Concentration

$C_{(x,t)}$= Chloride concentration at depth x on time t

$\mathrm{erf}(*)$= Error function from mathematic equation chart

2.4.3 **Thresholds for Chloride Content**

Reinforcement corrosion in non-carbonated, alkaline concrete can only start once the chloride content at the steel surface has reached a certain threshold value. This value is often referred to as critical chloride content or chloride threshold value, as shown in Figure 2-5. (Angst, 2009)

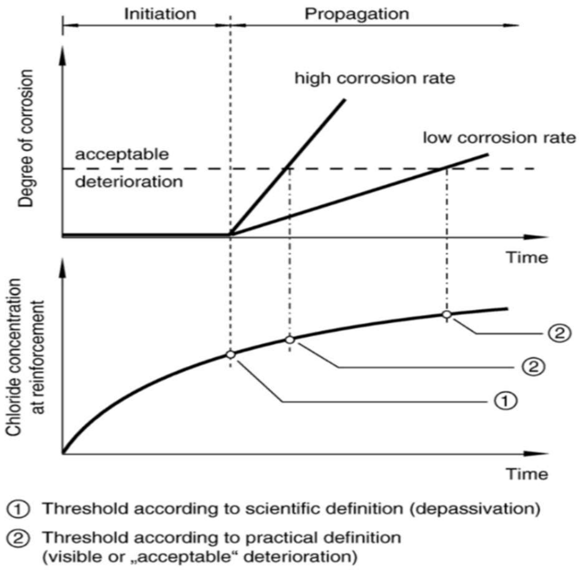

Figure 2-5 Definition of Chloride Threshold Value (Angst, 2009)

The threshold value for chloride concentration can be defined in two different ways: from a scientific point of view, the critical chloride content can be defined as the chloride concentration required for corrosion initiation; whereas from a practical point of view, the chloride threshold value can be defined with visible or physical deterioration of the reinforced concrete structure.

The critical chloride concentration is commonly expressed as total chloride, free chloride and Cl^-/OH^-.

The main reason for using total chloride as the measurement of chloride threshold value is that the test is relatively simple and well documented in standards. The value is quantified by the weight ratio of chloride ions and the cement/binder. While the binder content is hard to determine, the total chloride concentration can be also expressed relative to the weight of the concrete.

By assuming the bound chloride has no contribution to the corrosion process, it is reasonable to remove all the bounded chloride from the total chloride concentration and using the free chloride as an indicator to the potential of corrosion initiation. This value could be related to either the weight of the cement or the weight of the concrete.

Also, critical threshold values could be also expressed in the terms of Cl^-/OH^-. Publication often cited in this regard are those by Hausmann (1967). A conservative value of Cl^-/OH^- is set as 0.6 as the critical value for corrosion initiation.

The critical values for chloride contents in the literature has been summarized and attached in Appendix B. The critical values are either estimated by the numerical model or determined from the experiments directly. Due to the numerous factors affecting the corrosion process, the critical values show a large variance under different circumstances.

The ranges of chloride thresholds span through the following limitations based on the literature reviewed:

- (% by weight of concrete): 0.05 to 0.1. (2-4 lb/cu.yd.)
- Total chloride (% by weight of cement): 0.02 to 3.08. (Typically 0.4-0.6)
- Free chloride: 0.045 to 3.22 (mole/l) or 0.07 to 1.16 % by weight of cement.
- [Cl-]/[OH-] ratio: 0.01 to 20.

2.4.4 **Chloride Surface Concentration**

Chloride surface concentration is another vital input parameter for chloride induced corrosion models. As discussed before, the apparent surface concentration could be adopted by curve fitting using Equation 2.9 while assuming the diffusion coefficient and surface concentration are both constant. This simplified method is extremely suitable for old marine concrete structures. However, for younger structures, this approach may overestimate the diffusion penetration by a large margin so that the result may not coincide with what is now found in practice. The surface concentration estimated by this approach will also deviate from the experimental result if fly ash and silica fume are used in the binder.

Another problem that arises with the curve fitting approach is that the actual chloride content profile has a maximum chloride concentration few millimeters below the actual surface of the concrete, known as skin effect as shown in Figure 2-6.

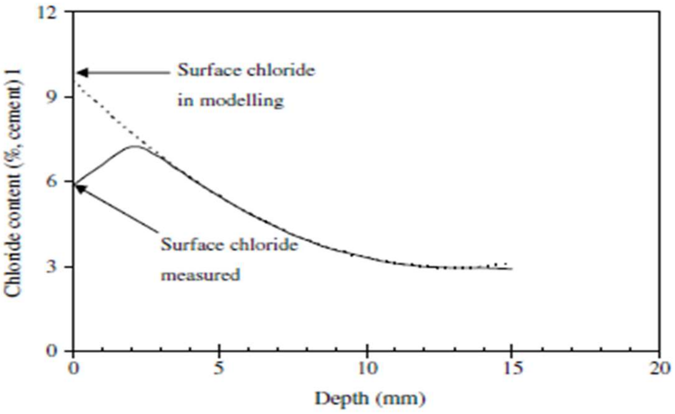

Figure 2-6 Skin Effect of the Concrete (Ann, 2009)

The skin effect is caused by various reasons. The degree of contact of chloride environment contributes to this surface chloride content decrease. If the concrete surface is submerged in sea water, the surface concentration may not be changed with time. However, for tidal zones and concrete exposed to aerial marine atmosphere, or seasonally applied deicing agents, the surface concentration may fluctuate since the chloride ions may be washed out during wet and dry cycles. Another reason that causes the skin effect is that the "skin" of the concrete usually has a different composition than the inner portions of concrete. This different skin composition may be the result of wall effect introduced during casting, carbonation or the precipitation of brucite formed by contact of hydrated cement with sea water. Therefore, the real surface chloride concentration is usually measured by taking the average chloride content on a thin surface layer, e.g., the chloride concentration in the layer within 1 inch below the surface is averaged.

2.4.5 **Chloride Diffusion Coefficient**

In order to apply the chloride diffusion model based on Fick's law, the diffusion constant needs to be specified. The diffusion constant is a function of the permeability and condition of the concrete, environmental factors such as exposure and climate, quality of workmanship, and extent of wearing and use. The input diffusion coefficient for NCDOT chloride ingress model is $1.6{\sim}3.0 \times 10^{-11}$ cm^2/s. Table 2-3 shows diffusion constants specified by several states departments of transportation (DOTs). (Ward-Waller, 2004) More diffusion coefficient published in the literature are listed in Appendix C.

Table 2-3 Mean Diffusion Constants for Various States (Ward-Waller, 2004)

	Mean Value of *Dc* (m^2/s)
California	5.114E-11
Delaware	1.022E-11
Florida	6.75E-11
Indiana	1.841E-11
Iowa	1.022E-11
Kansas	2.454E-11
Minnesota	1.022E-11
New York	2.659E-11
West Virginia	1.432E-11
Wisconsin	2.250E-11

2.5. Summary

The lack of knowledge about the long-term performance of concrete and the severity of environmental impacts has caused serious problems. Existing structures are experiencing higher deterioration rates and lasting for shorter service lives due to different causes of deterioration of reinforced concrete structures such as corrosion, freezing and thawing action, carbonation and alkali-silica reaction, in which corrosion is the most dominating factor.

Chloride induced corrosion is the most common root cause for concrete bridge deterioration. Once the chloride content reaches a certain threshold value, the passive layer formed on the surface of reinforcement rebar dissolves and corrosion initiates. Due to the manner of chloride transportation mechanism, diffusion is used to model the long-term chloride ingression in our research.

The typical values of diffusion coefficient for normal concrete were reported between 10^{-12} m^2/s and 10^{-11} m^2/s. If silica fume, fly ash or other alternative cementitious materials are used, the diffusion coefficient may reduce to 10^{-13} m^2/s.

Chloride diffusion coefficient is affected by the freeze and thaw cycles dramatically. The value may increase to 3 times of the original chloride diffusion coefficient after 75 freeze and thaw cycles. Furthermore, once the freeze and thaw cycles exceeds 300 to 500, the concrete may experience weight loss larger than 5%. The average annual freeze and thaw cycle for New York City, Syracuse, and Buffalo are 39, 61 and 59 times respectively. Therefore, for unprotected bridge components, the structures are prone to freeze and thaw damage and the bridge may deteriorate more rapidly due to the combined effect of chloride induced corrosion and freeze and thaw.

The chloride threshold value could be assumed as a constant of 1.97 lb/cu.yd. by weight of the concrete for ordinary Portland cement with black steel as a conservative estimation from the literature reviewed. The use of stainless steel will increase the chloride threshold value as much as 20 times of the threshold value for carbon steel. MMFX steel has also presented a higher chloride threshold value. As far as epoxy coated rebar, it exhibits similar chloride threshold value as black steel, but requires more time to initiate corrosion due to the barrier effect of the epoxy coating.

The chloride diffusion process can be determined by knowing the value of diffusion coefficient, exposure condition and the chloride threshold value. Therefore, the methods for testing and estimating these time-dependent variables are discussed in the following chapter.

3. CHLORIDE DIFFUSION VARIABLES

3.1. Introduction

For non-steady-state conditions, the concentration gradient changes with time, the flux can be simply described according to Fick's second law as shown in Equation 2-8.

Chemical NDTs can test the surface concentration, chloride diffusion coefficient, and concrete cover depth of the concrete specimen, directly. The chemical NDT data would allow fine tuning of the equation into a more precise and practical model. When the diffusion coefficient and the surface concentration are assumed to be constants, the future penetration of the chloride could be simplified as presented in the following equation, and described by (Collepardi, 1972):

$$\mathrm{C}_{(\mathrm{x,t})} = \mathrm{C}_0 + (\mathrm{C}_\mathrm{s} - \mathrm{C}_0)(1 - \mathrm{erf}\frac{\mathrm{x}}{2\sqrt{D_a \mathrm{t}}}) \tag{3.1}$$

Where,

$\mathrm{C(x,t)}$= Chloride concentration at depth x when time= t

C_i= Chloride concentration for virgin concrete

D_a= Achieved diffusion coefficient

C_s=Achieved surface chloride concentration

t= Time

$\mathrm{erf}(*)$= Error function from mathematic equation chart

The achieved diffusion coefficient and the achieved surface chloride concentration are determined from in-situ concrete exposed to the environment by curve-fitting. The chloride profile of the element could be obtained by chloride content tests. There are many lab techniques and field measurements for measuring chloride content in reinforced concrete structures, such as potentiometric and Volhard methods, ion selective electrodes, electrical resistivity and optical fiber sensor. (AASHTO-T 260, NT Build 208)

This simplified method is extremely suitable for old marine concrete structures. However, for younger structures, this approach may overestimate the diffusion penetration by a large margin, such the result may not coincide with what is now found in practice. In this case, numerical models should be used to determine the diffusion parameters.

3.2. Determination of the Chloride Threshold Value (*Cth*)

3.2.1 **Requirements for Newly Constructed Elements**

With reference to critical chloride content, also standards and regulations are occasionally cited, as they often present limits on the tolerable chloride content in concrete.

According to the AASHTO LRFD bridge construction specification (AASHTO, 2010), water used in mixing and curing of concrete shall be subject to approval and shall be reasonably clean and free of oil, salt, acid, alkali, sugar, vegetable, or other damaging substances. Mixing water for concrete in which steel is embedded shall not contain a chloride ion concentration in excess of 1,000 ppm or sulfates as SO_4 in excess of 1,300 ppm. Admixtures containing chloride ion in excess of one percent by weight (mass) of the admixture shall not be used in reinforced concrete. Admixtures in excess of 0.1 percent shall not be used in prestressed concrete.

The ACI code (ACI 318, 2014) also has a limit for chloride for new construction. The acid-soluble and water-soluble chloride limits are listed in the Table 3-1.

Table 3-1 Chloride Limits for New construction (ACI 318-14, 2014)

W0	N/A	2500	None		
W1	0.5	4000	None		
			Maximum water-soluble chloride ion content in concrete, percent by weight of cement		**Additional Provisions**
			Nonprestressed Concrete	**Prestressed Concrete**	
C0	N/A	2500	1	0.06	None
C1	N/A	2500	0.3	0.06	
C2	N/A	5000	0.15	0.06	Concrete Cover

The European standard EN 206-1 also restricts the chloride content to 0.2% - 0.4% chloride by weight of cement for reinforced concrete and 0.1% - 0.2% for prestressed concrete.

3.2.2 **Influencing Parameters**

3.2.2.1 Steel-Concrete Interface

The importance of entrapped air voids adjacent to the reinforcement steel surface needs to be emphasized since corrosion starts at the interface. The presence of the air voids may trigger the corrosion process prematurely before the chloride concentration reaches the threshold value at the surface of the steel. The absence of the cement material would cause local falling of the pH value around the steel, which may lead to a premature corrosion initiation.

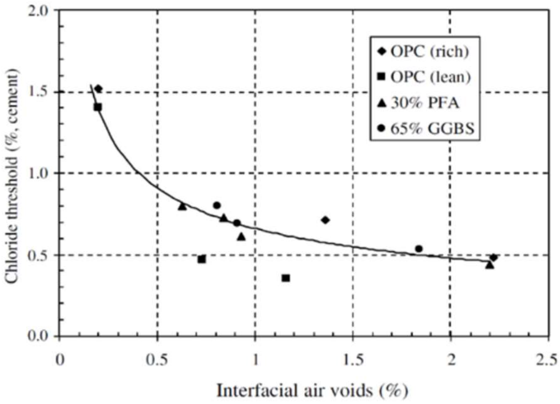

Figure 3-1 Chloride threshold as function of interfacial voids (Ann, 2007)

Although the physical condition of the steel–concrete interface in terms of the entrapped air void content has an effect on the critical value of chloride content, it is still hard to quantify the effects since there are only limited methods to detect air void content at the interface non-destructively and the method is only valid for large voids and ribbed bars.

3.2.2.2 pH value of the pore solution

The pore solution in concrete is an electrolyte, which is physically absorbed in the pores of the concrete. It may contain various ions, such as sodium, potassium, calcium, hydroxyl, sulphate and sulfite, etc. The chemical composition of the pore solution has a great impact on the pH value of the concrete. However, the carbonation process, leaching or proceeding hydration can also affect the pH value of the pore solution at later stages. Once the pore solution is polluted by chloride ions or de-alkalized by carbon dioxide, corrosion may occur.

The inhibiting effect of hydroxide ions against chloride induced corrosion, as a major factor influencing chloride threshold values for corrosion initiation was recognized early. The suggestion to present the threshold values of $\mathrm{Cl^-/OH^-}$ratios reflects this influence. (Angst, 2009)

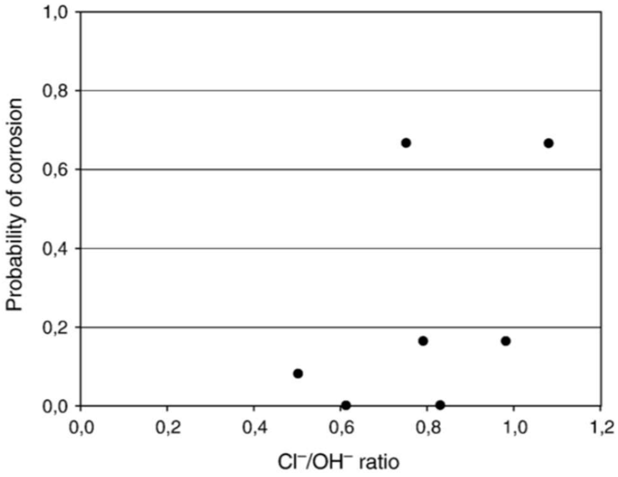

Figure 3-2 Probability of Corrosion vs. Cl^-/OH^-ratio (Angst, 2009)

In addition, the pH value may also affect the binding capacity of the chlorides. Studies have shown that a reduction of the pH to a value below 12.5 results in the release of a considerable part of the bound chlorides, while yet another part is released if the pH value is reduced to a value around 12. (Poulsen, 2012)

Based on the experiments by Hausmann (1967), the chloride threshold value is most accurately expressed by using $\mathrm{Cl^-/OH^-}$ ratio. A value of 0.6 is suggested and in succeeding studies.

3.2.2.3 Electrochemical Potential of Steel

The availability of oxygen and moisture content at the steel surface are the two main factors determining the electrochemical potential of steel embedded in concrete. In order for pitting corrosion to occur, the equilibrium potential must be higher than the pitting potential. The pitting potential is dependent on the concentration of chloride and higher contents of chlorides can be tolerated if the steel has a greater negative potential.

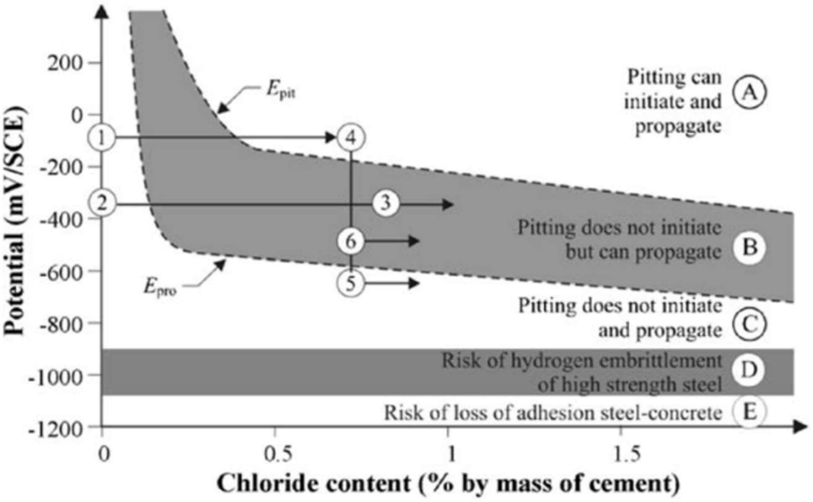

Figure 3-3 Steel potential versus chloride content in concrete (Bertolini, 2009)

Furthermore, compared with carbon steel, stainless steel has chloride threshold values as high as 20 times of the ones of carbon steel. It may remain passive and experience almost no corrosion even in relatively high chloride environment. MMFX2, another type of steel, also achieves a better performance compared to plain steel in corrosive environment by modifying the microstructure of the steel. Galvanized steel, by introducing the sacrificial zinc coating as a corrosion delay mechanism, also manage to have a longer service life. All these types of steel are more expensive than the plain steel. However, considering the savings in long term, in extreme corrosive environment, these corrosion resistant steels should be recommended in future construction projects.

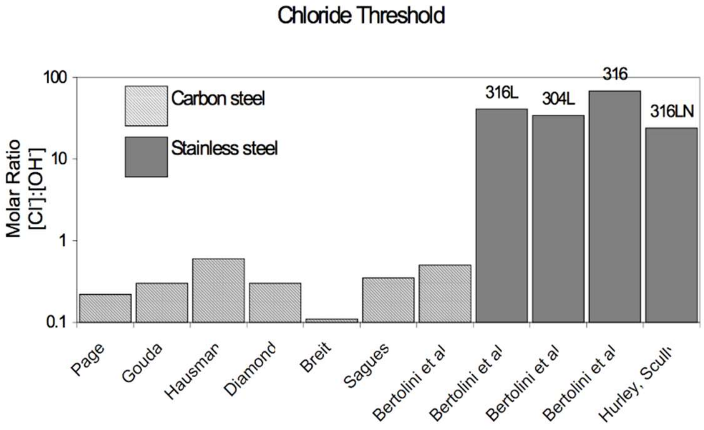

Figure 3-4 Chloride threshold value for Carbon steel and Stainless Steel (Hurley, 2008)

3.2.2.4 Binder Type

Binder type has great impact on the chloride threshold value. The effect of ground granulated blast-furnace slag (GGBS), fly ash (FA) and silica fume (SF) will change the critical chloride concentration in different ways.

GGBS has the effect of reducing the pH value of the pore solution, which promotes the initiation of pitting corrosion. However, it will increase the binding capacity of the concrete that may lead to a decrease in the free chloride content. Thus the overall effect of GGBS is hard to evaluate theoretically. Researchers give experimental reports that the GGBS either increase the chloride threshold value or decrease the value, and some other reports shows that the GGBS has no effect on the chloride threshold value. (Poulsen, 2012)

Fly ash has the same impact on the pH value of the pore solution as well as the binding capacity of the binder. Fly ash may have no effect on the chloride threshold value. Since it alters the pore structure in the concrete, the diffusion coefficient is affected by the presence of fly ash and may slow the chloride ingress process and lead to an extended service life for the concrete component.

Unlike the other two substances, Silica fume has a negative effect on the chloride threshold value. The pH value of pore solution is decreased and the binding capacity is decreased. The negative effect of silica fume on the chloride threshold value has been demonstrated in a number of studies. (Hansson, 1990; Petersson, 1993; Manera, 2008)

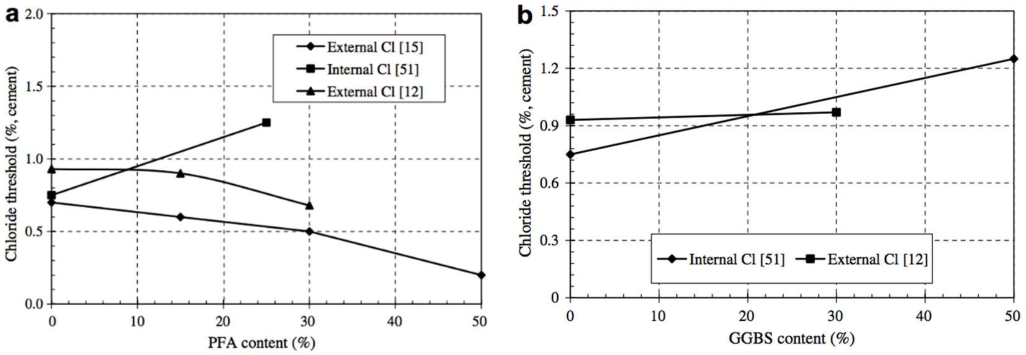

Figure 3-5 Chloride Threshold Values for Different Binder Type (Poulsen, 2012)

3.2.2.5 *Relative Humidity*

The effect of relative humidity on the chloride threshold level in laboratory-exposed mortars is shown below, as presented by Pettersson (1996). The threshold value for chloride ions increases when the available moisture is controlled.

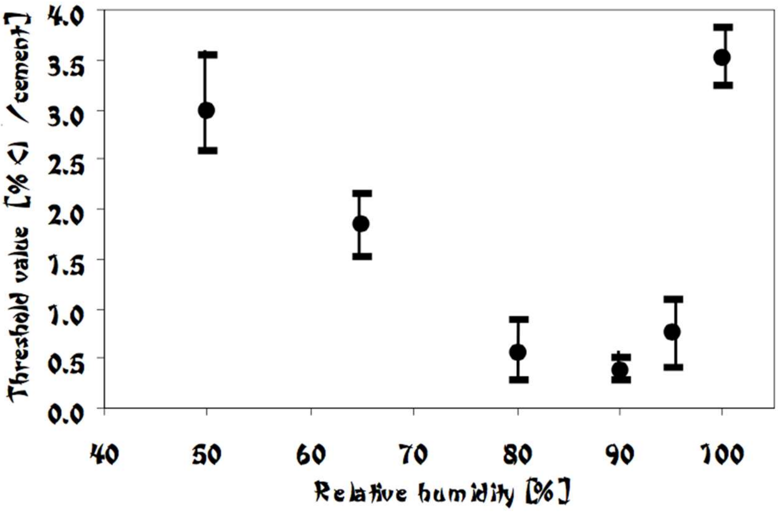

Figure 3-6 Relative humidity Vs. Chloride Threshold Value (Frederiksen, 2002)

3.2.2.6 Water-cement Ratio

Experimental data have indicated that concrete with lower water-cement ratio will have a higher chloride threshold value and vice versa, as shown below. (Pettersson, 1992, 1994; Schiessel and Breit, 1995) This is mainly due to the following consequences of a low water-cement ratio (Nilsson et al., 1996):

- Reduced area available for pitting corrosion development at the interface between steel and concrete
- Higher resistivity of the concrete
- Lower chloride mobility
- Improved ability to maintaining a high alkalinity

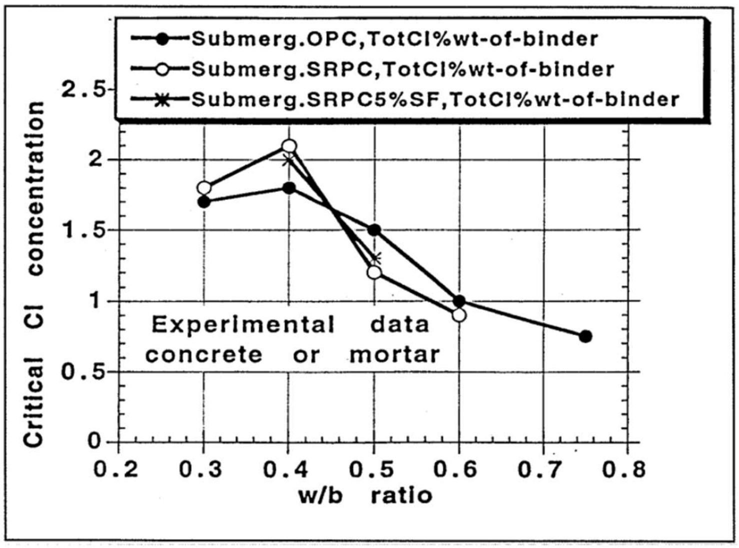

Figure 3-7 Water-cement Ratio vs. Chloride threshold Value (Poulsen, 2012)

3.2.2.7 *Degree of Hydration*

The water-cement ratio as well as the degree of hydration has an effect on the porosity of the paste and by this the availability of moisture and oxygen at the reinforcement. The threshold concentration increases with increased concrete age. This is particularly evident when it is assumed that chloride and alkali is only dissolved in capillary water (Fagerlund, 2011)

3.2.2.8 *Inhibiting Substances*

The presence of corrosion inhibitors can affect the threshold value dramatically. The $Ca(NO_2)_2$ inhibitor exhibits an inhibition effect only when the molar ratio between nitrite ions and chloride ions is less than 0.21. The ZnO and DMEA inhibitors can also effectively reduce the corrosion rate of steel in a saturated $Ca(OH)_2$ solution. All the inhibitors have a marginal effect on increasing the chloride threshold value for steel corrosion in a saturated $Ca(OH)_2$

solution. The reason may be due to the fact that the composition of the passive film on the steel surface does not change with the additions of the inhibitors. (Xu, 2013)

3.2.2.9 Surface Condition of the Steel

Different types of steel have different microstructures and compositions, so different steels usually have different corrosion behaviors in concrete. According to the experiment conducted by Ghods (2009), the polarization resistance is tested for as-received and polished surfaces as an indicator to the corrosion resistance. For both conditions, there is a threshold chloride concentration for the simulation pore solution above which the polarization resistance drops down dramatically. And it can be seen from Figure3-8, the polished rebar can endure a much higher chloride concentration without the breakdown of the passive layer compared to the as-received rebar.

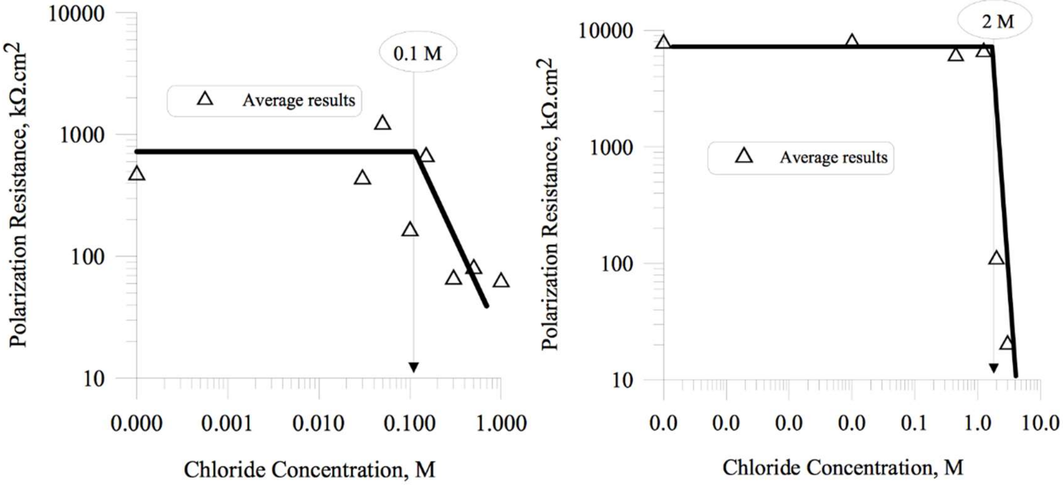

Figure 3-8 Polarization resistance of a) as-received rebar samples b) polished rebar samples (Ghods, 2009)

3.2.3 **Test Methods**

Generally, the experimental determination of the chloride threshold value must include the following four steps:

- Placing a reinforcement bar into a cement-based material or submerging it in a solution.
- Introducing chloride into the system.
- Detecting the corrosion initiation.
- Quantifying the chloride concentration at the time of corrosion initiation.

In order to quantify the chloride concentration at the time of corrosion initiation, the chloride content tests could be used. The chloride threshold value is usually expressed as either total chloride, free chloride or free chloride ion concentration.

The following test methods could be used to determine the corrosion initiation:

- Potential Shift
- Linear Polarization Resistance
- Macrocell Current
- Electrochemical Impedance Spectroscopy
- Galvanostatic Pulse Method
- Visual Examination

Except visual examination, all the other methods use an electrical approach to detect corrosion initiation, which gives a more accurate result compared to visual examination.

3.2.4 **Numerical Models**

Frederiksen (1997) proposed an equation to make semi-objective estimates for the threshold concentrations. The values could be obtained by:

$$C_{cr} = k_{cr,env} \times \exp(-1.5 \times eqv({}^{W}/_{C})_{cr}) \ [\%mass\ binder] \tag{3.2}$$

$k_{cr,env}$ is arbitrary to represent the environment factor. Suggested design values for threshold levels for black steel could be derived, as shown in Table 3-2, 3-3 and 3-4.

Table 3-2 The constant $\boldsymbol{k_{cr,env}}$ for the road environment (Frederiksen, 1997)

Environment: Constant:	Wet Road environment Splash (WRS)	Dry Road environment Splash (DRS)	Distant Road Atmosphere (DRA)
$k_{\mathrm{cr},\,env}$	1	1.25	1.25

Table 3-3 The constant $\boldsymbol{k_{cr,env}}$ for the marine environment (Frederiksen, 1997)

Environment: Constant:	Submerged marine environment (SUB)	Marine environment Splash (SPL)	Marine Atmosphere (ATM)
$k_{\mathrm{cr},\,env}$	3.35	1.25	1.25

Table 3-4 The activity factors for corrosion initiation in the road environment to be used when calculating the $\boldsymbol{eqv(^{w}/_{c})_{cr}}$ (Frederiksen, 1997)

Activity factor	Silica fume	Fly ash
k	-4.7	-1.4

The Suggested design values for chloride threshold levels (black steel) in various Nordic exposure zones are expressed in Table 3-5. These values are only suitable for crack free concrete with a maximum crack width of 0.1 mm and a minimum cover of 25mm. (Frederiksen, 1997)

Table 3-5 Suggested design chloride threshold level (Frederiksen, 1997)

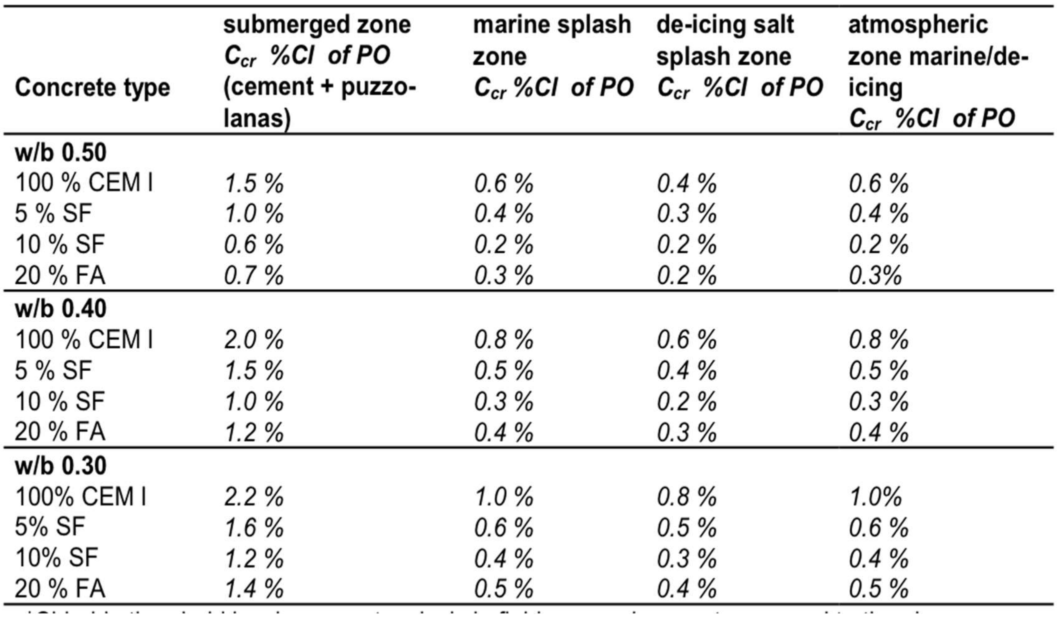

Concrete type	**submerged zone** C_{cr} ***%Cl of PO*** **(cement + puzzolanas)**	**marine splash zone** C_{cr} ***%Cl of PO***	**de-icing salt splash zone** C_{cr} ***%Cl of PO***	**atmospheric zone marine/de-icing** C_{cr} ***%Cl of PO***
w/b 0.50				
100 % CEM I	*1.5 %*	*0.6 %*	*0.4 %*	*0.6 %*
5 % SF	*1.0 %*	*0.4 %*	*0.3 %*	*0.4 %*
10 % SF	*0.6 %*	*0.2 %*	*0.2 %*	*0.2 %*
20 % FA	*0.7 %*	*0.3 %*	*0.2 %*	*0.3%*
w/b 0.40				
100 % CEM I	*2.0 %*	*0.8 %*	*0.6 %*	*0.8 %*
5 % SF	*1.5 %*	*0.5 %*	*0.4 %*	*0.5 %*
10 % SF	*1.0 %*	*0.3 %*	*0.2 %*	*0.3 %*
20 % FA	*1.2 %*	*0.4 %*	*0.3 %*	*0.4 %*
w/b 0.30				
100% CEM I	*2.2 %*	*1.0 %*	*0.8 %*	*1.0%*
5% SF	*1.6 %*	*0.6 %*	*0.5 %*	*0.6 %*
10% SF	*1.2 %*	*0.4 %*	*0.3 %*	*0.4 %*
20 % FA	*1.4 %*	*0.5 %*	*0.4 %*	*0.5 %*

A more detailed model was proposed by Fagerlund (2011) and the equation for estimating chloride threshold value is expressed as:

$$C_{cr} = 0.125 \cdot \alpha \cdot a \cdot \left(\frac{K \cdot k}{\frac{w}{c} - 0.19 \cdot \alpha}\right)^{b} + 3.55 \cdot K \cdot k \cdot \frac{\frac{w}{c} - 0.39 \cdot \alpha}{\frac{w}{c} - 0.19 \cdot \alpha} \tag{3.3}$$

Where,

$\frac{w}{c}$= water cement ratio

a, b = coefficients

α= Degree of hydration

k= amount of water soluble alkali in cement (mole/kg cement)

The threshold value of total chloride as weight of binder is determined by four parameters, in which, a and b are the coefficients represents the isotherm of chloride binding capacity governed by the following equation:

$$C_{bound} = a \cdot C_{free}{}^{b} \tag{3.4}$$

Where,

C_{bound}=Bound chloride (mg/g)

C_{free}= Free Chloride (mole/L)

For the typical isotherm shown below, a=13.5 and b=0.41.

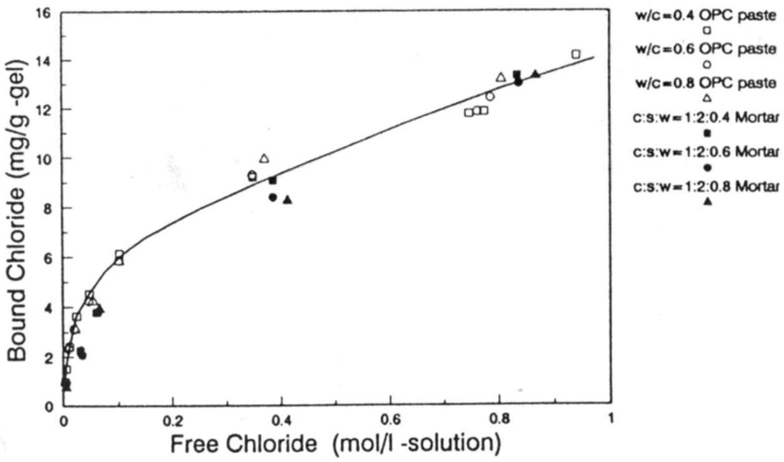

Figure 3-9 Relation between free and bound chloride in OPC (Tang, 1996)

3.2.5 **Summary**

The chloride threshold value is essential for estimating the service life of a concrete structure since it is a vital parameter to estimation the corrosion initiation time. It is vital for bridge engineers to develop a reliable testing procedure that could experimentally determine the chloride threshold value accurately. Given the numerous factors acting on the chloride threshold value, the reported chloride threshold value covers a wide range in the literature reviewed. Numerical methods have been investigated by some scholars, however, they still give roughly estimated values considering the different variables for the real structure. The chloride threshold value should be tested using one of the tests methods after completion of the construction in order to give a base value of the threshold value. If the tests are not performed and sufficient data is not available for the researcher, Fagerlund's model could be used to obtain a rough estimate for the chloride threshold value.

3.3. Determination of the Surface Chloride Concentration

3.3.1 Surface Chloride Concentration in Literature

Models for predicting chloride surface concentration have been proposed by many researchers. The surface concentration will increase with exposure time which makes it a function of time.

$$C_s = \emptyset(t) \tag{3.5}$$

Linear relation and square root relations are generally used to describe the surface chloride build up process, and are described as $\emptyset(t) = kt$ and $\emptyset(t) = k\sqrt{t}$ respectively.

McGee (1999) has investigated the relations between the surface concentration and the distance between the structure and the coastline *d*. When *d* is smaller than 0.1 km, $C_s = 2.85\ kg\ Cl^-/m^3$ concrete; while *d* is between 0.1 km and 2.84 km, $C_s = 1.15 - 1.81\lg(d)\ kg\ Cl^-/m^3$concrete; when *d* is greater than 2.84 km, $C_s = 0.03\ kg\ Cl^-/m^3$ concrete. While Bamforth (1998) suggested an estimated value for surface chloride concentration between 0.25% to 0.30% by weight of the concrete.

Ann (2009) states that the surface concentration is not zero even at the early stages of exposure. The initial surface concentration ranges between 2.0 to 2.5% right after the concrete is exposed to the environment. A modified square root build-up equation is developed and described as:

$$C_s = C_{s0} + k\sqrt{t} \tag{3.6}$$

Where k is the constant, t is the time of exposure and C_{s0} is the initial build-up of surface chloride.

Life 365 (Bentz, 2014) uses the linear model to demonstrate the build-up process for surface chloride concentration. The maximum surface chloride concentration is assumed to be 1.0%, 0.8%, 0.6% for marine splash zone, tidal zone and 800m away from the coast line respectively.

3.3.2 Determination of the Surface Concentration

The surface chloride concentration could be determined by averaging the chloride content with the thin surface layer. The depth of the layer should be selected carefully in order to rule out the skin effect while getting the relatively constant chloride concentration for further modelling.

Life-365 introduced a module that uses measurements obtained using ASTM C1556 for estimating the maximum surface chloride concentration. Once the concrete chloride concentration at different depth of a concrete sample is detected following ASTM C1556, the maximum surface concentration could be estimated by combining parameters including initial chloride concentration and exposure duration.

The estimation is done by fitting the laboratory data to a diffusion equation:

$$C(x,t) = C_s + (C_s - C_i)erf\frac{x}{\sqrt{4Dt}} \tag{3.7}$$

Where, $C(x,t)$ is chloride concentration at depth x when time= t; C_i is the chloride concentration for virgin concrete; D and C_s represents the constant diffusion coefficient and constant surface chloride concentration respectively; t is exposure time and *erf(*)* is the error function from mathematic equation chart.

The values of D and C_s are determined by minimizing the following function:

$$\sum[C_x^t - C(x,t)]^2 \tag{3.8}$$

By using a Levenberg-Marquardt nonlinear squares algorithm (Life-365,2014), the values of D and C_s could be determined. The ranges of initial guess for these two parameters are $C_s \in [0.01, 2.0]$ and $D \in [1 \times 10^{-15}, 1 \times 10^{-10}]$.

As discussed previously, this method is valid for estimating maximum surface concentration for old structures. The surface concentration is an average which does not reflect the seasoning changes. It is useful in calibrating the maximum surface concentration of a concrete structure after years of service.

3.3.3 **Numerical Models**

In order to better estimate the surface chloride concentration for concrete structures, a number of models are developed by scholars. Since the increase of chloride concentration will slow down with the aging of the concrete, the linear time depended model will overestimate the chloride concentration for long term exposure and underestimate the value for the initial stage. The square root model has the same problem. Therefore, Zhao (2010) have proposed a modified model to estimate the surface chloride concentration:

$$C_s(t) = C_{s0} + C_{smax}(1 - e^{-rt}) \tag{3.9}$$

In which, C_{s0} is the initial surface concentration by percent of the weight of the concrete; C_{smax} is the stable value of the surface chloride concentration; r is the accumulation constant; and C_{smax} could be estimated by the Duarte's model (Duarte, 2000):

$$C_{smax} = A \times {}^{W}/_{C} + \varepsilon \tag{3.10}$$

Where, A and ε are the regression constants and ${}^{w}/_{c}$ is the water cement ratio. According to the experiment done by Zhao, $A = 0.746$ and $\varepsilon = 0.2809$. The estimated value coincides well with the experimental outcomes.

Costa (1999) investigated 54 concrete panels exposed to marine environment for three to five years. The surface chloride concentration is model by the following equation:

$$C_s(t) = C_1 t^n \tag{3.11}$$

In which, $C_s(t)$ is the surface concentration at t years after exposure; C_1 is the surface concentration measured after 1 year of exposure; n is the empirical constant that ranges between 0.37 and 0.54.

Song (2008) has summarized the published data on C_s and proposed a refined model for the time-dependent parameter. The initial build-up of chlorides on the surface of concrete is shown as below:

$$C_s(t) = C_0 + \alpha \ln(t) \tag{3.12}$$

Where, C_0 is the initial surface concentration; α is the empirical constant. Based on the data collected by Song, $C_0 = 3.0431$ and $\alpha = 0.6856$.

Life-365 also gives exposure tab to give a rough estimation for the surface concentration build-up based on the exposure condition, as shown in Figure 3-10.

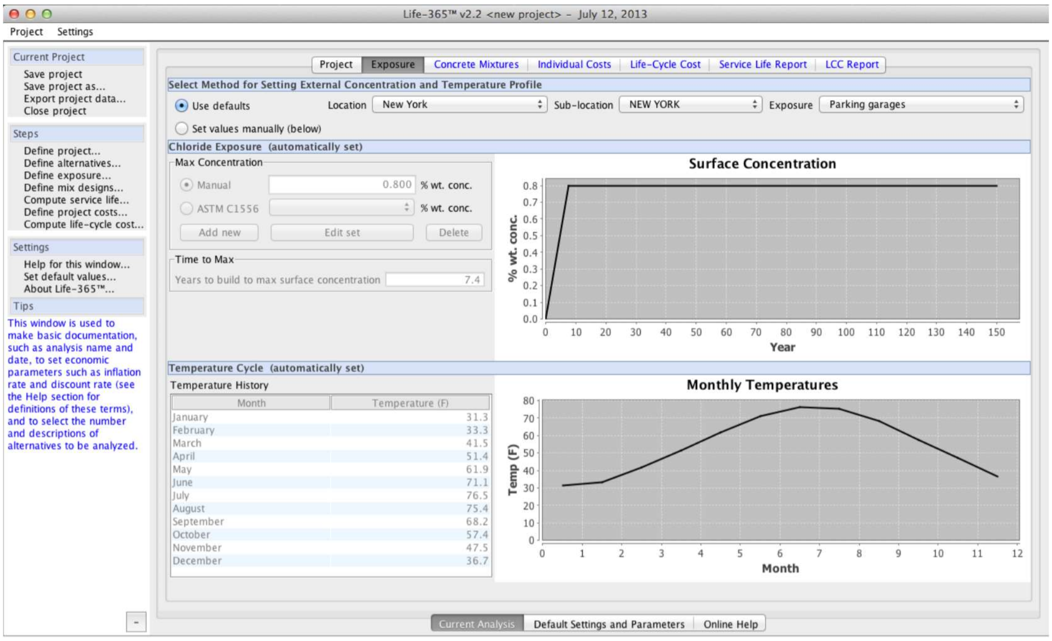

This window is used to make basic documentation, such as analysis name and date, to set economic parameters such as inflation rate and discount rate (see the Help section for definitions of these terms), and to select the number and descriptions of alternatives to be analyzed.

Select Method for Setting External Concentration and Temperature Profile

● Use defaults Location: New York Sub-location: NEW YORK Exposure: Parking garages

○ Set values manually (below)

Chloride Exposure (automatically set)

Max Concentration

● Manual 0.800 % wt. conc.

○ ASTM C1556 % wt. conc.

Time to Max

Years to build to max surface concentration 7.4

Temperature Cycle (automatically set)

Temperature History

Month	Temperature (F)
January	31.3
February	33.3
March	41.5
April	51.4
May	61.9
June	71.1
July	76.5
August	75.4
September	68.2
October	57.4
November	47.5
December	36.7

Figure 3-10 Exposure tab from Life-365 (Life-365, 2014)

3.3.4 **Summary**

Chloride surface concentration (C_s) is a vital parameter for estimating the corrosion initiation time. Chloride surface concentration has a great impact on the rate of chloride ingression, thereby influencing the prediction of chloride profile and corrosion risk.

Chloride surface concentration should be detected following the ASTM 1556 procedure. Nominal surface concentration could be estimated by numerical regression. It can also be estimated by averaging the chloride content for the top layer of the concrete. In practice, the chloride content within the top 1 in of the concrete could be calculated and treated as the surface chloride concentration at 1in below the actual surface of the concrete in order to rule out the skin effect of the concrete.

The experimental data for surface concentration of a newly constructed bridge tend to show scattered values that fluctuate and cover a wide range. Song's and Bentz's models are considered most favorable scientific models to predict surface chloride concentration as a time depended variable. In this research, the model proposed by E. C. Bentz is used since it is adopted by the widely used software Life-365.

3.4. Determination of the Diffusion Coefficient

3.4.1 **Diffusion Coefficient Estimation in the Literature**

Due to the importance of determination of the chloride diffusion coefficient (*D_c*), numerous scholars devoted their studies to this area through experimenting and numerical modeling.

JSCE (2002) proposed the following equations to estimate chloride diffusion coefficient by:

$$log\mathrm{D}_c = -3.9\left(\frac{\mathrm{w}}{\mathrm{c}}\right)^2 + 7.2\left(\frac{w}{c}\right) - 2.5 \qquad For\ OPC \tag{3.13}$$

$$log\mathrm{D}_c = -3.0\left(\frac{\mathrm{w}}{\mathrm{c}}\right)^2 + 7.2\left(\frac{w}{c}\right) - 2.5 \qquad For\ concrete\ with\ slag\ or\ SF \tag{3.14}$$

Boulfiz et al. (2003) investigated mathematical models and numerical simulations for water movement and chloride ions ingress by diffusion and advection in cracked and uncracked concrete under saturated or unsaturated conditions and derived the following equations:

$$log\mathrm{D}_c = -3.9\left(\frac{\mathrm{w}}{\mathrm{c}}\right)^2 + 7.2\left(\frac{w}{c}\right) - 14 \qquad For\ OPC\ or\ Concrete\ with\ FA \tag{3.15}$$

$$log\mathrm{D}_c = -3.0\left(\frac{\mathrm{w}}{\mathrm{c}}\right)^2 + 5.4\left(\frac{w}{c}\right) - 13.7 \qquad For\ concrete\ wi\quad slag\ or\ SF \tag{3.16}$$

The initial diffusion coefficient (D_{ref}), known as the reference diffusion coefficient of the concrete element is primarily correlated with the water cement ratio and the composition of the cementitious materials.

Ehlen's Life-365^{TM} Life Prediction Models and computer program also provide an approach to estimate the diffusion coefficient. The base case concrete mixture is plain Portland cement concrete with no special corrosion protection strategy. For this case, the following values are assumed:

$$\mathrm{D}_t = (\frac{1}{t})^m \mathrm{D}_{28} \tag{3.17}$$

$$\mathrm{D}_{28} = 1 \times 10^{(-12.06 \quad 2.40 \quad /c)} \tag{3.18}$$

In which, D_{28} is the diffusion coefficient after 28 days of curing. m stands for the aging factor that represents the decaying of diffusion coefficient in time due to effect of concrete aging.

The addition of silica fume is known to produce significant reductions in the permeability and diffusivity of concrete. In Ehlen's model, the presence of the silica fume affects the diffusion coefficient as shown below:

$$\mathrm{D}_{SF} = \mathrm{D}_{PC} \cdot e^{-0.165 \cdot SF} \tag{3.19}$$

Neither fly ash nor slag are assumed to affect the early-age diffusion coefficient, D_{28}, or the chloride threshold, C_t. However, both materials impact the rate of reduction in diffusivity and hence the value of m. The presence of the silica fume is affecting the diffusion coefficient decay factor as shown below. (Life-365, 2014)

$$m = 0.2 + 0.4^{(\%FA/50\ +\ \%SG/70)} < 0.6 \tag{3.20}$$

(Only valid up to replacement levels of 50% of fly ash or 70% of slag)

Ferreira (2010) provide a model suitable for concrete with high-performance Portland cement, silica fume, fly ash and slag. And the influence of temperature has been addressed in his models as shown below:

$$\mathrm{D(t)} = \mathrm{D_{ref,294}Kf(t)f(T)} \tag{3.21}$$

$$\mathrm{f(T)} = ({}^{T}\!/_{294}) \cdot \exp[{}^{U}\!/_{R} \cdot ({}^{1}\!/_{294} - {}^{1}\!/_{T})] \tag{3.22}$$

$$\mathrm{f(t)} = \left(\frac{\mathrm{t}_{ref}}{\mathrm{t}}\right)^{m} \tag{3.23}$$

Where,

U = Activation energy of diffusion process (J mol^{-1})

R = Gas constant (8.314 J mol^{-1} K^{-1})

In addition, a more detailed diffusion coefficient estimation model was presented by Saetta (1993) for silica fume concrete that also incorporates the influence of relative humidity as shown below;

$$\mathrm{D} = \mathrm{D_{ref} f_1(T) f_2(t) f_3(h)} \tag{3.24}$$

$$\mathrm{f_1(T)} = \exp\left[{}^{U}\!/_{R} \cdot \left({}^{1}\!/_{T_{ref}} - {}^{1}\!/_{T}\right)\right] \tag{3.25}$$

$$\mathrm{f_2(t)} = \zeta + (1-\zeta)\left(\frac{28}{t}\right)^{0.5} \tag{3.26}$$

$$\mathrm{f_3(h)} = [1 + {}^{(1-h)^4}\!/_{1-{h_c}^4}]^{-1} \tag{3.27}$$

Where,

ζ = Constant from 0 to 1

h = Current humidity (%)

h_c = Critical humidity level at which the diffusion coefficient drops halfway between the maximum and minimum value (%)

Besides the parameters included in the scientific models introduced above, such as temperature, water cement ratio, binder type and hydration process, the chloride diffusion coefficient is also affected by other parameters. Various experiments are designed and conducted by researchers to investigate these influencing parameters.

Construction workers can significantly influence the final coulomb value for a concrete specimen. Poor consolidation, and poor curing increase concrete permeability and increase the coulombs passing through the concrete. Using a 7-day moist cure instead of a 1-day moist cure can even decrease the chloride permeability by about 30%. The chloride diffusion coefficient is determined by Rapid chloride permeability test. Curing condition compared with the charge passed through the concrete slice is shown below.

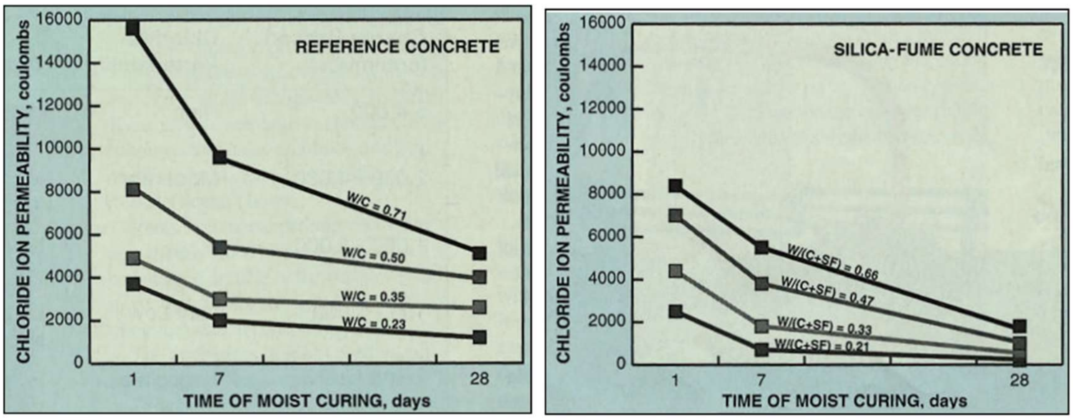

Figure 3-11 Time of moist curing Vs. Chloride Ion Permeability (Suprenant, 1991)

The porosity and the permeability of the concrete will also affect the diffusion coefficient. Higher porosity and larger pore sizes lead to more severe corrosion damage in the steel. If the concrete has low permeability, then the chlorides and carbon dioxide would be difficult to access the reinforcement and the possibility of corrosion would be low. Based on Sugiyama (1996) investigation, the correlation between gas permeability and chloride diffusion coefficient is valid in particular when the water-cement ratio of concrete dominates the gas permeability. The correlation is based on the fact that the chloride diffusion coefficient is also a factor that significantly affected by the water-cement ratio. The correlation may become poor if the specimen experienced a longer period of drying for gas permeability due to the micro-cracks formed during the elongated drying period.

The presence of cracks will also have a great impact on the chloride diffusion coefficient. Gerard (2000) states that for Ordinary Portland Cement with a water cement ratio of 0.45, the chloride diffusion coefficient jumped from $9.7 \times 10^{-9} cm^2/s$ for the virgin concrete to $76.52 \times 10^{-9} cm^2/s$ after experiencing 95 freeze and thaw cycles. Relations regarding to the ratio between the chloride diffusion coefficients for undamaged and damaged concrete specimen have been correlated with the ratio of effective elastic modulus of concrete under these two different conditions. Jang (2011) also conducted research on the effect of crack width on chloride diffusion coefficients of concrete. Zhang (2011) also investigated the relation between cracks and the diffusion coefficient.

Care (2003) and Liu (2011) studied the impact of different types of aggregates on the diffusion coefficient of the concrete.

In addition, the influence of deterioration during service, exposure conditions and the impact of chloride binding are also investigated by different scholars. The chloride diffusion coefficient reported from published data is given in Appendix C, which includes the diffusion information on the type of sample and the exposure condition from which that data was obtained.

3.4.2 **Test Methods**

Diffusion coefficient is defined as the rate of transfer of the diffusing substance across a unit area of a section divided by the space gradient of concentration at the section.

Two types of diffusion coefficients can be tested by different tests: steady-stated diffusion coefficient refers to the pore solution concentration and non-steady-state diffusion coefficient, measured by the units of percentage of the mass of cement.

The commonly used tests are the rapid chloride permeability test (RCPT), salt ponding test, rapid migration test and bulk diffusion test.

3.4.2.1 RCPT

The rapid chloride permeability test (RCPT) was developed in 1981 by David Whiting for the Federal Highway Administration, FHWA (Gergely, 2006). It was developed to provide an alternative to the salt ponding test, which is a long-term test.

The basic principle behind the RCPT is the applied voltage technique. This technique is based on the principle that a charged ion, such as chloride ions, will migrate in an electric field in the direction of the pole of the opposite charge.

Although the test shows good correlation for Portland cement concrete, it does not provide high correlations with concretes with admixtures or supplementary cementitious materials. The presence of silica fume and fly ash will change the pore fluid conductivity and the micro-structural characteristics of the concrete, and it will cause an increase in the amount of charge passed during the RCPT test, which may lead to an overestimated value for the chloride permeability.

Mineral admixtures are not the only concrete additives that disrupt the RCPT. Nitrite-based corrosion inhibitors also cause unduly high RCPT values. These inhibitors are used to fend off corrosion of rebars due to chemical attacks.

3.4.2.2 Salt Ponding Test

The salt ponding test is the most widely accepted test method for determining the chloride permeability of concrete. There are two versions of this test: AASHTO T259 and

ASTM C1543 (AASHTO & ASTM, 2002). The AASHTO test consists of 42 days of preparation and 90 days of ponding. The ASTM method lasts for a subjective length of time determined by the concrete type. Both tests require a 3% salt solution to be ponded on concrete slabs measuring 12” square by 3” thick. This solution is changed every two months for the ASTM method, while it is not changed for AASHTO. The chloride concentration is determined for 0.5-inch slices of the slab. (Gergely, 2006)

There are some criticisms for the salt ponding test. The first one is that due to the nature of the test, the method gives an average chloride concentration over a 0.5” section instead of a real chloride profile. This difference will introduce error during the curve fitting process.

Another issue is that the salt ponding test allows chloride ingression by other chloride transpiration mechanisms. This test allows for other transport mechanisms including sorption and wicking. The concrete should be dried for 28 days before the solution is added. When the solution is added, there will be suction of the chloride solution due to the wetting effect.

3.4.2.3 Rapid Migration Test

Tang and Nilsson proposed a variation on the conventional migration cell unique enough to be mentioned separately. A migration cell is set up with a specimen 50 mm thick and 100 mm in diameter, and an applied voltage of 30 V, as shown in Figure 3-12. (Stanish, 1997)

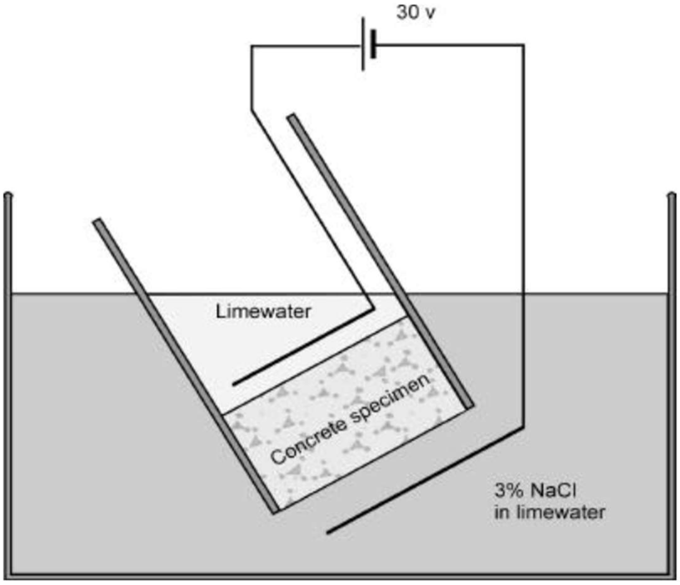

Figure 3-12 Tang and Nilsson migration cell (Stanish, 1997)

This test method is similar to the RCPT in that a 2-inch thick cylinder with a 4-inch diameter is subjected to an applied voltage for a period of time. The difference in this test is the length of time, typically 24 hours, and the voltage used, ranging from 10-60 VDC. This test method has been suggested to be a better option than the RCPT test for a wider variety of concrete mixes.

One of the major benefits of this test is that it allows for the calculation of a non-steady state diffusion coefficient. This diffusion coefficient is a function of the applied voltage, temperature of the solution, thickness of the specimen and the depth of chloride penetration. Also, the use of corrosion inhibiting admixtures did not affect the RMT results as in the case for RCPT results. This suggests that the RMT is capable of testing a wider range of concretes than the RCPT.

3.4.2.4 *Bulk Diffusion Test*

A bulk diffusion test has been developed to overcome some of the deficiencies of the salt ponding test to measure diffusion. The NordTest is the first formally standardized version of the bulk diffusion test. Compared with salt ponding test, the test specimen is saturated with limewater instead of dried for 28 days in order to eliminate the wetting effect. The only face left uncovered is the one exposed to a 2.8 M NaCl solution. And the specimen is left this way for a minimum of 35 days before evaluation. The typical set up for the test is shown in Figure 3-13.

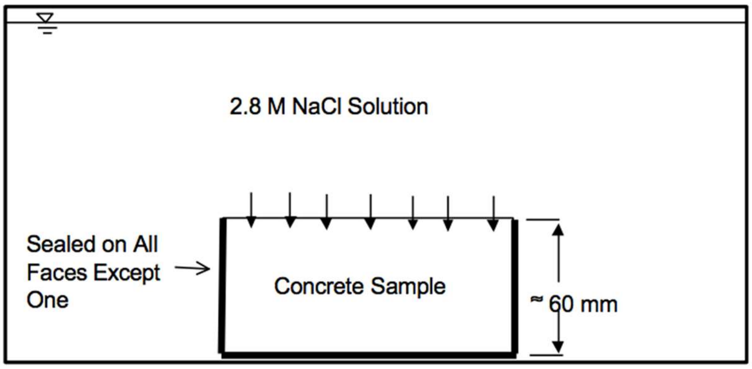

Figure 3-13 Bulk Diffusion Test (Stanish, 1997)

To evaluate the sample, the chloride profile of the concrete is determined by mounting the sample in either a mill or lathe with a diamond tipped bit. The chloride content of the powder is then determined according to AASHTO T260. The error function solution of Fick's Second Law is then fit to the curve and a diffusion value and surface chloride concentration is determined.

This test is still a long-term test. For low quality concretes, the minimum exposure period is 35 days. This period must be extended to 90 days or longer for higher quality concrete, which resulting in a test duration similar to the one of to salt ponding test. (Gergely, 2006)

3.5. Proposed Refined Numerical Models for Estimating *Dc*

Chloride diffusion coefficient is a vital parameter in estimating the chloride-induced corrosion for reinforced concrete. The chloride diffusion coefficients can be classified as:

- The real but unknown chloride diffusion coefficient.
- The apparent chloride diffusion coefficient obtained by curve fitting to a chloride profile.
- The instant chloride diffusion coefficient as measured by RCP test, etc.

The derivation of chloride diffusion coefficient is usually based on the curve fitting of the chloride profile extracted from the field data using Fick's law. The chloride profile of the element could be obtained by chloride content tests. There are many lab techniques and field measurements for measuring chloride content in reinforced concrete structures, such as potentiometric and Volhard methods, ion selective electrodes, electrical resistivity and optical fiber sensor.

The curve fitting method yields to the apparent chloride diffusion coefficient over a period of time, which is extremely suitable for estimating the chloride profile for old marine concrete structures. However, due to time-dependent nature of chloride diffusion coefficient, this method gives unreliable estimation of the chloride profile for younger structures since it overestimates the diffusion penetration by a large margin. In such cases, the time-dependent diffusion coefficient should be predicted by scientific method.

In this study, a revised equation for estimating time-dependent chloride diffusion coefficient is proposed. In order to do so, the decisive parameters governing the chloride diffusion coefficient have been identified and evaluated. The major factors incorporated in the scientific model that dominate the diffusion coefficient are the water cement ratio of the concrete, the type and proportion of cementitious materials. Factors reflect the aging of the concrete, presence of cracks, exposure conditions, curing conditions and stress level are also investigated.

The proposed equation is expressed as:

$$D_c(x,t) = k_t k_b k_c k_T k_E k_{RH} k_d k_l D_{ref} \tag{3.28}$$

Where,

$\mathrm{D_{ref}}$ = Reference chloride diffusion coefficient

k_t= Effects of aging of the concrete

k_b = Effects of chloride binding capacity

k_c = Curing conditions

k_T= Effects of temperature

k_E = Environmental factor

k_{RH}= Effects of relative humidity

k_d = Effects of cracking

k_l = Content of Latex

3.5.1 Reference Chloride Diffusion Coefficient ($\boldsymbol{D_{ref}}$)

The reference chloride diffusion coefficient is usually measured by CTH or similar tests, usually at a maturity age of 28 days. It is the base chloride diffusion coefficient that is measured in the lab, under controlled environment conditions. The concrete specimen should be well cured and stored at a constant temperature while fully saturated.

The reference chloride diffusion coefficient reflects the initial resistance of the concrete to chloride penetration. It is mainly affected by the water cement ratio and the type of the binder, which controls the micro structure in the concrete.

If the experimental data is not available, the chloride diffusion coefficient could be estimated by the following equation used in Life-365 (2014):

$$D_{28} = 1 \times 10^{(-12.06+2.4^{W}/_{c})} \cdot e^{-0.165 \cdot S} \tag{3.29}$$

Where, SF= the percentage of silica fume (%)

3.5.2 Aging Factor (k_t)

Time dependency of chloride diffusion coefficient plays a vital role in the service life prediction of concrete structure. In general, chloride diffusion coefficient often decreases with time due to the process of hydration. The commonly used equation to quantify the time dependency is as follows:

$$k_t = \left(\frac{\mathrm{t}_{ref}}{\mathrm{t}}\right)^m \tag{3.30}$$

In which, t_{ref} is the time corresponding to the reference chloride diffusion coefficient, t is the exposure time and m is a constant.

This exponential equation is widely used by researchers. The age factor, m, is important for service life prediction. It depends on the concrete mixture proportions, especially on the water cement ratio of various mixes. (Song, 2013) The exposure condition may also affect the age factor. It is obtained by fitting Equation (2.8) and (2.9) using several chloride diffusion coefficients for different time values. Therefore, the diffusion coefficient of the concrete should be examined periodically in order to better calibrate the age factor.

If sufficient data is not available, the age factor, m, could be also estimated by using the following equations proposed by Jin (2008):

$$m = \begin{cases} 0.8\,{}^{w}/_{c} + 0.35\left({}^{FA}/_{50} + {}^{SG}/_{70}\right)(Atomospheri\ \ Zone) \\ 0.8\,{}^{w}/_{c} + 0.35\left({}^{FA}/_{50} + {}^{SG}/_{70}\right) - 0.04\ (Splash/Tidal\ Zone \\ 0.8\,{}^{w}/_{c} + 0.35\left({}^{FA}/_{50} + {}^{SG}/_{70}\right) - 0.14\ (Submerged\ Zone \end{cases} \tag{3.31}$$

In which, ${}^{w}/_{c}$ is the water cement ratio of the mix, FA and SG represent the proportion of Fly ash and Slag by weight of the cement. This equation is only valid up to replacement levels of 50% of fly ash or 70% of slag. And the maximum value for m is 0.6 as stated in (Life-365, 2014).

3.5.3 Chloride Binding Factor (k_b)

The chloride ions in the concrete could be separated into two parts: the free chlorides in the pore solution, and the bound chlorides that reacts or bound to the concrete surface, in which, only the free chlorides can react with other chemicals such as the corroding the reinforcing steel. Therefore, the chloride binding capacity has an important impact on the service life of concrete structures and should be incorporated in the chloride diffusion coefficient.

The relation between free chlorides and bound chlorides is expressed as binding isotherm. There are three mathematical equations that are commonly used by researchers to describe the binding isotherm: linear isotherm, Langmuir isotherm or Freundlich isotherm. Due to the complexity of the latter two, it is impractical to consider those isotherms in estimating the chloride diffusion coefficient for a real structure since a myriad of parameters is required. Therefore, in this report, only the linear isotherm is used.

The binding capacity of concrete is affected by a number of parameters, the most critical ones are the binder type, chloride concentration in the concrete, and the pH value of the pore solution. Since the linear isotherm is selected, the chloride concentration will not contribute to differentiate binding factor.

Mohammed (2003) has conducted a thorough investigation on the relationship between free chloride and total chloride contents in concrete in Japan, and the k_{b} value was reported to range from 0.813 to 0.898. Xu (2008) has determined the k_{b} for ordinary Portland cement concrete and high performance concrete exposed to sea water and k_{b} equals to 0.877 and 0.81 respectively. Based on the literature review done by Zhao (2011), the range of the chloride binding factor could be determined as:

$$k_b = \begin{cases} 0.7 - 0.9\ (OPC) \\ 0.6 - 0.7\ (HPC\ with\ Slag\ or\ Fly\ Ash) \\ 0.7 - 0.8 (HPC\ with\ Silica\ Fume) \end{cases} \tag{3.32}$$

Since the chloride binding capacity depends on the pH value of the pore solution, the chloride binding factor can be simplified and expressed as a function of the pH value of the pore solution. According to the HETEK report (Nilsson, 1996), concrete loses its binding capacity once it is fully carbonated, which means $k_b = 1$ if the pH value is less than 10. Also, the pH value for a fresh concrete is always above 13.5 and the steel is fully protected under the high alkalinity of the concrete. The minimum value of k_b is set once the pH is higher than 13.5. While the pH value equals 11.5, the concrete still has small portion of its binding capacity, therefore, the minimum value from the literature is assigned at pH value of 11.5. A linear relationship is assumed between the pH value and the chloride binding factor. The chloride binding factor could be determined from Figure 3-14.

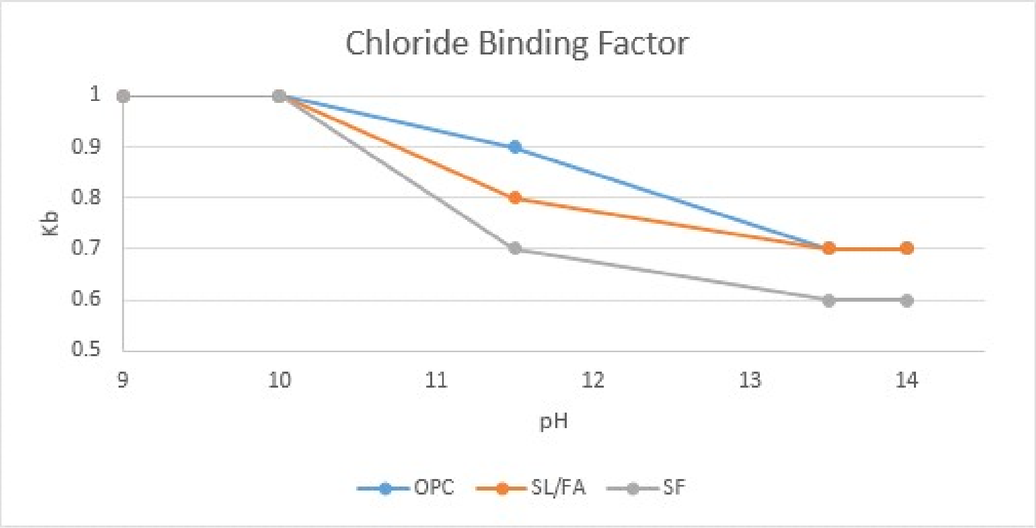

Figure 3-14 Chloride Binding Factor

3.5.4 Curing Factor (k_c)

Initial curing has a vital impact on the chloride diffusion coefficient. Concrete will show a higher chloride diffusion coefficient under a short curing period due to the micro cracks formed inside the concrete. Based on the research done by Alizadeh (2008), Costa (1999) and the Duracrete (2000), a chart has been created to estimate the curing factor under various curing regimes.

Table 3-6 Curing Factor for Different Curing Time

Curing time (days)	1	3	7	28
k_c	2.7	1.8	1.4	1

3.5.5 **Effects of Temperature (k_T)**

The impact of temperature on chloride diffusion has been well published by researchers. Ferreira (2010) investigated the influence of temperature on concrete with different binder mixtures and the equation to quantify k_T was expressed as:

$$k_T = ({}^{T}/_{T_{re}}\ ) \cdot \exp[{}^{U}/_{R} \cdot \left({}^{1}/_{T_{ref}} - {}^{1}/_{T}\right)] \tag{3.33}$$

In which, T is the temperature of the concrete and T_{ref} is the temperature used when the reference diffusion coefficient is measured (K); U is the activation energy of diffusion process (J mol-1) and R is gas constant (8.314 J mol-1 K-1).

The activation energy of diffusion is related to the water cement ratio and the binder type. It could be calculated by the following equation using two sets of test conducted at different temperatures for a specific concrete mix.

$$ln\left({}^{D_1}/_{D_2}\right) = -{}^{U}/_{R} \cdot \left({}^{1}/_{T_1} - {}^{1}/_{T_2}\right) \tag{3.34}$$

In which, D_1 and D_2 is the diffusion coefficient measured at temperatures T_1 and T_2.

So (2014) conducted experimental research for OPC and concrete with fly ash for different water cement ratio. The reported values are summarized in the Table 3-7.

Table 3-7 U/R for different water cement ratios for OPC and concrete with Fly Ash (So, 2014)

	U/R (1/K)		
w/c	0.4	0.5	0.6
OPC	3067	3284	2093
Concrete with FA	3873	3464	2213

Interpolation of the values in the chart could be used for simplification if the experimental tests data is lacking.

3.5.6 Environmental Factor ($\boldsymbol{k_E}$)

Exposure condition of the concrete element exhibits a great impact on the chloride diffusion coefficient. For marine structures, chloride diffusion coefficient shows a great difference for bridge elements exposed in submerged zone, tidal zone, splash zone and atmospheric zone. It is obvious that the impact is due to the amount of chloride available in the surrounding environment, the temperature, relative humidity, mechanism of chloride transportation. Since the temperature and relative humidity is discussed by another factor, this environmental factor mainly counts for the chloride transportation mechanism as well as the amount of chloride available.

Unlike the concrete in the submerged zone, the concrete in splash and tidal zone is constantly experiencing wet and dry cycle, the surface chloride concentration is much higher due to the crystallization of salt in the pore structure. Also, the chloride ions will transport into the concrete by capillary suction besides diffusion which result in a higher diffusion coefficient compared to submerged zone. The atmospheric zone is exposed to chlorides in the air and it also yields to a different value.

Wang (2008) has reviewed the environmental factor published by various researchers and the range for environmental factor has been listed in the following table.

Table 3-8 Environmental Factor Range (Wang, 2008)

Binder	OPC			HPC		
Exposure Condition	Tidal Zone	Splash Zone	Aero Zone	Tidal Zone	Splash Zone	Aero Zone
k_e	0.9-2.0	0.4-1.3	0.5-0.7	2.7-3.6	0.7-1.2	1.9-2.4

In this paper, the initial value for environmental factor is selected based on the research from Duracrete (2000). The equation is expressed as:

$$k_E = k_{E1}k_{E2} \tag{3.35}$$

In which, k_{E1} is the location index and k_{E2} is the concrete mix factor.

The value of $k_{E1}$and k_{E2} is selected as follows:

Table 3-9 Value of k_{E1} (Duracrete, 2000)

Location	Submerged Zone	Tidal/Splash Zone	Atmospheric Zone
k_{E1}	0.757	1.087	1.47

Table 3-10 Value of k_{E1} (Duracrete, 2000)

Concrete mix	OPC	HPC
k_{E1}	1	0.345

Environmental factor for road application that subjected to deicing salts can be chosen from the value for splash zone due to the similarity of the exposure condition. However, the amount of deicing salt used, the geographical location of the bridge, exposure to rain, amount of traffic will also impact the environmental factor. Therefore, the value of k_E for road condition should be selected with extra caution.

3.5.7 Effects of Relative Humidity (k_{RH})

Relative humidity in the concrete is a decisive parameter for the continuity of the pore solution in the concrete, thus, it also has a great impact on the diffusion coefficient. Based on the research done by Saetta (1993), the reduction of diffusion coefficient could be quantified by the equation shown below:

$$\mathrm{k}_{RH} = [1 + {(1-h)^4}/{(1-h_c)^4}]^{-1} \tag{3.36}$$

In which, h is current humidity (%); h_c is the critical humidity level at which the diffusion coefficient drops halfway between the maximum and minimum value (%), commonly set as 75%.

The inner relative humidity of the concrete could be tested through NDT methods, such as moisture meter.

A simplified chart for k_{RH} is presented in Table 3-11.

Table 3-11 Effects of Relative Humidity

RH	<54%	65%	75%	85%	>95%
k_{RH}	0.07	0.2	0.5	0.88	1

Relative humidity of the concrete is mainly determined by surrounding environment. For submerged zone, k_{RH} equals to 1 in most cases. Relative humidity for concrete exposed to air can be estimated by the relative humidity in the air for long term evaluation.

3.5.8 Damage Factor ($\boldsymbol{k_d}$)

Reference chloride diffusion coefficient is always measured on a specimen that is cast and cured in a controlled environment which makes the specimen crack free. At the same time, the specimens are often left stress free in both laboratory and field exposure tests. However, it is not always true for the concrete from a real structure. Cracks may form at the surface of concrete due to plastic shrinkage at early age. Through years of service, other reasons, such as temperature, loading, excessive settlement, freeze-thaw cycling, may also cause cracks. Besides, the bridges elements are subjected to various loading through its service life, the concrete property will be greatly affected by the load conditions as well.

Chloride diffusion coefficients in the damaged concrete is much higher than the ones in virgin concrete since the chloride ions may move more freely in the micro cracks within the concrete. Researchers have stated that the crack width has a vital impact on the diffusion coefficient for crack width greater than 0.1mm. For crack width smaller than 0.1mm, the impact is negligible since it does not have significant impact on the diffusion coefficient. The maximum diffusion coefficient of chloride in the crack is limited as the diffusion coefficient for pore solution. Also, if the crack is wide enough, the surface of crack could be treated as surface directly subjected to the exposure environment.

In order to investigate the internal damage caused chloride diffusion variation, Rahman (2012) and Teggure (2013) has conducted several experiments. The impact of the damage is quantified through a damage index, which is evaluated based on the differences of dynamic modulus of elasticity of cracked and uncracked concrete. The equation used to evaluate the damage factor is expressed as follow:

$$k_d = \frac{7.826(E_0 - E_d)}{E_0} + 1 \tag{3.37}$$

In which, E_0 and E_d are the dynamic modulus of elasticity of uncracked and cracked concrete, respectively.

The dynamic modulus of elasticity of concrete can be determined nondestructively using resonance tests based on measuring the fundamental flexural and torsional frequencies of concrete specimens using a Grindosonic apparatus (Teggure, 2013). The tests should be carried out for new structures in order to achieve a base understanding of the dynamic modulus of elasticity of the concrete.

Another advantage of using damage index to quantify cracking impact is that the change of modulus also relates to the freeze-thaw effect. If the concrete experiences severe freeze-thaw cycles, micro cracks will form in the concrete which will also affect the diffusion coefficient. By using the damage index, which is the difference of moduli of concrete, the impact of freeze-thaw cycles on the diffusion coefficient is also evaluated.

Depending on the point in the service life of the bridge, the dynamic modulus of elasticity is calculated as (Salman and Al-Amawee, 2006):

$$E_d(t) = 7.3[f_c(t)]^{0.533} \tag{3.38}$$

In which, $E_d(t)$ is the dynamic modulus of elasticity at time t in GPa, and $f_c(t)$ is the concrete compressive strength at time t in MPa; t is the time of evaluation. By adopting this equation, the dynamic modulus of elasticity can be estimated based on the compressive strength of the concrete.

3.5.9 **Latex Content**

Several studies have been conducted to investigate the impact of polymers in the concrete mix. The polymer modified concrete has shown different mechanical properties when compared with ordinary Portland cement concrete, such as compressive strength, and flexural strength. Meanwhile, polymer will also change the microstructure of the concrete, resulting in a considerable difference considering the durability parameters such as chloride diffusion coefficient.

Won (2008) has conducted a set of tests to evaluate the diffusion property of latex modified concrete. Different water cement ratio, latex cement ratio and unit cement contents have been used to inspect these parameters separately. The concrete mix table is shown as below.

Table 3-12 Concrete Mix Table of Different water-cement ratio, latex content (Won, 2008)

Type of mix(W/C-LS/C-unit cement contents)	W/C (%)	LS/C (%)	S/a (%)	(kg/m³)				
				C	W	S	G	Latex
33-15-400	33	15	55	400	64	887	760	128
33-10-400		10			87	914	783	85
39-10-400	39	10			111	881	755	85
39-5-400		5			133	908	778	43
45-5-400	45	5			157	874	749	43
33-15-350	33	15		350	56	942	807	112
39-15-350	39	15			77	913	782	112
39-10-350		10			97	937	803	74
45-10-350	45	10			118	908	778	74
39-15-300	39	15		300	66	972	833	96
45-15-300	45	15			84	947	812	96
45-10-300		10			101	968	829	64

The time dependent constant and average diffusion coefficient is summarized in the following table.

Table 3-13 Average Diffusion Coefficient of Different Concrete Mix (Won, 2008)

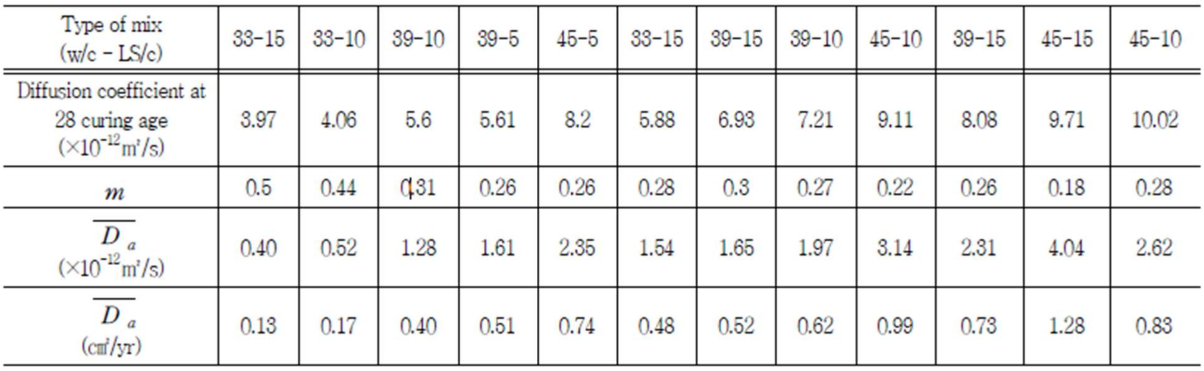

Type of mix (w/c - LS/c)	33-15	33-10	39-10	39-5	45-5	33-15	39-15	39-10	45-10	39-15	45-15	45-10
Diffusion coefficient at 28 curing age ($\times 10^{-12}$ m²/s)	3.97	4.06	5.6	5.61	8.2	5.88	6.93	7.21	9.11	8.08	9.71	10.02
m	0.5	0.44	0.31	0.26	0.26	0.28	0.3	0.27	0.22	0.26	0.18	0.28
$\overline{D_a}$ ($\times 10^{-12}$ m²/s)	0.40	0.52	1.28	1.61	2.35	1.54	1.65	1.97	3.14	2.31	4.04	2.62
$\overline{D_a}$ (cm²/yr)	0.13	0.17	0.40	0.51	0.74	0.48	0.52	0.62	0.99	0.73	1.28	0.83

By grouping the mix with the same water cement ratio, the normalized diffusion coefficient of different latex-cement ratio could be extracted.

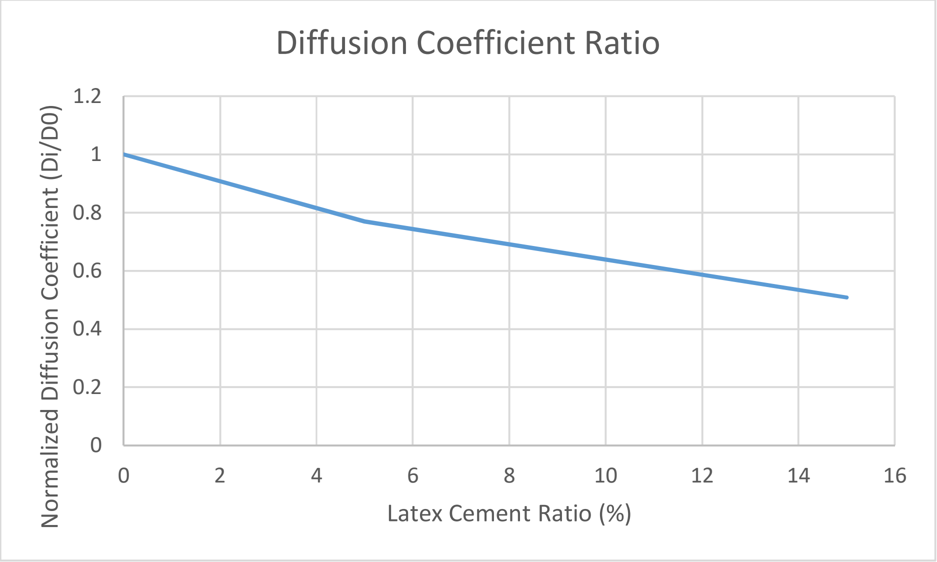

Figure 3-15 Diffusion Coefficient Ratio Vs. Latex Cement Ratio (Won, 2008)

However, there are several points that need to be identified. The water cement ratio is relatively high for latex modified concrete, and the change unit cement contents also have an influence on the diffusion coefficient ratio.

Another research conducted by Yang (2009) has identified that latex improved the chloride penetration resistance of the mortar, as indicated by the reduced apparent diffusion coefficients of chloride ions, D_{Cl}. When the P/C ratio was 16%, the value of D_{Cl} decreased by 65% compared with conventional Portland cement mortar. D_{Cl} decreased linearly with the increase in P/C ratio under the experimental conditions of this study.

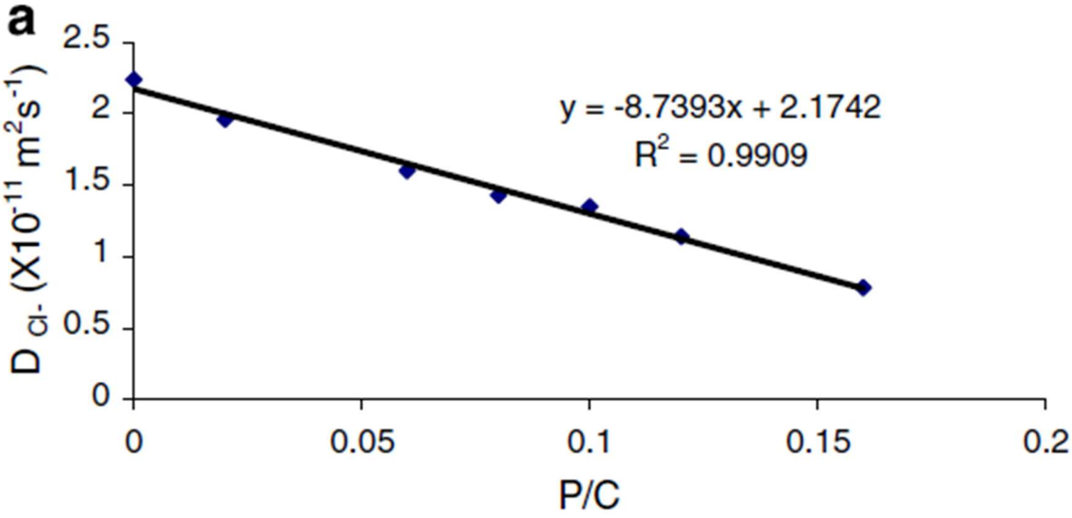

Figure 3-16 Diffusion Coefficient Ratio Vs. Latex Cement Ratio (Yang, 2009)

Combining the two experimental results, the equation for estimating the diffusion coefficient of latex modified concrete has been revised as:

$$D_{28} = 1 \times 10^{(-12.06+2.4 W/c)} \cdot 0.8^{(20 \cdot P/c)} \tag{3.39}$$

In which, $P/_C$ is the polymer cement ratio.

The effect of polymer in this model is compared with the data reported by Won (2008) and Yang (2009), as shown in Figure 3-17.

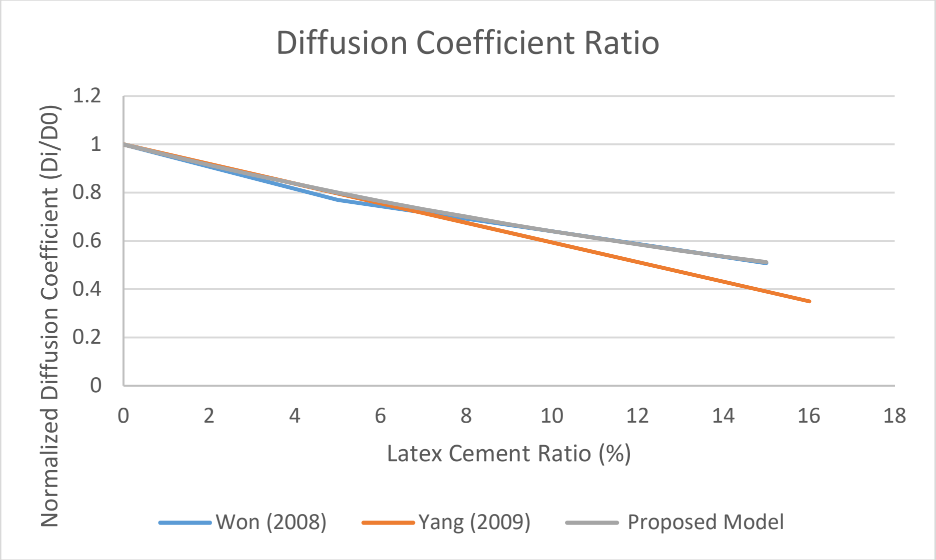

Figure 3-17 Diffusion Coefficient Ratio Vs. Latex Cement Ratio

Also, based on the data from Won (2008), the polymer will also affect the aging factor m. In general, the water cement ratio is the most influential factor. Therefore, the equation for estimating m is modified accordingly:

$$m = 1.2 - 2.4\,{}^{w}/_{c} + 0.35\left({}^{FA}/_{50} + {}^{SG}/_{70}\right) \tag{3.40}$$

m should still be smaller than 0.6.

Based on the equation derived by Bentz, effect of silica fume could be measured by the following equation:

$$\frac{D_{sf}}{D_{pc}} = e^{-0.165 \cdot SF} \tag{3.41}$$

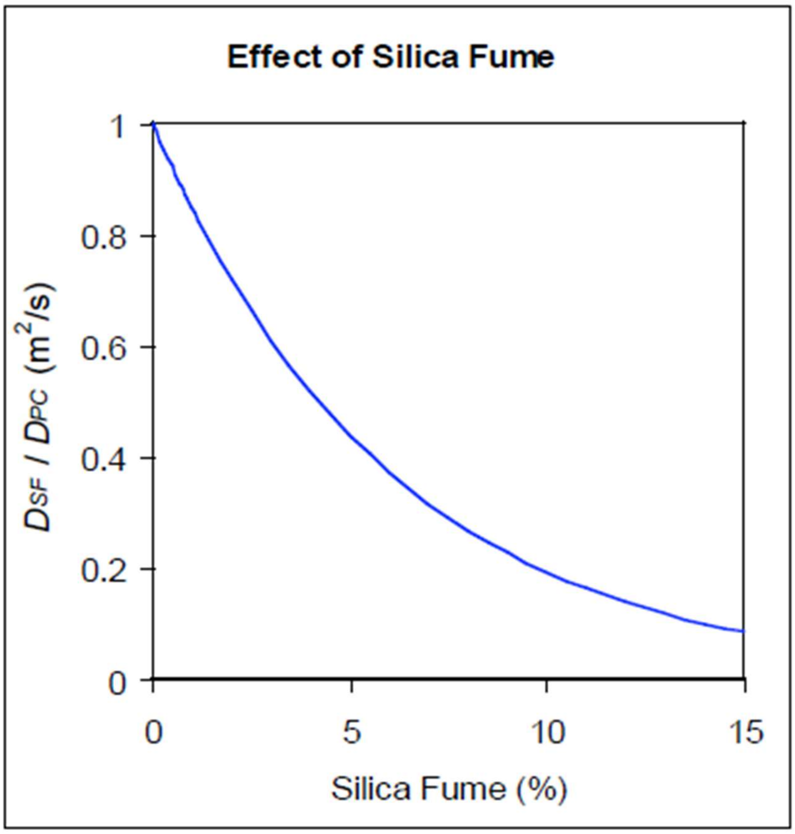

Figure 3-18 Effect of Silica Fume on *Dc* (Bentz, 2014)

The effect of Latex has been determined as:

$$\frac{D_{Lx}}{D_{pc}} = 0.6^{(20 \cdot P/C)} \tag{3.42}$$

Where, $P/_C$ is the polymer-cement ratio.

However, these two factors cannot be put together by simple multiplication. Gao (2002) conducted experimental study on properties of polymer-modified cement mortars with silica fume. And based on his study, effective diffusion coefficient of chloride ion decreases significantly by addition of SF and polymers in cement mortar. However, the equation needs further calibration based on his experimental research.

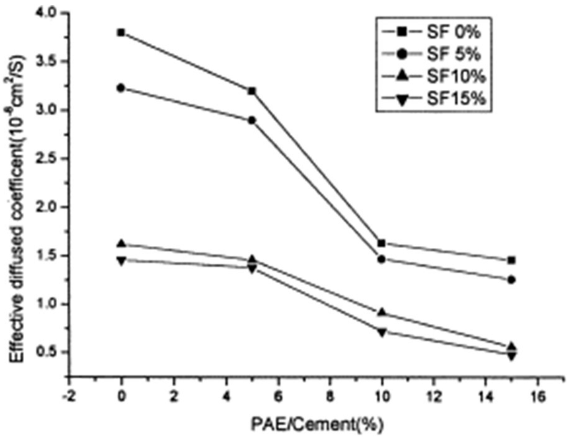

Figure 3-19 Effective Diffusion Coefficient for Concrete with Latex and SF (Gao, 2002)

One additional term is added in order to compensate the difference caused by the interaction between latex and silica fume. The calibrated equation is shown as:

$$D_{28} = 1 \times 10^{(-12.06+\ .4 W/c)} \cdot e^{-0.165 \cdot SF} 0.8^{(20 \cdot P/c)}((1 + \mathrm{SF}/(-0.04\mathrm{SF}^2 + 0.74\mathrm{SF} + 0.9))) \tag{3.43}$$

Different concrete specimens have been made with various proportions of SF, latex polymers and water cement ratios. The comparison of the predicted diffusion coefficient and the data is shown in Table 3-14 and Figure 3-20, 3-21 and 3-22.

Equation 3-39 is valid for SF and Latex up to 15% by weight of the cement.

Table 3-14 Comparison of Predicated Diffusion Coefficient of HPC with Latex and SF

Mix	**w/c**	**SF**	**LMC**	**D_{28}(m^2/s)**	
				Model	**Data**
D (0% SF)	0.35	0	0%	4.73E-12	3.79E-12
	0.35	0	5%	2.83E-12	3.14E-12
	0.35	0	10%	1.70E-12	1.48E-12
	0.35	0	15%	1.02E-12	1.29E-12

Mix	**w/c**	**SF**	**LMC**	**D_{28}(m^2/s)**	
				Model	**Data**
D (5% SF)	0.28	5	0%	3.53E-12	3.17E-12
	0.28	5	5%	2.12E-12	2.83E-12
	0.28	5	10%	1.27E-12	1.3E-12
	0.28	5	15%	7.63E-13	1.06E-12
D (10% SF)	0.26	10	0%	1.96E-12	1.46E-12
	0.26	10	5%	1.17E-12	1.29E-12
	0.26	10	10%	7.04E-13	7.16E-13
	0.26	10	15%	4.22E-13	3.46E-13
D (15% SF)	0.24	15	0%	1.40E-12	1.28E-12
	0.24	15	5%	8.42E-13	1.19E-12
	0.24	15	10%	5.05E-13	4.94E-13
	0.24	15	15%	3.03E-13	2.43E-13

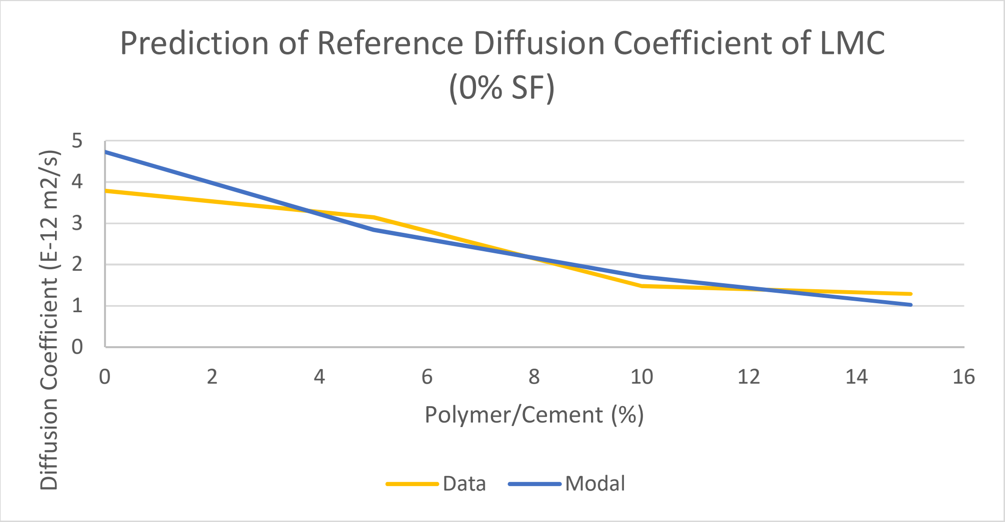

Figure 3-20 Prediction of Reference Diffusion Coefficient of LMC with 0% Silica Fume

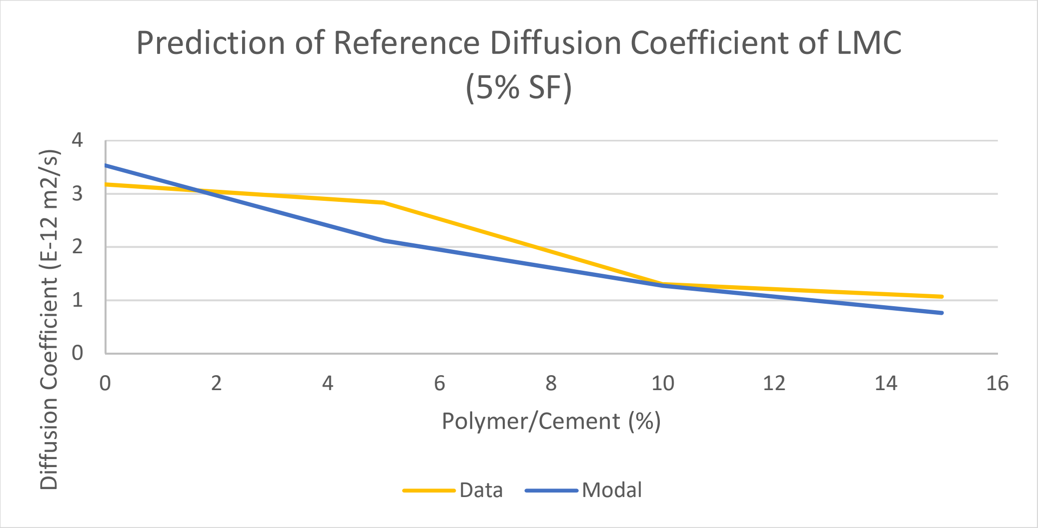

Figure 3-21 Prediction of Reference Diffusion Coefficient of LMC with 5% Silica Fume

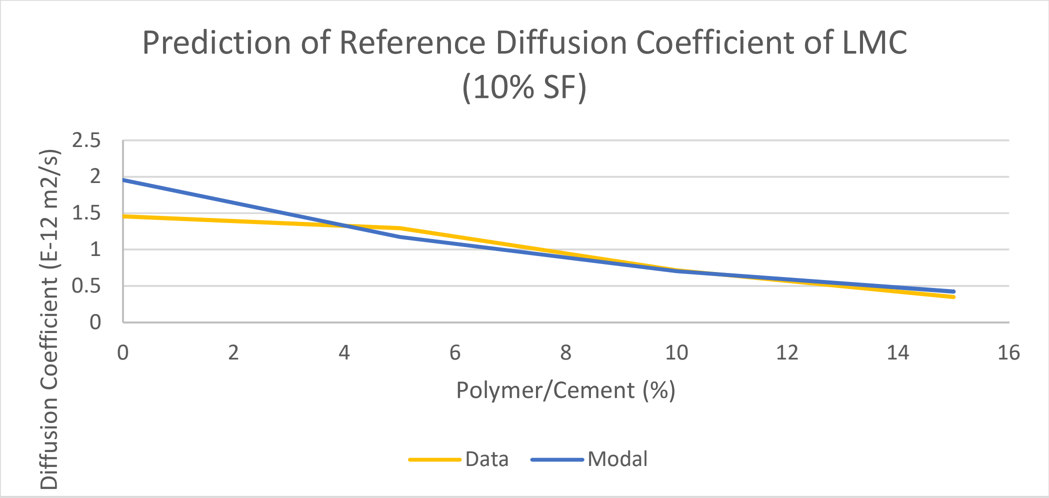

Figure 3-22 Prediction of Reference Diffusion Coefficient of LMC with 10% Silica Fume

3.6. Calibration of the Model

Experimental Data of Folkestone blocks (Thomas, 1999)

In order to investigate the impact of fly ash and slag on the transportation mechanism of chloride ions into marine-exposed concrete, eighteen reinforced concrete blocks (1.0×0.5×0.3 m) were cast in 1987 by Thomas. The blocks were exposed in the splash zone on the sea front at Folkeston, southeast coast of England. Three different concrete mix were used including ordinary Portland cement concrete (OPC), high performance concrete with fly ash (P/PFA) or slag (P/GBS). The blocks were cured for 1 to 3 days before they were exposed to the splash zone. The details of the concrete mixes are listed in Table 3-12.

Table 3-15 Details of concrete mix (Thomas, 1999)

	Mix proportions(kg/m^3)		
Mix designation	PC	P/PFA	P/GBS
Portland cement	288	227	110
Fly ash	—	98	—
Slag	—	—	255
Total cementitious content	288	325	365
Water-to-cementitious	190	170	177
Water-to-cementitious ratio	0.66	0.54	0.48
Stone	1240	1305	1240
Sand	660	585	600
28-day strength (MPA)	39.4	49.6	37.9

For the concrete mix OPC, the reference diffusion coefficient D_{ref} is calculated based on equation, $D_{\text{ref}} = 1 \times 10^{(-12.06+2.4^{w}/c)}$; m=0.488; w/c=0.66; $k_b = 0.8$; k_T is the calculated based on the average monthly temperature; k_E=1.087; k_c =1.8; k_d=1, no damage is assumed. Based on these parameters, the predicted chloride diffusion coefficient for OPC compared with the diffusion coefficient derived from the best fit of the Fick's law solution is compared in Figure 3-23.

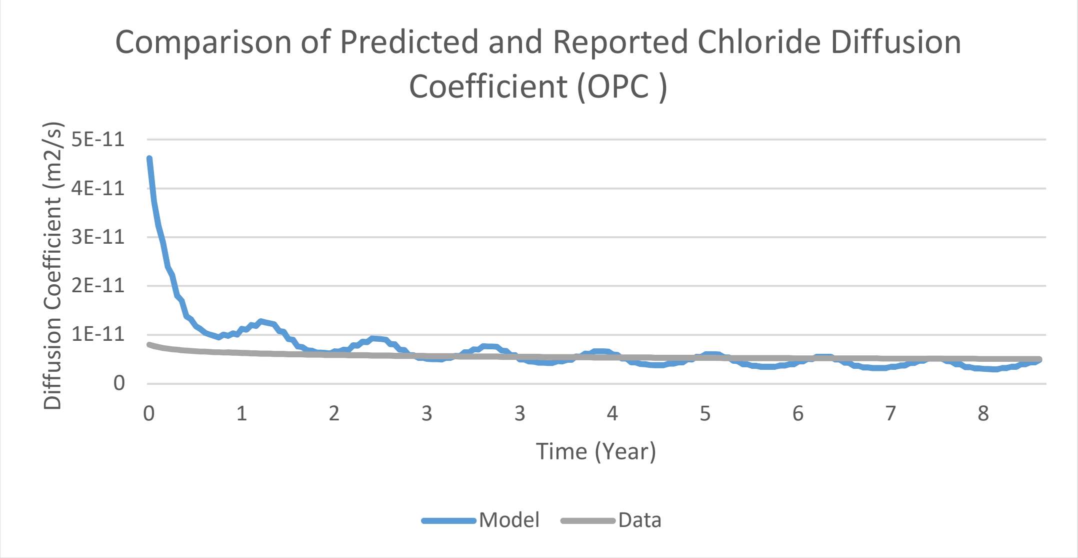

Figure 3-23 Predicted and Reported Chloride Diffusion Coefficient OPC

As shown in the figure, the equation gives reasonable predication of the chloride diffusion coefficient as a function of exposure environment and age. Due to the impact of the temperature change, the predicted chloride diffusion wobbles around the apparent diffusion coefficient which is regressed from the chloride profile of the exposed blocks. The initial diffusion coefficient is relatively high and decreases dramatically due to the early age hydration of the concrete, which complies with the experimental findings.

The same comparison has been made for high performance concrete with fly ash and slag. The aging factor *m* is 0.358 for concrete mix with 54% of fly ash. And it is assigned as 0.6

for concrete mix with 70% slag since 0.6 is the maximum allowable value for aging factor as stated in (life-365, 2014). The concrete mix will also affect the value used for binding factor and environmental factor. In this case, it is assumed that $k_b = 0.65$ and $k_e = 0.375$ respectively. The comparison between the predicted and reported chloride diffusion coefficient for concrete mix with fly ash and slag is presented in Figure 3-24 and 3-25.

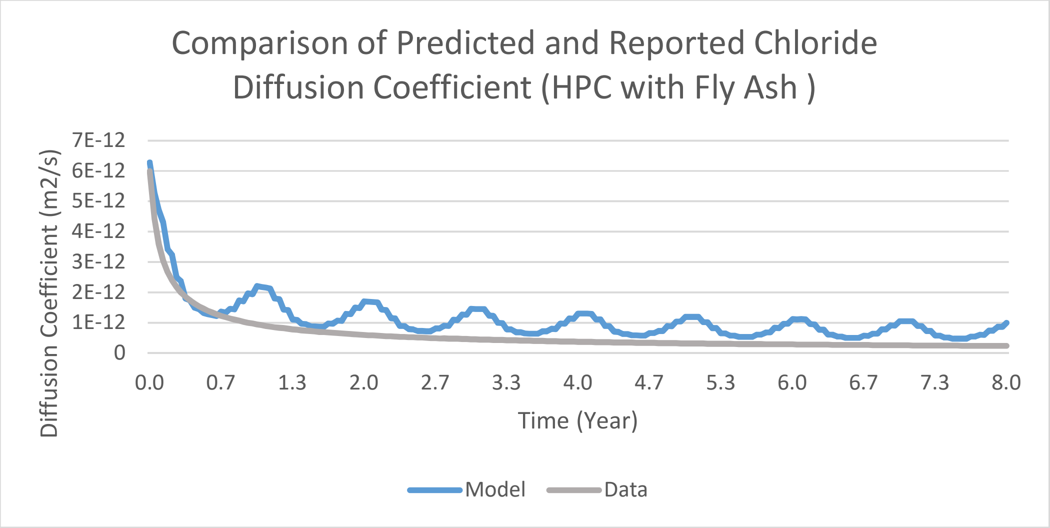

Figure 3-24 Predicted and Reported Chloride Diffusion Coefficient HPC with Fly Ash

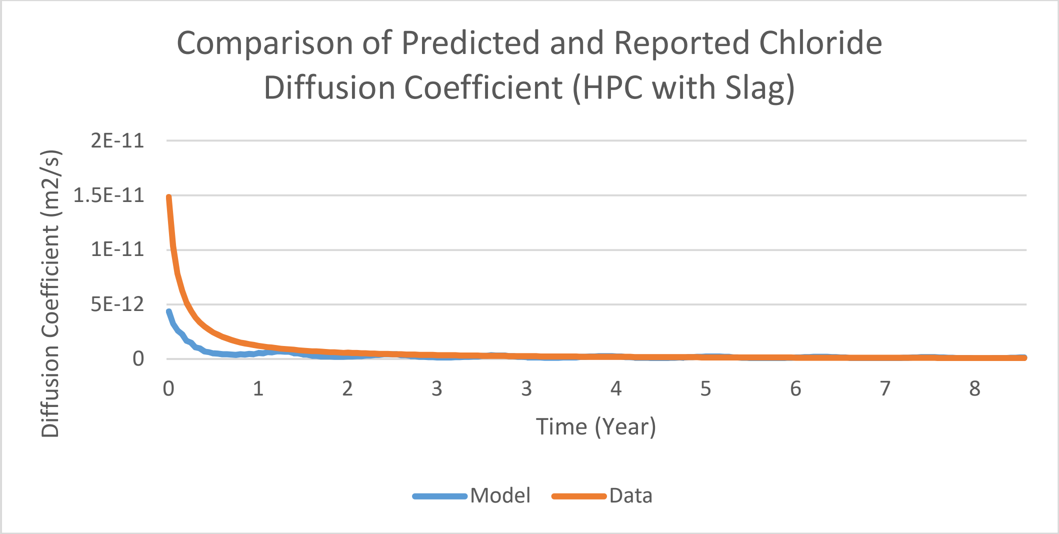

Figure 3-25 Predicted and Reported Chloride Diffusion Coefficient for High Performance Concrete with Slag

3.7. Summary

Chloride induced corrosion is the most common root cause for concrete bridge deterioration. Once the chloride content reaches a certain threshold value, the passive layer formed on the surface of reinforcement rebar will dissolve and corrosion initiates. Due to the manner of chloride transportation mechanism, diffusion is used to model the long-term chloride ingression in our research.

The chloride profile, surface concentration and chloride diffusion coefficient should be tested and monitored for all the concrete bridge elements. It is also important to test and record the concrete properties for newly constructed elements in order to get a reference value for chloride diffusion coefficient and the damage index. The dynamic elastic modulus of concrete should also be tested.

The typical values of diffusion coefficient for normal concrete were reported between 10^{-12} m^2/s and 10^{-11} m^2/s. If silica fume, fly ash or other alternative cementitious materials are used, the diffusion coefficient may reduce to 10^{-13} m^2/s.

The chloride threshold valued could be estimated by the equation proposed by Fagerlund. For simplification purpose, a value of 0.05% of the weight of the concrete (1.97 lb./cu.yd.) can be used for ordinary Portland cement with black steel.

If sufficient data is not available, the diffusion variables should be estimated based on the proposed numerical equations.

4. FINITE ELEMENT ANALYSIS

4.1. Introduction

In severe exposure conditions, service life of the concrete bridge component mainly depends on the chloride-induced corrosion. In order get a more refined prediction for the remaining service life, a variety of numerical models are available. In order to do so, the chloride profile should be predicted, which is the chloride concentration at certain depth at a given time. ABAQUS is selected to perform the finite element analysis. In the analysis, diffusion variables can be estimated using proposed numerical models. Temperature and exposure condition will also be specified to be part of the external load conditions. Combined with all the inputs, the finite element model can be constructed. It will be able to determine the chloride profile for the concrete specimen for any given time. Compared with the average concrete cover thickness and the chloride threshold value for corrosion initiation, the time for corrosion initiation will be identified for the finite element model for the concrete bridge component under a certain exposure condition and a condition state.

The results of the FEA are compared with the experimental data in literature for both the chloride concentration and the corrosion initiation time. The achieved chloride profiles from FEA are also compared with experimental/ field data in order to validate the model.

Slab is selected to be the bridge element modeled by ABAQUS since the slab is under the most severe exposure condition among all the bridge components. The presences of deicing salt, the effect of the traffic load, and the possible pond water due to precipitation will have a negative effect on the service life of the components. The surface of the slab may also experience scaling and cracks caused by other deterioration mechanisms. The average thickness of the concrete for slabs is also smaller than those for other components. Therefore, a typical concrete bridge deck element is used in the FEA.

4.2. Element Type

Due to the similarity of the partial differential equation, the FEA of chloride diffusion could be achieved by using the heat transfer modular in ABAQUS. DC2D8, an 8-node biquadratic element, are selected since they are capable of conducting mass diffusion analysis.

4.3. Material Properties and Real Constants

The Soret effect is set equal to 1 and the solubility is defined by the Fick's Law. The element type is assumed to be isotropic so the diffusion coefficient is a constant in any direction. The concrete diffusion coefficient is estimated by the refined equation. And the temperature, surface chloride concentration and other input parameters are estimated based on the exposure.

However, ABAQUS does not recognize time as a variable for diffusivity. The time was set as a field variable, and the diffusion coefficient is then tabulated as dependents of this field variable. As the field variable was constantly updated to correspond to the current time increment, and the diffusivity was also changed according to the current field variable value. In this way, the time dependent diffusivity could be implemented throughout the analysis.

4.4. Boundary Conditions and Loading

Chloride surface concentration is set as a time-dependent variable based on the exposure conditions, while the diffusion coefficient for the chloride ions is mapped to diffusivity, with the solubility set to a value of 1. The diffusion coefficient is tabulated as dependents of the field variable defined as time. The steel bars in the concrete are set as the reflective boundary since the chloride ions tend to accumulate when they reach the surface of the reinforcing steel.

4.5. Validation of the FEA Model

4.5.1 **Chloride Profile: Experimental Data of Folkestone blocks (Thomas, 1999)**

Based on the chloride diffusion coefficient predicted from the model, the chloride profile after certain years of exposure could be derived from FEA analysis. The chloride profile shows the chloride concentration at different depth below the concrete cover, which is the most direct value to assess the potential of ongoing corrosion. In this study, Abaqus is used as the Finite Element Analysis software.

The finite element model is a block of a typical concrete bridge deck, shown in Figure 4-1. A sketch of the element has been developed according to the experiment set up as shown in Figure 4-1. A 8 in by 8 in (as in 20.32 cm*20.32 cm) block is modeled. Two No. 6 rebar are placed into the concrete in order to better simulate the chloride profile for real structure. 1 in (2.54 cm) cover is provided for the bottom reinforcement. An additional 1.5 in (3.81 cm) cover is used for top reinforcement. Since only the top surface is exposed to the environment, the chloride transportation are assumed to start from the top side of the deck. Transient analysis is performed in order to find out the chloride concentration in the model based on the boundary condition and initial condition.

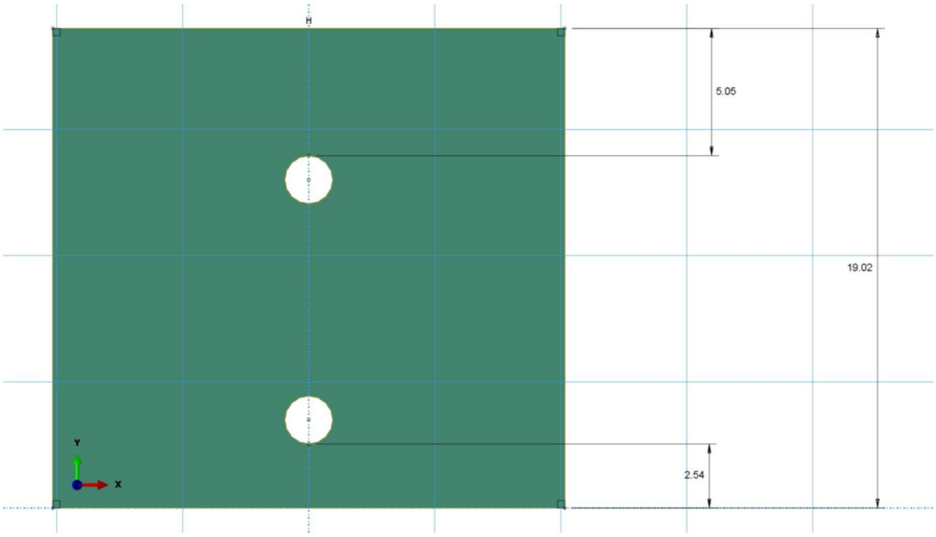

Figure 4-1 Sketch of the Bridge Deck Section

The properties of concrete and chloride diffusion coefficient is obtained from the proposed equation. The surface concentrations of the chloride ions are given as 3.5% and 5% by weight of the concrete in the literature for OPC and HPC, respectively.

In order to simplify the model, several assumptions are made. The temperature used in the model is the monthly average in Folkestone, England. The temperature factor is updated monthly. The first period is taken from July's data since the experiment starts at fall, which may give a more conservative prediction. Also July's data is assumed as the beginning of one year to avoid construction during the winter season. Given the average temperature, the temperature factors are calculated accordingly.

The comparison between the simulated and reported chloride profile for OPC, HPC with FA and HPC with slag after 8 years of exposure is shown in Figure 4-2,3,4.

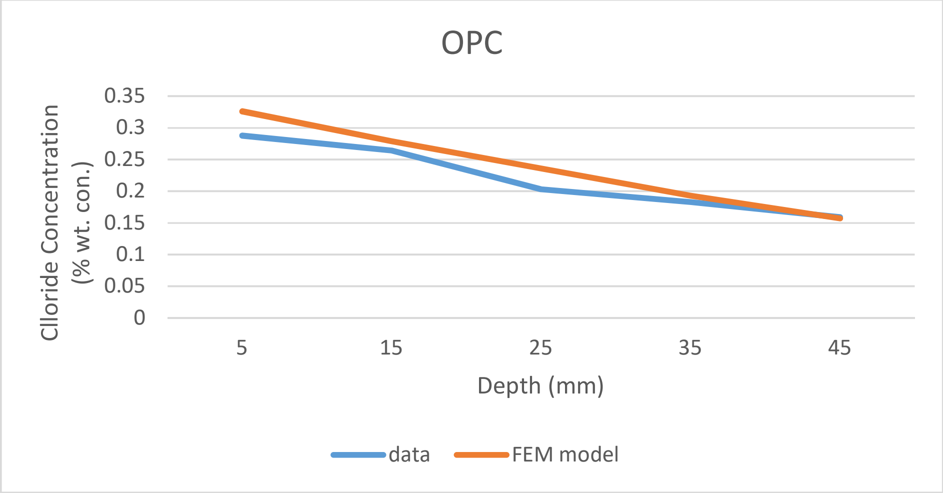

Figure 4-2 Comparison of the Simulated and measured chloride Profile for OPC

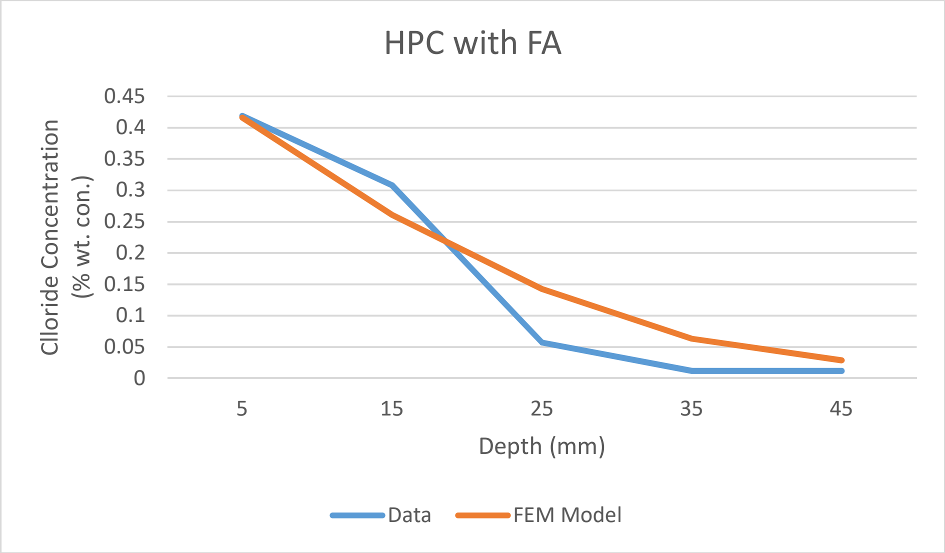

Figure 4-3 Comparison of the Simulated and measured chloride Profile for HPC with FA

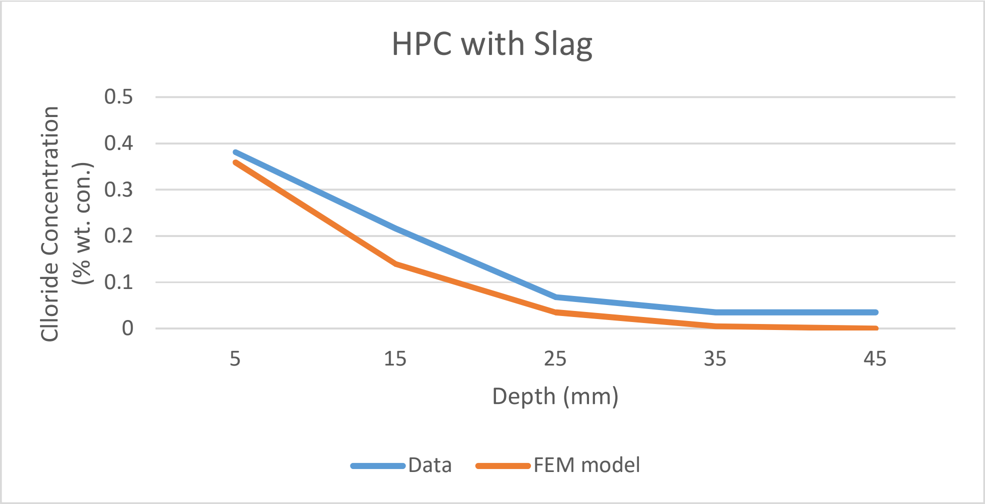

Figure 4-4 Comparison of the Simulated and measured chloride Profile for HPC with Slag

Based on the figure, it can be seen that the proposed model gives a good prediction of the chloride concentration for concrete blocks after 8 years of exposure. The proposed model gives a conservative prediction for both OPC and HPC since the predicted chloride concentration is higher than the reported one. The predicted chloride concentration is small than the data in the literature for HPC with slag. The error may come from the variation of the concrete quality, change in the exposure condition and temperature fluctuation.

Also, the aging factor reported in the paper is 1.2 which is considerable greater than normal. It means that the concrete specimen may experience some early age cracking or deficiency which leads to a high diffusivity at early age of exposure. Therefore, nondestructive tests are recommended to determine the reference diffusion coefficient and other decisive factors used in the prediction equation.

4.5.2 **Chloride Profile: Sea Wall (Thomas, 1999)**

Thomas (1999) also presented data from a field investigation of a 30-year-old concrete sea wall in South Wales. The wall is situated a few meters above the high tidal level and having a slightly milder exposure condition than the Folkesttone blocks. The concrete has a water cement ratio approximately 0.5 to 0.6 where no exact data is available. w/c=0.5 is selected in order to estimate the reference diffusion coefficient. 25% of fly ash is also used in the concrete mix. The temperature profile for South Wales is inputted. Other parameters are determined from the proposed equation.

The result is shown in Figure 4-5.

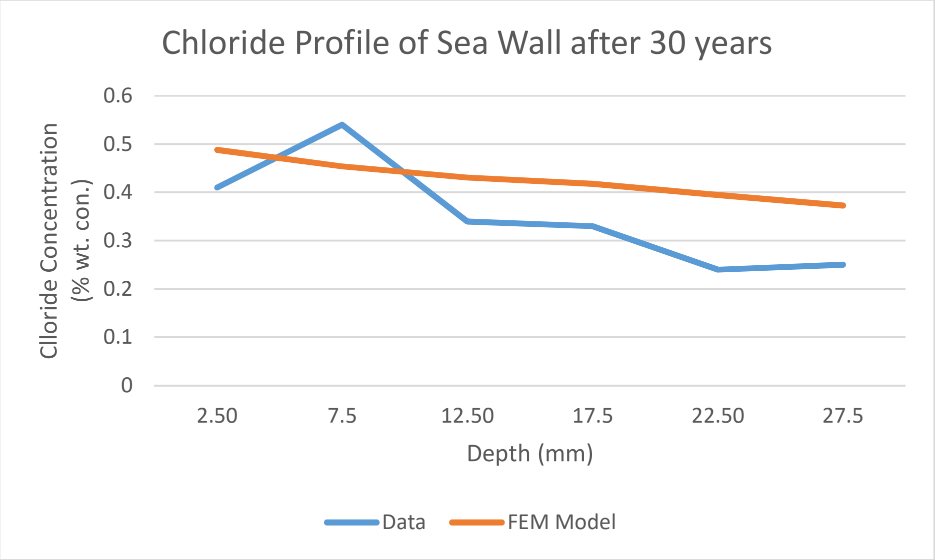

Figure 4-5 Chloride Profile of Sea Wall after 30 years of Exposure

4.6. Effectiveness of Surface Sealers

4.6.1 Modeling Verification with Life 365

In order to quantify the impact of surface sealer application on the chloride ingression process, the finite element models are developed. One typical model of a concrete bridge deck has been constructed. The concrete block is 8 in *8 in (20.32 cm* 20.32 cm), where 2 No.6 bars are placed. Concrete cover is 1 in (2.54 cm) for the bottom rebar and an additional 1.5 in (3.81 cm) concrete cover is provided for the top reinforcement to represent the wearing surface. The sketch of the model is shown in Figure 4-6. The concrete mix is designed with a water cement ratio of 0.49 and a base diffusion coefficient is assumed as 1.3×10E-11 m^2/s.

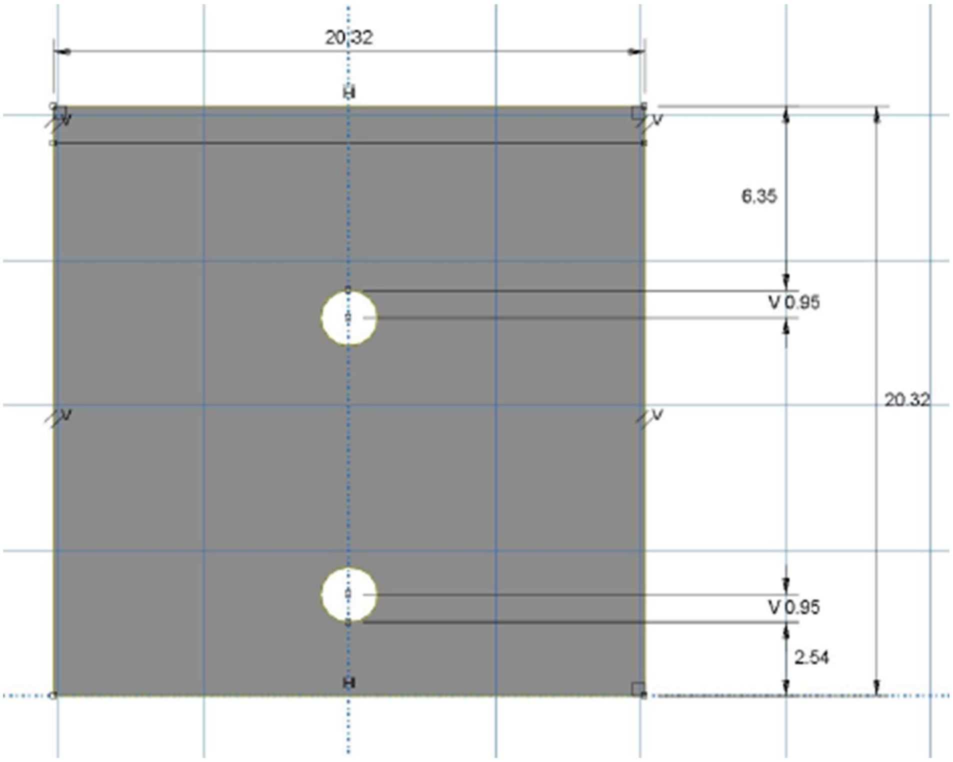

Figure 4-6 Model Sketch

The sealers are applied to the concrete at the beginning of its service life and reapplied every 5 years since the surface coating lifetime is assumed to be 5 years. The initial efficiency of the sealer is assumed as 90% as dictated in the life 365. The concrete bridge is assumed as a rural highway bridge in Syracuse, NY. The surface chloride concentration build-up equation is described as:

$$Cs = \begin{cases} 0.1167t & (0 < t < 6) \\ 0.7 & (t \geq 6) \end{cases} \tag{4.1}$$

In which, Cs is the surface chloride concentration measured in percentage of the weight of the concrete; t is time in years.

The surface concentration with the use of sealer is shown in the Figure4-7. In the Finite element software, the surface concentration can be assigned as a time dependent boundary condition. Therefore, these values are used to tabulate the time dependent surface concentration in ABAQUS.

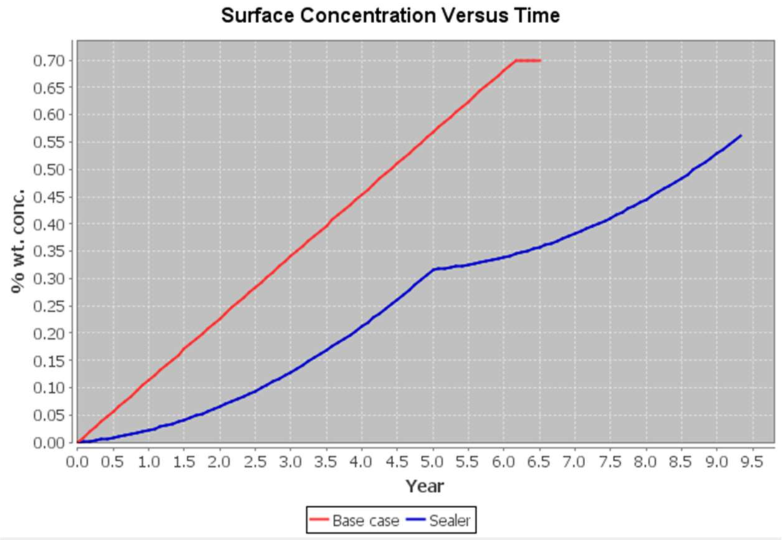

Figure 4-7 Surface Concentration with time

The result of life-365 is provided in Figure 4-8. Since the maximum allowable chloride concentration is 0.05 by weight of the concrete, the corrosion initiation is assumed to start when the threshold value is reached at depth of 6.4 cm which is the top clear cover of concrete. It can be seen that the base case, where no preventive maintenance methods are applied onto the concrete, shows that corrosion initiates at the end of 6.5 years. On the other hand, the blue line, which represents the use of surface sealers, shows a longer period of time passes before active corrosion. In this particular simulation, the application of sealer elongated the service life of the bridge deck by approximately 3 years.

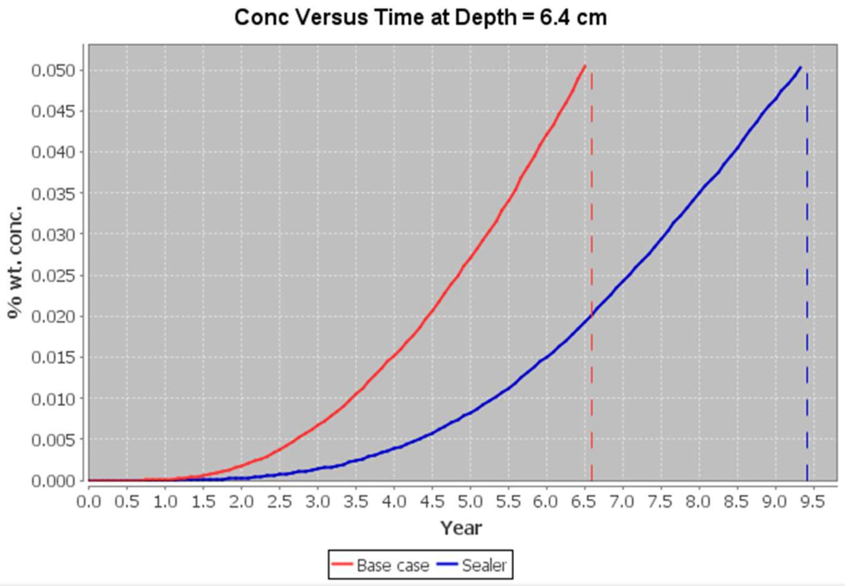

Figure 4-8 Chloride Concentration at Depth=6.4 cm

The result of FEA is provided in Figure 4-9.

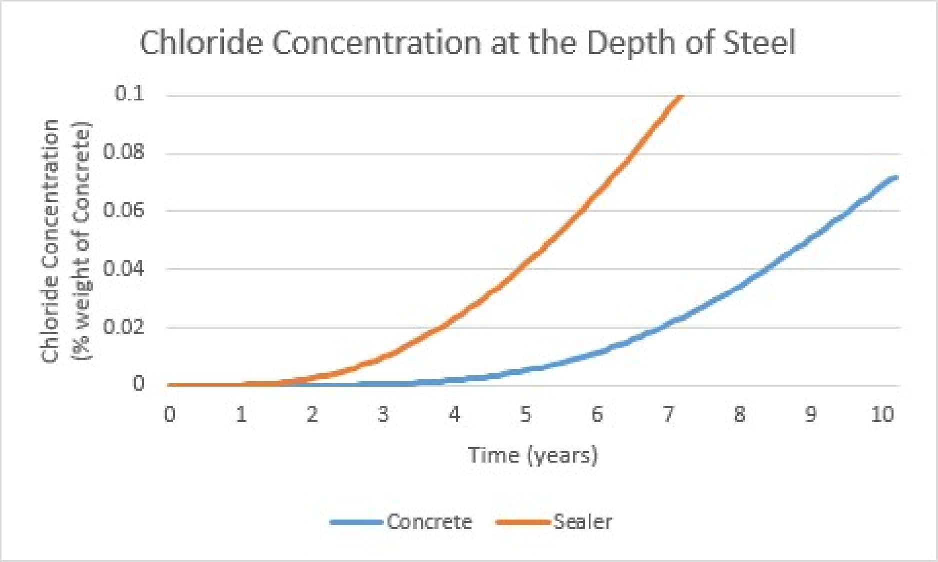

Figure 4-9 Chloride Concentration at the depth of Steel

From the figure, it can be seen that the result agrees with the prediction from Life-365. The chloride concentration reaches the threshold value at the depth of steel after nearly 6 years of exposure for bare concrete. And for the sealer application, the corrosion initiation time is assumed to be 9 years after exposure.

The results show that the effectiveness of the sealer can be modeled by quantifying its impact on the surface chloride concentration with time. The initial effectiveness and the surface coating lifetime should be examined in order to get a good estimation of the service life of the concrete treated with coatings. And the finite element model using the parameters derived from the proposed model gives reliable estimation compared with other commercial software.

4.6.2 **Modeling Verification with Experimental Results**

In order to further investigate the effectiveness of different types of sealers, experimental data by Moradllo (2012) are used to compare with the results of the finite element models.

Based on the experiment done by Moradllo, a concrete mix with water cement ratio of 0.5 is used. Different types of surface coating are used, including aliphatic acrylic and epoxy polyurethane. The concrete specimens are cast into 150mm×150mm×600mm blocks in steel molds and then compacted using a vibrating table. The specimens are removed from the molds after 24 hours after casting and then cured in water saturated with calcium hydroxide at 21℃ for 28 days. After the curing period, the specimens are moved to Bandar-Abbas cost and subjected to tidal zone exposure condition in Persian Gulf for 5 years. The average monthly temperature of Bandar Abbas is shown in Figure 4-10.

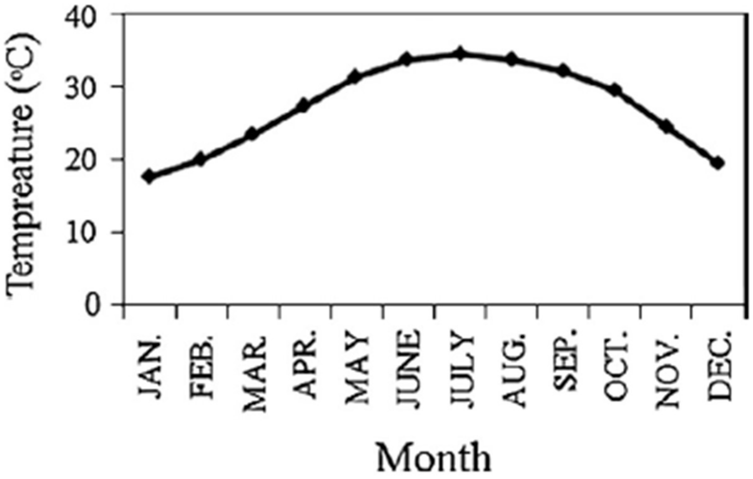

Figure 4-10 Average Monthly Temperature of Bandar Abbas

During the simulation, the base diffusion coefficient is calculated with the proposed model as 1.38×10E-11 m^2/s. And the aging factor is 0.4. The chloride binding factor is assumed as 0.8 and the environmental factor is set as 1.087 since the specimens are placed in tidal zone. The assumed chloride diffusion coefficient is shown in Figure 4-11.

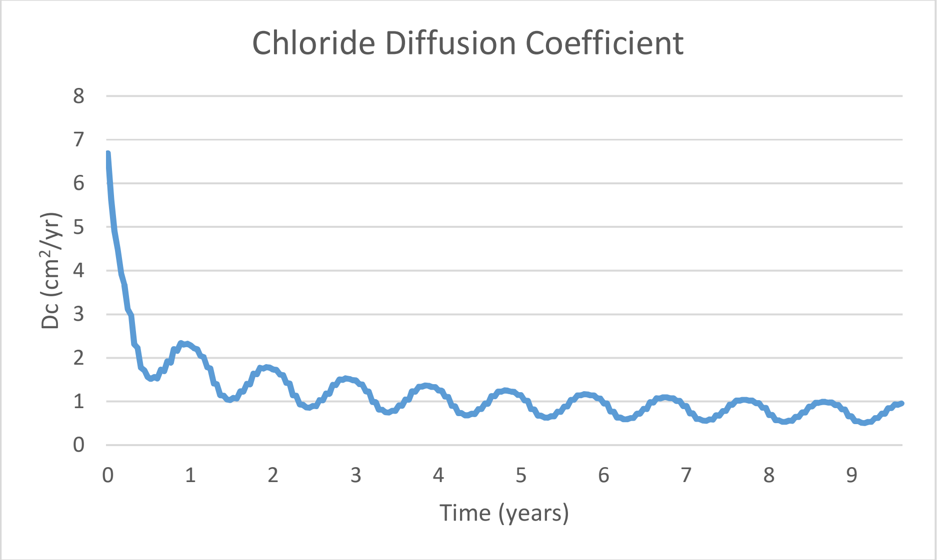

Figure 4-11 Estimated Diffusion Coefficient

The concrete model has been revised according to the experiment. A 15cm×15cm block is modeled as shown in Figure 4-12. The chloride diffusion coefficient is uniformly assigned to the concrete block. Only the top surface is subjected to the external chloride and all the other three edges are assigned as reflecting boundaries.

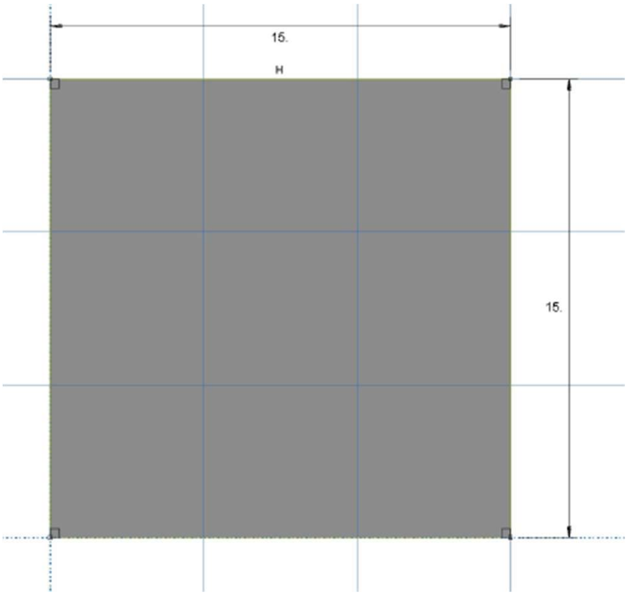

Figure 4-12 Model Sketch

The Surface concentration is extracted from the report, as shown in Figure 4-13.

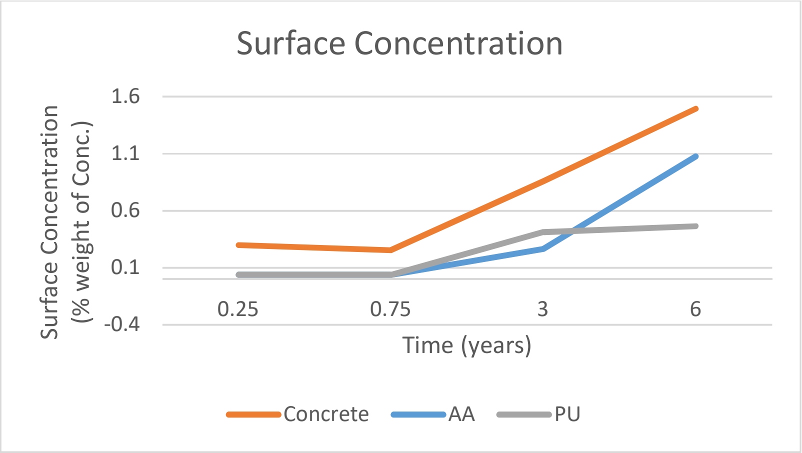

Figure 4-13 Surface Concentration

It can be seen that the use of surface treatment dramatically affects the chloride build up rate on the surface of the concrete. The effectiveness of the sealers can be shown in two parameters, the initial effectiveness and the durability of the sealer. Based on Moradllo's (2012) research, most of the sealers are effective in early ages. However, epoxy polyurethane (PU) and aliphatic acrylic (AA) are the most efficient coating which resist appropriately against harsh environment of tidal zone and improve service life of concrete most aptly.

The simulated chloride concentration after 60 month of exposure is shown in Figure 4-13.

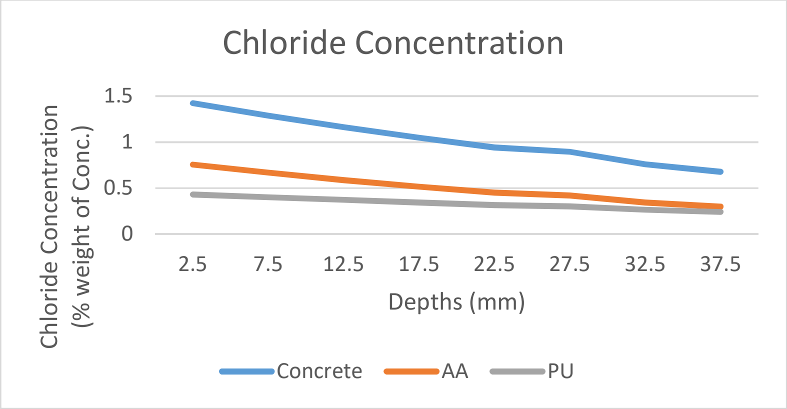

Figure 4-14 Chloride Concentration after 5 years of Exposure

In comparison, the chloride profiles of the concrete specimens with coatings of aliphatic acrylic and epoxy polyurethane from the experimental data and the finite element models are shown in Figure 4-15 and Figure 4-16.

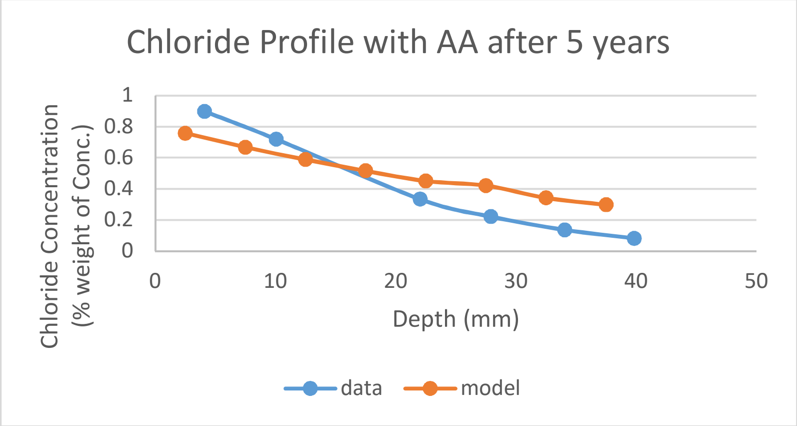

Figure 4-15 Chloride Profile after 5 years of exposure with AA

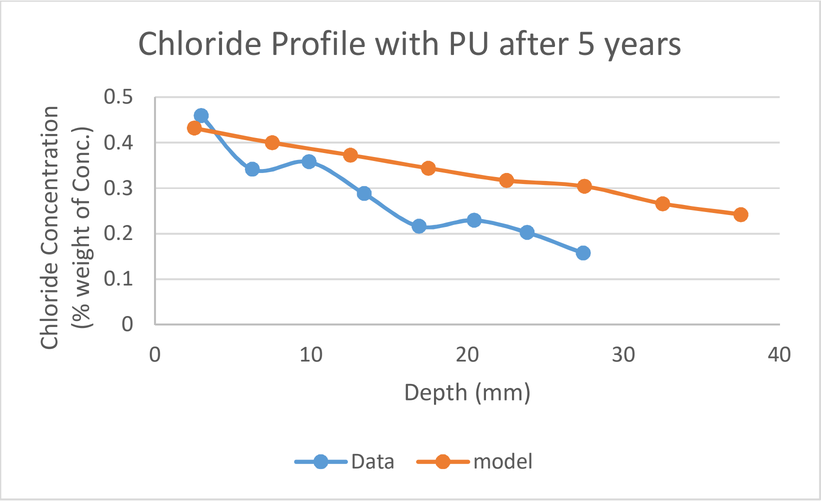

Figure 4-16 Chloride Profile after 5 years of exposure with PU

It can be seen that the results from the finite element models are close to the experimental data and the predicted chloride concentration is conservative. The reason of the difference may come from the impact of the sealer on the diffusion coefficient for the top layer of the concrete. However, based on research done by Morse (2009), Oman (2014) and Rahim (2006), the sealers impact on the diffusion coefficient is decreasing in the first several months of exposure and will diminish in further exposure times. As the sealer deteriorates, the chloride penetration may accelerate. Therefore, the impact of the coatings on the diffusion coefficient is not considered in this research. Another explanation of the error is that the surface chloride is measured for the top layer of the concrete, which may result a higher concentration assigned to the extreme surface of the concrete in the finite element model instead of several millimeters beneath the surface.

4.7. Effectiveness of Overlay

The Virginia pilot bridge is located at the junction of US Route 15 and Interstate 66, south of Gainesville. The bridge was built in 1979. The bridge is a two-span continuous structure, with a cast-in-place composite concrete deck of 8.5 inch. The deck was built with a maximum water cement ratio of 0.45 and a minimum 2 in. cover depth was required. During the modeling process, the water cement ratio is set as 0.45 and the average monthly temperature is used to calculatek_T; $k_b = 0.8$; k_E=1.087 since the exposure condition for road bridges with the use of de-icing salt in the winter season can be treated as marine exposure in the splash zone (Duracrete, 2010). Although the amount of chloride available and the surface chloride build up rate may be different, the diffusion coefficient will not show significant difference since the chloride diffusion coefficient mainly depends on the concrete property; k_c =1, assuming 28 days of wet curing; the damage factor is tabulated from experimental data.

Since no data is available for the change of dynamic modulus of elasticity or compressive strength, the damage factor is assumed to be dictated by the freeze-thaw effect. Based on the NRMCA (2004) reports, an average region in the middle part of eastern US experience 15 or more freeze-thaw cycles annually. Lee (2005) has reported the relation between the freeze-thaw cycles and the change in dynamic modulus elasticity. Based on these research, the time-dependent damage factor for a typical bridge in Virginia can be modeled by the following equation:

$$k_d = 1 + 0.1346t - 0.000313t^2 - 2.817t^3 \times 10^{-6} \tag{4.1}$$

The surface concentration is assumed to increase linearly until it reaches its maximum value after 10 years of exposure as suggested by Life-365 (2014).

First of all, the max surface chloride concentration is calibrated based on the chloride concentration in the bridge deck after 29 years of service. The maximum surface chloride concentration is assumed to be 6 lb./ yd^3 based on the chloride profiles from the Virginia Report VTRC 09-R13. The accumulation rate, however, is still 10 years as indicated by life 365. For the chloride concentration, the FEM model shows a reasonable curve that cross the average of the sets of data points. In general, the FEM gives a conservative prediction since it does not consider the variation in the surface concentration from different data point.

The difference between the FEM and the data can be explained by routine maintenance and difference in the exposure.

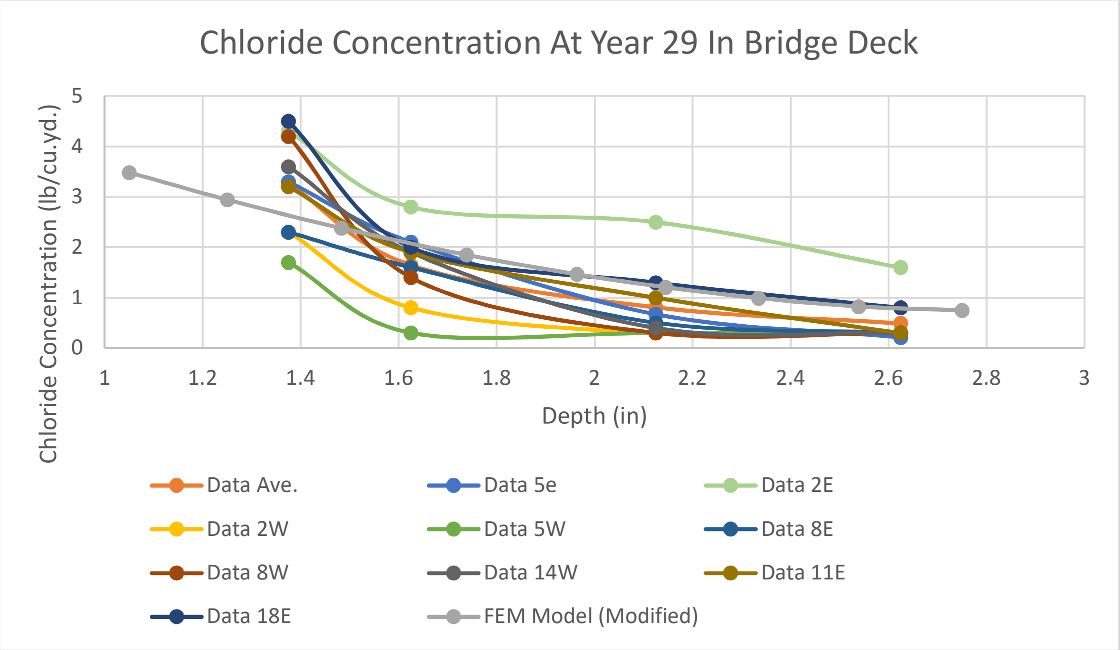

Figure 4-17 Chloride Concentration at Year 29 In Bridge Deck

Different overlay systems are used based on the report, in which, Overlay System A, B, C, D and E are selected to calibrate the finite element model.

With different concrete mix design, the reference diffusion coefficients (D_0) and the decaying factor (m) for different overlay systems varies. The reference diffusion coefficient calculated based on the concrete mix is displayed in the Table 4-1.

Table 4-1 Concrete Mix and estimated Reference Diffusion Coefficient

Mix	**w/c**	**FA**	**SF**	**Slag**	**LMC**	**D_0(m2/s)**	**m**	**D_0(cm2/year)**
OPC	0.5	0%	0%	0%	0%	1.38E-11	0.4	4.35
A	0.4	0%	7%	0%	0%	2.50E-12	0.32	0.79
B	0.4	0%	5%	35%	0%	3.48E-12	0.495	1.1
C	0.4	15%	5%	0%	0%	3.48E-12	0.425	1.1
E	0.25	15%	13%	0%	0%	1.75E-12	0.305	0.55

The chloride concentrations from the filed data used to calibrate the chloride concentration in the overlay are summarized in Table 4-2.

Table 4-2 Field Data from Virginia Pilot Bridge

Data									
Depth (in.)	Chloride Concentration (lb./cu.yd.)								
	A (7%SF)		B (5% SF 35%Slag)		C (5% SF 15% FA)		D (15% LMC)	E (13% SF 15%FA)	
	2E	2W	5E	5W	8E	8W	14 W	11E	18E
0-0.125	3.44	5.899	2.182	5.112	3.887	7.594	3.568	3.131	2.323
0.125-0.25	3.195	5.723	1.07	4.062	2.52	7.232	2.001	2.964	2.951
0.25-0.375	2.321	4.928	0.749	2.116	1.421	4.209	0.865	2.962	3.037
0.375-0.5	1.453	3.501	0.747	1.069	1.018	1.919	0.507	2.303	2.538
0.5-0.625	1.028	2.896	0.904	0.711	0.949	1.472	0.385	1.929	1.898
0.625-0.75	0.72	2.395		0.582	1.156	1.145	0.238	1.76	1.768
0.75-0.875		1.931		0.48		1.082	0.247	1.655	
0.875-1		1.849		0.516		0.925	0.359		
1-1.125		1.824		0.905		0.751	0.819		

All the chloride profiles are measured or simulated after 10 years of the overlay work. The chloride profiles for each different scenario are presented in the following figures.

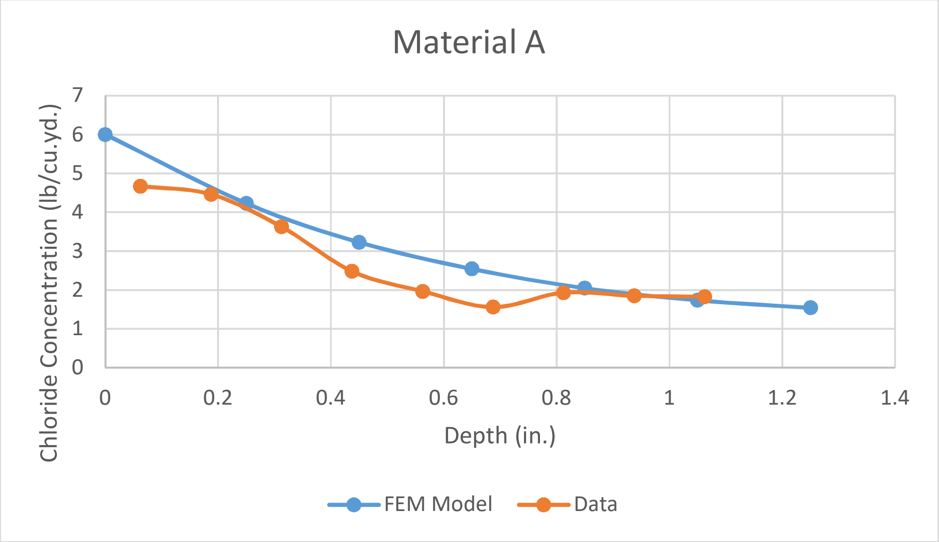

Figure 4-18 Chloride Profile of OPC with w/c=0.5 after 10 years of Treatment

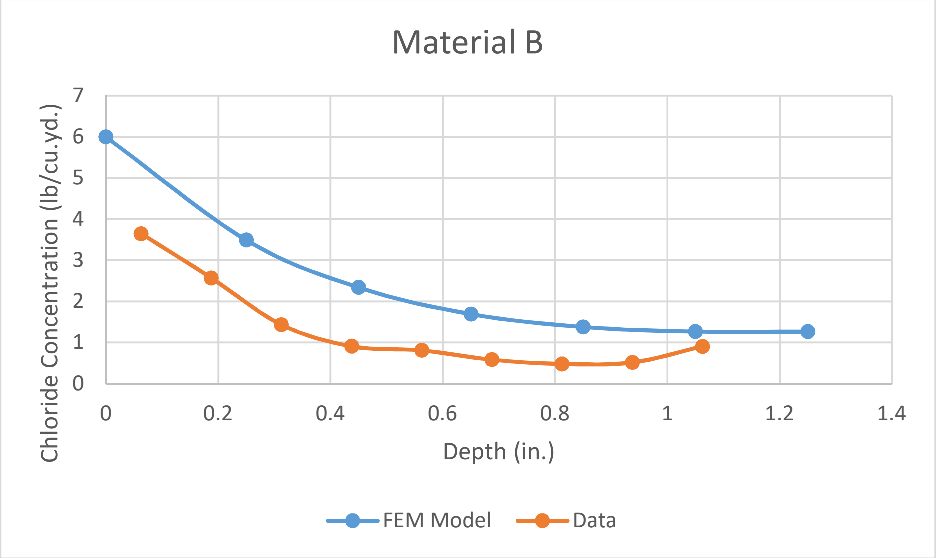

Figure 4-19 Chloride Profile of HPC with w/c=0.4 and 7% Silica Fume after 10 years of Treatment

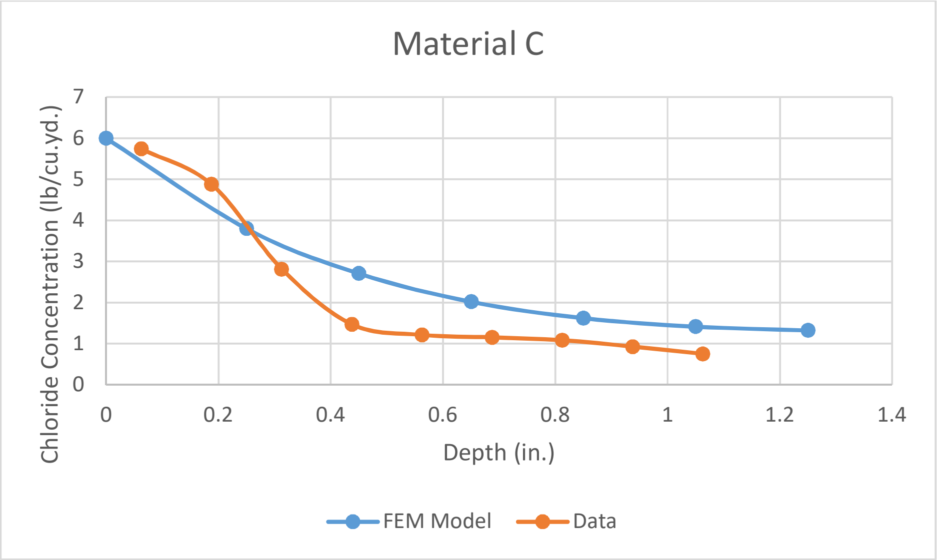

Figure 4-20 Chloride Profile of HPC with w/c=0.4 and 5% Silica Fume and 35% Slag after 10 years of Treatment

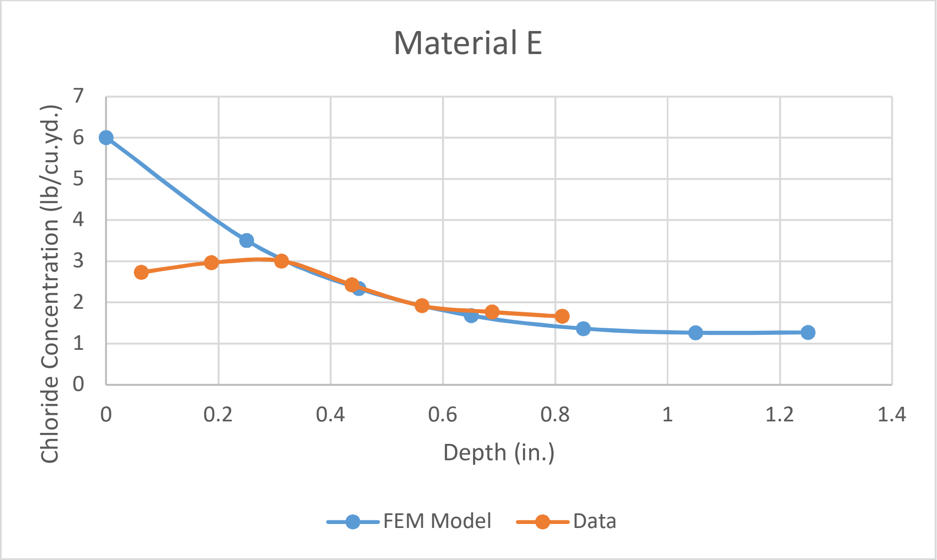

Figure 4-21 Chloride Profile of HPC with w/c=0.25 and 15% Fly Ash and 13% Silica Fume after 10 years of Treatment

4.8. Effectiveness of Latex Modified Concrete Overlay

The latex modified concrete overlay is used on the Virginia Pilot bridge and it was the overlay Type D. Latex has a great impact on reducing the permeability of the newly constructed overlay. As the other bridge deck models, the original bridge deck is 8 in thick. The clear cover for the bottom rebar is 1 in. The concrete cover for the top reinforcement is 2.5 in., including a 1 in wearing surface. After 29 years of service, the bridge deck is rehabilitated by cutting out the 1 in wearing surface and then overlaying with 1.25” thick latex modified concrete. The latex modified concrete has a water cement ratio of 0.4 and the latex-cement ratio is 15% by weight. The chloride concentration is measured after 10 years follows the rehabilitation. Based on the result, it can be seen that the model gives an accurate prediction for the chloride profile in the latex modified concrete overlay.

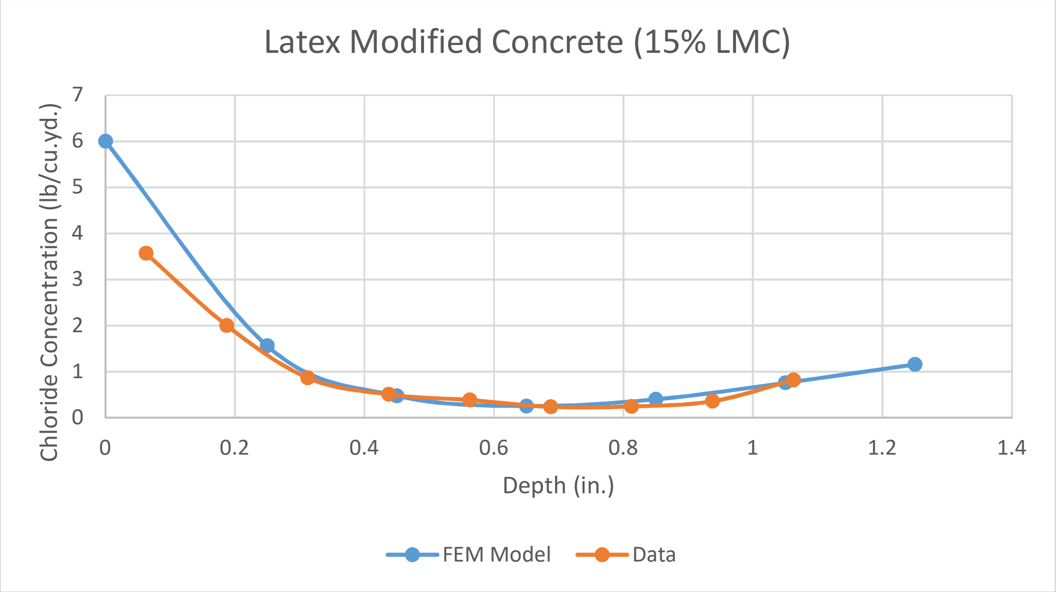

Figure 4-22 Chloride Profile of 15% Latex Modified Concrete after 10 years of Treatment

4.9. Effectiveness of Wearing of the Top of Concrete Deck

In order to investigate the impact of wearing on the diffusion process on bridge deck elements, a modified FEM is constructed. The same geometric parameters are used from the example where the latex modified concrete is analyzed. The bridge deck is originally 8 in high.

After 29 years of service, the top 1 in cover is removed and replaced with a 1.25 in LMC overlay.

The major difference of this model compared with the previous one is that the effects of wearing is considered. The impact is simplified by moving the boundary condition every 5 years to represent the abrasion of the top surface of the bridge deck. Based on the DOT report, the average wearing rate for a typical bridge deck is 0.5” per 20 years. Therefore, the boundary condition is moved every 5 years based on this rate of wearing.

The boundary conditions and the rehabilitation measures are shown in the following figure.

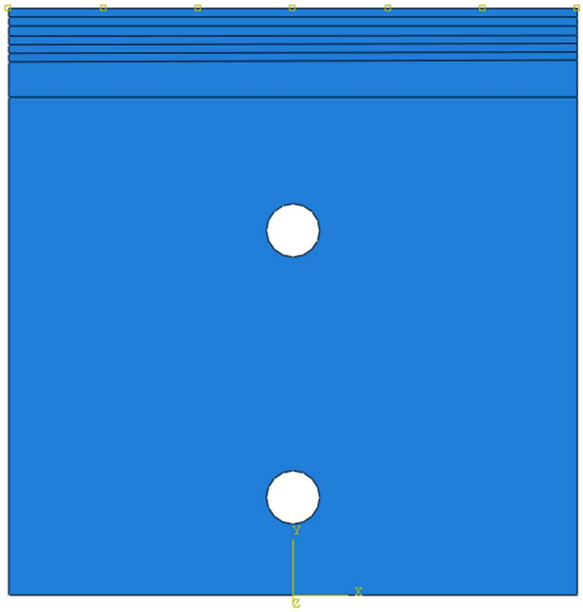

Figure 4-23 Moving Boundary Conditions to represent Erosion

The result for the FEM at the end of 29 years of service is shown in the following figure.

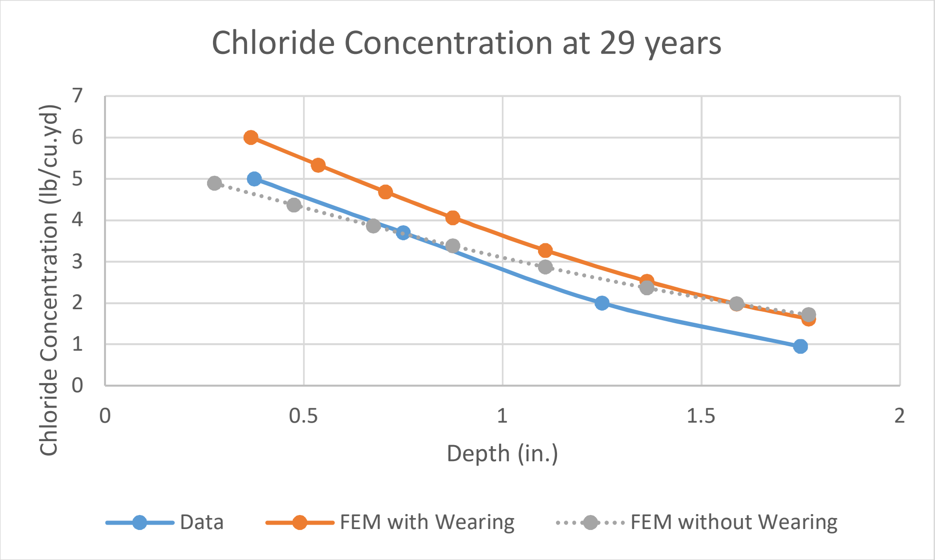

Figure 4-24 Comparison of Chloride Profile of FEM with or without Considering Wearing

It can be seen that the FEM considering wearing has a good correlation with the data. Since the surface concentration used as an input was actually the average over a long span of the bridge, a new max surface concentration representing the local exposure condition, 5 lb. /cu. yd. is assumed based on the trajectory of its own data. The FEM result considering wearing is closer to the reported data. It gives an accurate estimation concentration near the surface of the concrete and does not overestimate the chloride concentration compared to the field data.

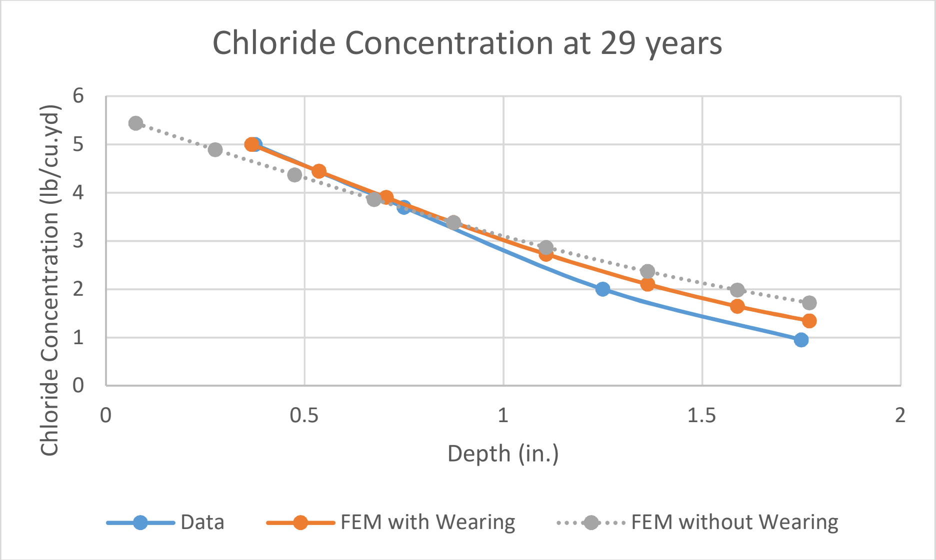

Figure 4-25 Chloride Profile of the original bridge deck at 29 years

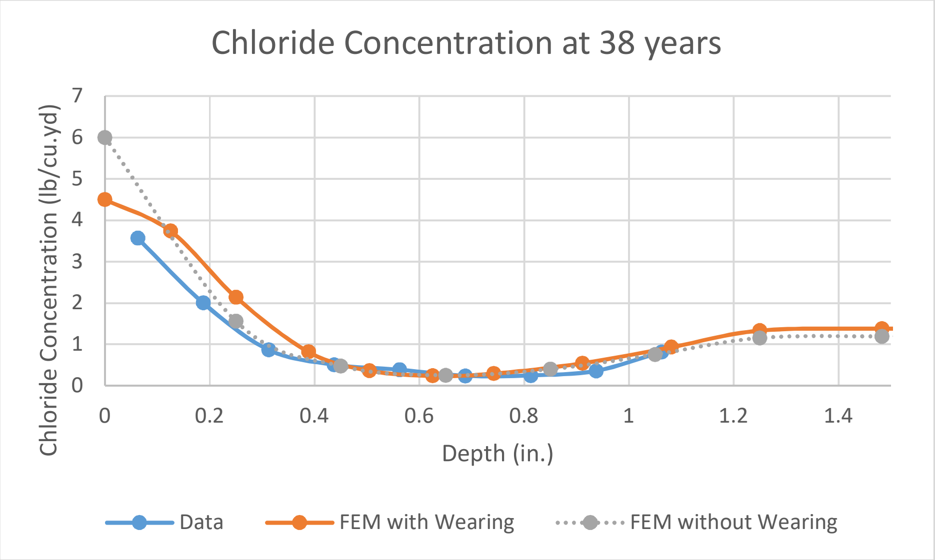

Figure 4-26 Chloride Profile after 10 years of treatment with 15% Latex Modified Concrete

4.10. Summary and Conclusions

Through the comparison of the FEA results with the estimation derived from other software and field data, it can be seen that the FEA can be used as an efficient tool to predict the chloride profile, therefore to predict the remaining service life of the concrete bridge element and guide future maintenance rehabilitation work.

Once the exposure condition is constant or the structure has been exposed for a long period of time, the average diffusion coefficient and achieved average surface concentration can predict the chloride profile accurately. However, it may not be accurate for younger structures, or complex exposure conditions. In that case, it is very necessary to perform periodic NDTs to evaluate and monitor the condition state of the concrete bridge elements.

When performing the analysis, extreme care should be taken for the surface concentration accumulation and the reference diffusion coefficient. As the implantation of ongoing NDT, the accumulated inspection data could not only serve as a reference value in the record, but also help to calibrate the estimating equations.

In this chapter, the impact of the combination of Latex modified concrete and silica fume into the concrete mix is evaluated. The degradation of the concrete caused by wearing is also considered.

The FEA model, however, is used for further investigation in the next chapter to perform a life cycle cost analysis model.

5. COST ANALYSIS FOR A TYPICAL BRIDGE DECK ELEMENT

5.1. Introduction

The bridge construction and operation cost to an agency is never a one-time expenditure. Since following its planning, design, and construction, a bridge requires periodic maintenance and possibly repair or rehabilitation actions to ensure its continued function and safety.

In this chapter, a 75-year design service life is considered for comparison of the cost for different maintenance strategies. The timing to apply preventive maintenance actions are determined based on the results from the finite element analysis and the cost for individual application of the preventive maintenance measure are identified. The maintenance cost is compared by covering all the cost to the present value considering the time value. No user cost is considered in this analysis. The life cycle cost is used to compare different maintenance strategies for different concrete quality and exposure conditions.

In this segment, only the agency cost, which includes the material cost and labor are investigated. Whenever a repair or rehabilitation work is necessary on a bridge, a significant portion of the cost of the activity comes from incidental costs, rather than the actual repair or material costs. Incidental costs include mobilization, traffic control, and repairs and improvements to other parts of the bridge, such as drains, barrier rails, and approaches (Kepler, 2000). This part of the cost is not included due to its nature of uncertainty.

Also, there is another cost associated with preventive maintenance activities on bridges that is not considered in this economic analysis, which is the user cost. The user costs are the costs incurred by the traveling public attributable to the application of the bridge preservation actions, which includes time lost due to delays or detours, accidents and other resources used.

These costs are site specific and can make the total cost considerably higher than the cost used in this analysis. Therefore, due to its nature of case sensitivity, user costs are also not included in the analysis.

5.2. Cost of Materials

5.2.1 **Alternative Reinforcement**

Based on the survey from SHRP 2, the rating value for different types of reinforcement reported by State DOTs are listed in Table 5-1.

Table 5-1 Rating Value for Different Types of Reinforcement (SHRP2, 2014)

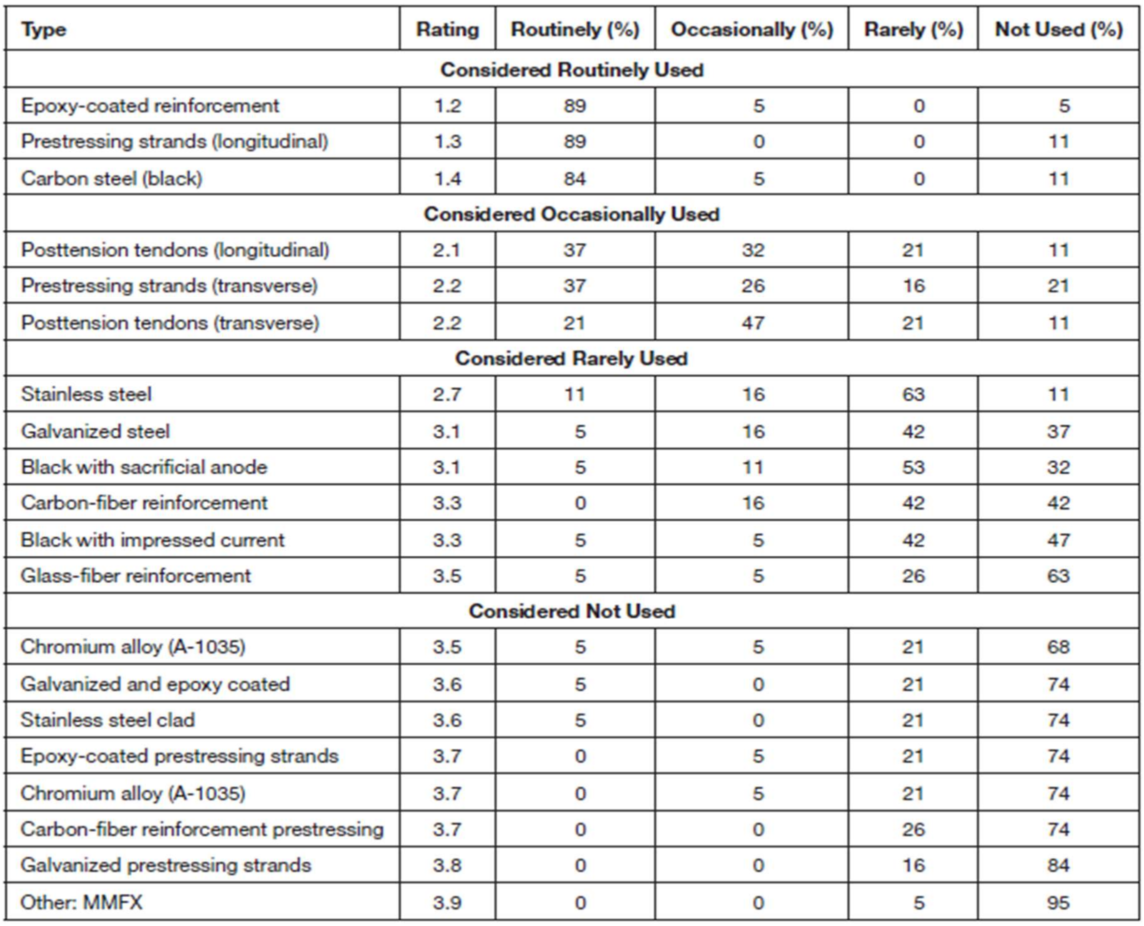

Type	Rating	Routinely (%)	Occasionally (%)	Rarely (%)	Not Used (%)
Considered Routinely Used					
Epoxy-coated reinforcement	1.2	89	5	0	5
Prestressing strands (longitudinal)	1.3	89	0	0	11
Carbon steel (black)	1.4	84	5	0	11
Considered Occasionally Used					
Posttension tendons (longitudinal)	2.1	37	32	21	11
Prestressing strands (transverse)	2.2	37	26	16	21
Posttension tendons (transverse)	2.2	21	47	21	11
Considered Rarely Used					
Stainless steel	2.7	11	16	63	11
Galvanized steel	3.1	5	16	42	37
Black with sacrificial anode	3.1	5	11	53	32
Carbon-fiber reinforcement	3.3	0	16	42	42
Black with impressed current	3.3	5	5	42	47
Glass-fiber reinforcement	3.5	5	5	26	63
Considered Not Used					
Chromium alloy (A-1035)	3.5	5	5	21	68
Galvanized and epoxy coated	3.6	5	0	21	74
Stainless steel clad	3.6	5	0	21	74
Epoxy-coated prestressing strands	3.7	0	5	21	74
Chromium alloy (A-1035)	3.7	0	5	21	74
Carbon-fiber reinforcement prestressing	3.7	0	0	26	74
Galvanized prestressing strands	3.8	0	0	16	84
Other: MMFX	3.9	0	0	5	95

The considered rating scale was 1=routinely, 2=occasionally, 3=rarely, and 4=not used. In general, the most widely adopted reinforcement steel are carbon steel (black steel), epoxy-coated reinforcement and prestressing strands (longitudinal).

Carbon steel is the most commonly used reinforcement in the concrete and it has the lowest unit price compared to the others, despite the price may vary based on the size of the rebar. Triandafilou (2012) has identified the unit cost of carbon steel #4 bars at 0.48 $/lb. for materials only. The cost estimated from Life-365 has a similar value which is 0.45 $/lb. The 2013 National Construction Estimator gives a slightly different value which is 0.65 $/lb. for a #4 rebar, and if it is placed and tied in structural slabs, an additional 0.31 $/lb. cost should be added for labor.

Compared to carbon steel, epoxy coated rebar has a higher material unit cost coming from the epoxy coating. The epoxy coated steel reinforcing bars are introduced into bridge construction more than 40 years ago and they are suitable for any concrete subjected to corrosive conditions, including exposure to deicing salts or marine waters. Triandafilou (2012) reported a unit cost of epoxy coated rebar as 0.7 $/lb., similar to the Life-365's estimation, which is 0.6 $/lb. Based on the 2013 National Construction Estimator, the unit cost of epoxy coated rebar is 0.3 $/lb. higher than the black steel, which yields to a unit cost of 0.97 $/lb. Also, based on Sharp's Report (2009), the labor cost associated with placing epoxy coated rebar may be higher and unanticipated direct costs may occur during construction phase while using epoxy coated rebar, the actual in-place unit cost of epoxy coated rebar may be as high as 0.9 $/lb.

Galvanized steel is also considered rarely used based on Table 5-1. Hot-dipped galvanized, or zinc-coated rebar have been used since 1930s. However, the performance of its corrosion resistance is controversial. Some of the researchers say the threshold value for corrosion initiation is 4 to 10 times higher than the threshold value for black bar while others say galvanized steel will only produce a slight increase in the service life of a structure in severe chloride environment. (Basham, 1999) The unit cost for galvanized steel is slightly higher than the epoxy coated rebar, which is around 0.7 \$/lb. for materials only.

Stainless steel is another alternative for reinforcement which has a chloride threshold value at least 10 times greater than carbon steel. The threshold value for Type 304 stainless steel with a stainless steel cathode was 12 to 30 lb./yd^3. For Type 316 stainless steel in both mats, the threshold value for chloride concentration can range from 20 to 33 lb./yd^3. If stainless steel is used in concrete bridge elements, the element can easily achieve a 100-year life span without any other corrosion protection system. However, the initial cost for stainless steel is much higher compared to the other alternatives, reaching 2.99 \$/lb., which is 6 times more expensive than black steel.

One particular type of steel, MMFX, is listed in the table and it is barely used by State DOTs. Bar for bar in place cost estimates, MMFX rebar is approximately one-half the cost of stainless steel rebar. It is roughly 30% more than galvanized and 50% more than ECR bar for bar; however, the additional handling and field costs of galvanized and ECR need to be taken into account. Further, MMFX outperforms both galvanized and ECR for corrosion resistance resulting in the lowest life cycle cost over the competing products. According to the report (MMFX, 2016), upon the first repair of structures built with galvanized rebar or ECR the costs are estimated at 5 times or more than if constructed with MMFX rebar. Based on these information, the unit cost of the MMFX rebar could be estimated as 0.94 \$/lb.

The unit cost of different types of reinforcement that will be used in the cost analysis in this chapter is summarized in Table 5-2.

Table 5-2 Unit Cost of Different Types of Reinforcement

Type of Reinforcement	Unit Cost ($/lb.)
Carbon Steel (Black Steel)	0.45
Epoxy Coated Rebar	0.6
Galvanized Steel Reinforcement	0.7
Stainless Steel Bar	2.99
MMFX	0.94

5.2.2 Specialized Concrete

Concrete is the major construction material for concrete bridges and the material cost of concrete plays a significant role in the bid price. Based on the Life-365 estimation, the unit cost for concrete is about 76.5 \$/yd^3. However, in order to increase the workability, freeze-thaw resistance, durability and even the compressive strength of the concrete, different types of admixtures are often needed for the specific concrete mix, which will increase the unit cost of the concrete. However, due to the fact that high performance concrete is widely adopted in the new construction projects and the cost variation is not significant, the unit cost of concrete for newly constructed elements is assumed constant despite the difference in concrete mix design. The different costs for particular types of concrete mix are investigated as used in the overlays only which serve as preventive maintenance measures.

5.3. Cost of Preventive Maintenance Measures

5.3.1 **Sealers**

5.3.1.1 Crack sealing

The crack sealing is mainly used to prevent the intrusion of moisture and other harmful compounds through existing cracks. These treatments typically require high quality materials and good preparation. Sealants commonly used by State DOTs are Reactive Methyl Methacrylate (MMA), High molecular weight methacrylate (HMWM) and epoxy-based sealant.

Based on the Oman's (2014) research, the crack sealants used by Minnesota DOT were examined. The cost for MMA resins from different manufactures ranges from $42 to $87 per gallon. While the material cost for Epoxy-based sealant varies within a range of $42 to $81 per gallon.

However, since the crack sealant is not needed for the entire surface of the concrete structure, the actual cost of implementing crack sealant is significantly depending on the crack density. The unit price for the application is always measured in linear foot. Based on the NCHRP report 523, the cost is approximately $0.3-$1.5 per linear foot for crack filling and cracks sealing and the cost are slightly higher if it is for a small job.

5.3.1.2 Penetrating Sealers

Due to the effectiveness and the low cost of penetrating sealants, numerous products and systems are available in the market provided by different manufactures. The sealants could be installed with a common low pressure garden sprayer, as well as production field spraying equipment might also be used to improve installation time and application uniformity. Based on the rates reported by Soriano (2001), the cost ranges from \$0.16 to \$0.40 per square feet for the product materials cost. This cost covers the materials only, calculated from the unit price of the sealers and the application rate that recommended by the manufactures. According to the survey conducted by Krauss (2009), the cost for sealer applications is approximately \$3-\$5 per square feet, including the surface preparation, materials and application fees, as shown in Table 5-3.

5.3.2 **Overlays**

Based on the NCHRP report published by Krauss (2009), the cost for commonly used overlays are combined in Table 5-3. The cost and service life both covers a wide range and has a large standard deviation. The cost and expected service life in Table 5-3 are the mean values presented in Krauss's report.

Table 5-3 Rehabilitation Method Summaries (Krauss, 2009)

Rehabilitation Method	**Expected Service Life Range (Years)**	**Cost Range (\$/sq. ft.)**
Rigid Overlays		
High Performance Concrete Overlays	16-29	17-25
Low Slump Concrete Overlays	16-32	13-19
Latex Modified Concrete Overlays	14-29	18-39
Asphalt-Based Overlays		
Asphalt Overlays with a Membrane	12-19	3.1-7.6
Miscellaneous Asphalt Overlays	8-15	1-3
Others		
Polymer Overlays	9-18	10-17
Crack Repair	19-33	NA
Penetrating Sealers	4-10	3-5
Deck replacement	27-32	43-53

Other researchers also reported estimated values for different measures. According to the 2008 road report, asphalt overlays up to 2-inch thick cost \$2.2 per square feet, and it goes up to

$3.9 per square feet if the thickness reaches 2 to 4 inch. For polyester polymer concrete overlay, the application cost ranges from $8 to $17 per square feet with an average of $10.

The cost of overlays is strongly correlated with the oil price due to production and transportation costs. It is also affected by the scope of the project. The actual cost may vary based on the state and the current oil price.

5.3.3 Electrochemical Treatment

The cost of electrochemical treatment depends on bridge specific factors, such as accessibility. Damaged concrete also requires rehabilitation before the application of the electrochemical treatment, which may increase the total cost of the application. Spalled and delaminated concrete should be treated and contaminated steel should be cleaned before the installation of the electrochemical treatment.

The conceptual average cost for electrochemical re-alkalization is about $60 per square feet based on the Latah Bridge Rehabilitation Study (2012).

Table 5-4 shows the cost for cathodic protection systems and electrochemical chloride extraction summarized by Clemeña (2000). The cost for electrochemical chloride extraction ranges from $13 to $78 per square feet based on the SHRP-S-669 (1993). The cost includes single-use material, amortized materials, and labor, in which the labor cost contribute a major part for the increase of the cost. The cost of implementing ECE or CP for concrete bridges provided by Virginia DOT in 2000 is shown in the Table 4. Based on the values reported, the cost for ECE treatment ranges $11.9- $12.5 per square feet for bridge decks and $8-$29.8 for piers and abutments. Lee (2005) investigated the ECE applications in Iowa during the year of 2003, the average cost is reported $25 per square feet for the deck application.

Table 5-4 Cost for CP and ECE Application (Clemeña, 2000)

Corrosion Control Option	Bridge Component	Anode	Amount of Area Involved (m^2)	Unit Cost ($\$/m^2$)	Projected Life (yr)
Impressed-Current CP	Decks	Catalyzed Ti Mesh	740-38,500	57-97	60-90
	Piers/ Abutments	Conductive Paints	1,040-7,700	82-151	12-15
		Thermal-Sprayed Zn Coating	19-18,200	86-108	Up-27
		Thermal-Sprayed Ti Coating	66-280	105	20-40
Galvanic CP	Piers/ Abutments	Thermal-Sprayed Zn Coating	480-981	86-108	<10[a]
		Thermal-Sprayed Al-Zn-In Coating	42-4,180	118-160	10-15[a]
		Zn/Hydrogel	24-8,750	26-171	10-12[b]
ECE Treatment	Decks	Catalyzed Ti Mesh	720-1,560	128-135	> 10
	Piers/ Abutments	Steel/Catalyzed Ti Mesh	89-488	86-321	> 10

[a] At 12 mil.
[b] At 10 mil.

For cathodic protection system, the cost analysis is different due to various system types. Since the cathodic protection system is a long-term protection system, it is unfair to compare its huge capital investment with other protection systems. Therefore, the equivalent annual cost is used to compare CP for different anode system, as shown in Table 5-5. The equivalent annual cost is illustrated below. In general, the costs for CP falls in the range between \$10- \$30 per square feet of the surface treated.

Table 5-5 Equivalent Annual Costs for Anode System Per Unit Area (Etcheverry, 1998)

Service life (years)	Equivalent Annual cost ($\$/100ft^2$)			
	Bent			
	19	20	21	22
	Impressed Sprayed Zn	Impressed Sprayed Ti	Impressed Ti Mesh	Sacrificial Sprayed Zn
5				78
10	118	1,026	248	598
15	91	791	191	
20		680	164	
25		618	150	
30		581	140	
35		556	135	
40		541		

5.3.4 Summary of Preventive Maintenance Measure Costs

The NCHRP 14-23 report gives the unit cost for various preservation activities. The unit cost for different preventive maintenance and repair activities is shown in Table 5-6.

Table 5-6 Cost Estimation for Preservation Actions (NCHRP 14-23, 2014)

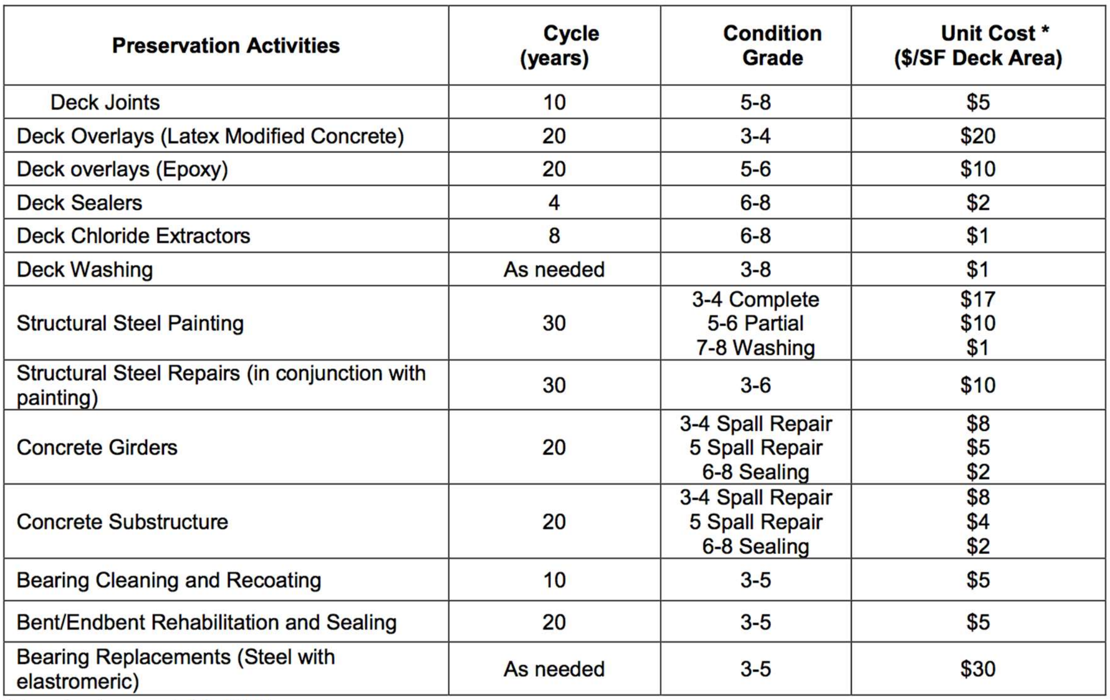

Preservation Activities	Cycle (years)	Condition Grade	Unit Cost * ($/SF Deck Area)
Deck Joints	10	5-8	$5
Deck Overlays (Latex Modified Concrete)	20	3-4	$20
Deck overlays (Epoxy)	20	5-6	$10
Deck Sealers	4	6-8	$2
Deck Chloride Extractors	8	6-8	$1
Deck Washing	As needed	3-8	$1
Structural Steel Painting	30	3-4 Complete 5-6 Partial 7-8 Washing	$17 $10 $1
Structural Steel Repairs (in conjunction with painting)	30	3-6	$10
Concrete Girders	20	3-4 Spall Repair 5 Spall Repair 6-8 Sealing	$8 $5 $2
Concrete Substructure	20	3-4 Spall Repair 5 Spall Repair 6-8 Sealing	$8 $4 $2
Bearing Cleaning and Recoating	10	3-5	$5
Bent/Endbent Rehabilitation and Sealing	20	3-5	$5
Bearing Replacements (Steel with elastromeric)	As needed	3-5	$30

* to raise to acceptable LOS

Based on the rate given in Table 5-6 and the literature reviewed in the previous sections, a cost estimation table is constructed and given below as shown in Table 5-7, which presents the unit cost for various preventive measures for concrete bridges. The cost may vary based on the accessibility of the materials, the construction experiences, location of the job site and oil price, etc.

It should be noted that the same activity may have a different cost based on the current condition state of the bridge element. A concrete bridge deck, for instance, once it was still in good condition, a thin overlay could be used as a preventive maintenance method and will cost much less than using overlay as a tool to rehabilitate the concrete bridge deck from a severely deterioration state.

Table 5-7 Estimated Cost for Preservation Actions

Type of Activities	**Cost ($/sq. ft.)**
Washing	1
Sealer	
Crack Sealer	0.4-0.8
Penetrating Sealer	1-3
Overlays	
High Performance Concrete Overlays	17-25
Low Slump Concrete Overlays	13-19
Latex Modified Concrete Overlays	18-39
Asphalt Overlays with a Membrane	4-7
Others	
Cathodic Protection	10-30
Electrochemical Chloride Extraction	10-30
Electrochemical Re-alkalization	10-30
Deck Replacement	80-100
Asphalt Replacement	2-5
Remove Overlay	8-15

The costs listed in table 5-7 are case sensitive. It includes the costs for surface preparation, material costs and the installation costs. The actual cost for overlay replacement may be higher for the reapplication due to the fact that the existing surface need to be removed and that activity introduce additional costs to the total costs. In addition, the actual cost for implementing electrochemical treatment such as cathodic protection, chloride extraction and re-alkalization might also be higher since major rehabilitation work always needs to be done before the treatment is done.

The values are used in this report for the cost analysis and comparison between different preventive maintenance systems and application strategies. The actual costs for each application need to be identified for the purpose of optimizing the preventive maintenance systems and the timing for implementing the actions.

5.4. Service Life Estimation under Different Preventive Maintenance Strategies

5.4.1 Finite Element Model

In order to estimate the service life of the concrete bridge deck element, a finite element model shown below in Figure 5-1 has been constructed. The original depth of the bridge deck is 20.32 cm (8 in). Due to the first Overlay application, 1” of the original concrete cover is removed and 1.25” overlay is applied, resulting in a total depth of the bridge deck to be equal to 20.955 cm (8.25 in). The succeeding overlay applications consist of 1.25” removal and 1.25” overlay, which will maintain the depth of the deck without composing too much excessive dead load onto the bridge system.

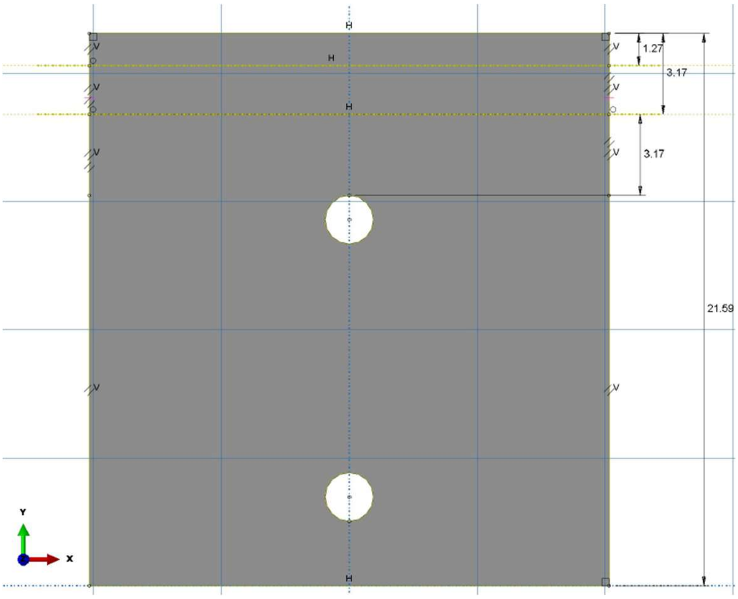

Figure 5-1 Sketch of the Finite Element Model

5.4.2 **Exposure Conditions**

Exposure condition is a vital parameter to estimate the service life of the concrete bridge elements. Temperature, freeze-thaw cycles, and surface chloride concentration are the major dependents of exposure condition. The exposure condition is identical for each bridge. However, in order to simplify the analysis, three exposure conditions are selected to conduct the life cycle analysis, which are severe, normal and mild exposure.

Three Rural highway bridges from New York, Virginia and North Carolina are selected to represent severe, normal and mild exposure respectively. The surface Chloride concentration for each State is summarized in Figure 5-2.

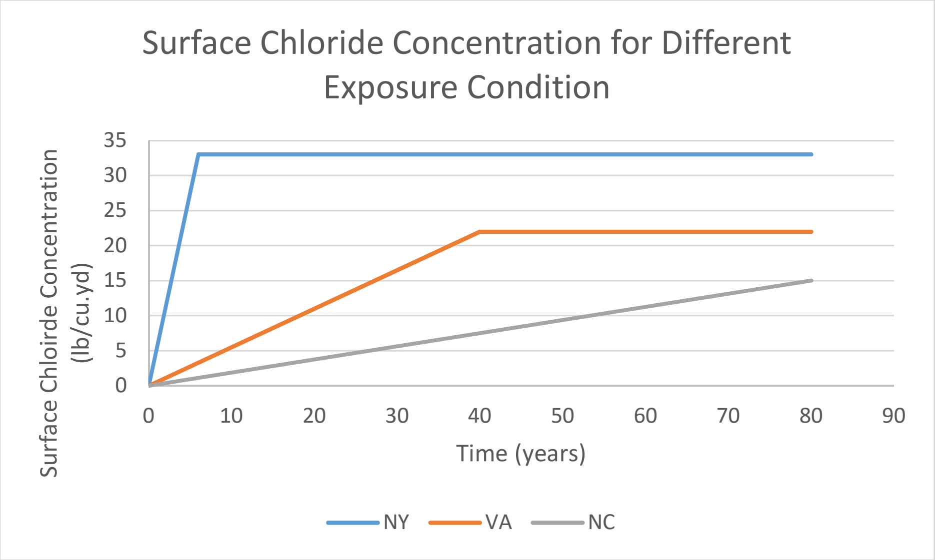

Figure 5-2 Surface Chloride Concentration for Different Exposure Condition

The average monthly temperature for each state is listed in Table 5-8.

Table 5-8 Average Monthly Temperature for NY, VA, NC

Month	**NY (°C)**	**VA (°C)**	**NC (°C)**
Jul	22	26	23
Aug	21	25	22
Sep	20	22	19
Oct	10	16	13
Nov	5	11	9
Dec	-1	7	4
Jan	-4	4	2
Feb	-4	5	4
Mar	1	9	9
Apr	8	14	13
May	14	19	17
Jun	20	23.5	21

5.4.3 **Concrete Quality**

Chloride diffusion coefficient of the concrete element should be tested and monitored using NDT methods mentioned in the previous chapter. If sufficient field data is not available, it could be estimated based on the proposed equation for predicting the chloride diffusion coefficient based on the concrete mix, exposure conditions, and other parameters such as the deterioration status.

Three different categories are generated to represent the concrete quality, Poor, normal and Good. An ordinary Portland cement concrete with water-cement ratio of 0.45 is assumed for poor quality concrete representing the old structures which have high water cement ratio and high diffusive concrete. An ordinary Portland cement concrete with water-cement ratio of 0.35 is assigned for normal quality concrete. For good quality concrete, the water-cement ratio is still 0.35, however, the top 1” cover is replaced with high performance concrete with 15% fly ash and 5% silica fume. In this case, the top 1 in. overlay consists of high performance concrete is cast during the construction of the concrete bridge deck.

5.4.4 **Identifying Preservation Actions**

The preservation actions are limited by the current condition state of the concrete bridge element. Some elements may have only one or two feasible actions especially when the bridge element is in excellent condition or totally deteriorated. In order to achieve active preventive maintenance, measures should be taken before any corrosion initiates.

Two main aspects of information need to be identified for preservation actions, the cost and the effects of the preservation actions.

The unit cost of the preservation actions is often influenced by the previous condition state, target condition state after maintenance, the amount of work, accessibility and other effects. Major rehabilitation works, like bridge deck replacement, is costly but effective for restoring the condition state to excellent or near new condition. On the other hand, minor rehabilitation works, like washing and sealing, will not be an appropriate solution to enhance the condition state of a bridge element, but cost much less than the major ones.

The effects of the preservation actions can be classified into two categories: restoration of the condition state or extension of time in the same condition state. The typical treatment that will result in a restoration in condition state for concrete decks is application of overlays, which will eliminate spalls and delamination on the deck surface and set the condition of the bridge deck to a better state. Application of sealers is a typical action that will lead to the extension of time that a bridge element could stay in the same condition state. The presence of sealers will postpone the deterioration while the condition state is still in the state of good or fair.

Table 5-9 Assumed Cost for Each Activity

Type of Activities	**Cost ($/sq. ft.)**
Penetrating Sealer	2
Crack Sealing	2
Patching	30
Concrete Overlays as Preventive Maintenance Measure	10
Concrete Overlays as Reactive Maintenance Measure	20
Cathodic Protection	30
Deck Replacement	90

The most likely cost of individual maintenance action is assumed within the range governed by Table 5-7 and listed in Table 5-9.

Also, for existing bridge element, the effectiveness of preventive maintenance measures is not only governed by the treatment effectiveness, but also the current deterioration state of the element. For instance, once the chloride concentration in the concrete slab exceeds a certain value, applying overlay will not contribute to extend the service life of the deck since the remaining chloride in the concrete slab will continue ingress into the concrete and cause corrosion. In this case, the chloride concentration at the surface of the steel is assigned as the threshold value to evaluate the effectiveness and the service life of the preventive maintenance activities.

5.5. Life-cycle Cost analysis

5.5.1 **Initial Construction Cost Using Different Materials**

From the previous research, it can be seen that based on different exposure environment and requirements, State DOTs have their own preference when choosing the construction materials.

The construction cost based on alternative reinforcement is discussed. The unit cost for carbon steel, epoxy coated rebar, stainless steel and MMFX is listed in Table 5-2. The concrete unit cost can be estimated as \$76.5/yd^3 as listed above if no special admixture is used.

Based on these information, the initial construction cost can be estimated for a typical bridge deck element which is 180 ft.×100 ft. ×8in. The reinforcement ratio of the bridge deck is assumed as 1.2% so that the volume of the rebar used can be estimated based on the volume of concrete consumed. The construction costs for various reinforcement is summarized in the following table.

Table 5-10 Construction Cost

Reinforcement Type	**Construction Cost ($/sq. ft.)**
Carbon Steel	$3.89
ECR	$4.56
Stainless Steel	$15.23
MMFX	$6.08

From the table, it can be seen that the carbon steel is the most appealing alternative since it gives the minimum construction cost estimation. Use of Epoxy coated rebar and MMFX will increase the construction cost by 16% and 58%, respectively. Stainless steel has an initial cost which is 3.7 times of the cost using carbon steel. This drastic increase in the capital investment makes it unacceptable for State DOTs to widely adopt stainless steel as the major type of reinforcement.

However, the construction cost is only a small portion in the life cycle cost through a concrete bridge deck's service life. A real concrete bridge deck element is highly unlikely to serve its service life without major rehabilitation. For instance, the service life of the bridge deck also has a great impact on the cost analysis.

A concrete bridge deck in Syracuse, NY is used as an example. The concrete mix is designed as normal concrete without any other corrosion protection measures. Four different reinforcement are evaluated based on their service life, which is the time needed from exposure to corrosion-induced cracking. The water cement ratio is constant as 0.42, and the same diffusion coefficient is achieved for different scenarios. Also, the exposure conditions are assumed to be the same. Therefore, the major variable is the chloride threshold value and the propagation time needed from corrosion initiation to cracking. The estimated service life is listed in Table 5-11.

Table 5-11 Service Life of Concrete Bridge Decks with Different Reinforcement

Reinforcement Type	**Construction Cost ($/sq. ft.)**	**Expected Service Life (Years))**
Carbon Steel	$3.89	13.9
ECR	$4.56	27.9
Stainless Steel	$15.23	93.3
MMFX	$6.08	28.3

From Table 5-11, it can be seen that concrete bridge decks reinforced with carbon steel has the shortest service life that equals 13.9 years, which means the element needs repair and rehabilitation after only 14 years of completion. If the designing service life is 100 years, it is guaranteed that the carbon steel reinforced bridge deck needs several rounds of major rehabilitation and even replacement of the entire element. MMFX and ECR exhibit better performance compared to carbon steel, achieving an estimated service life of 27.9 and 28.3 years respectively. However, the epoxy coating of on the ECR is prone to damage during construction, which may lead to pitting corrosion. It will accelerate the corrosion process once the chloride concentration at the break face reaches the threshold value. The actual service life of bridge deck using ECR is normally shorter than expected and needs close monitor.

On the other hand, stainless steel has outperformed all the other reinforcement alternatives by achieving a service life of 93.3 years without any other corrosion mitigation measures. The benefits from this extended service life is outstanding. No major rehabilitation is needed through its whole design service life, which will benefit the bridge management agencies by saving the possible cost for rehabilitation, rerouting, traffic control, etc. Also, user cost associated with traffic disturbance is also prevented if stainless steel is used.

In conclusion, for structures spanning important routes, stainless steel is highly recommended. Also, MMFX and ECR provides a longer service lives compared to carbon steel. If carbon steel is used as the reinforcement rebar for concrete bridge element that will be exposed in corrosive environment, preventive maintenance measures should be included in the design.

Since the majority of the DOTs are using carbon steel as the reinforcement, the following analysis are focusing on the life-cycle costs of carbon steel reinforced concrete bridge deck only. The impact of using ECR can be estimated by prolonging the estimated service life by 14 years, which presents the barrier effect of the epoxy coating.

5.5.2 Severe Exposure Condition

The estimated service life is determined by the corrosion initiation time, which is the chloride concentration at the surface of the steel reaches the chloride threshold value, as 1.97 lb./yd^3. Based on the finite element model, the resulted service lives for bridge deck elements exposed in severe exposure conditions are approximately 7.5 years, 10 years and 23 years, as shown in Figure 5-3.

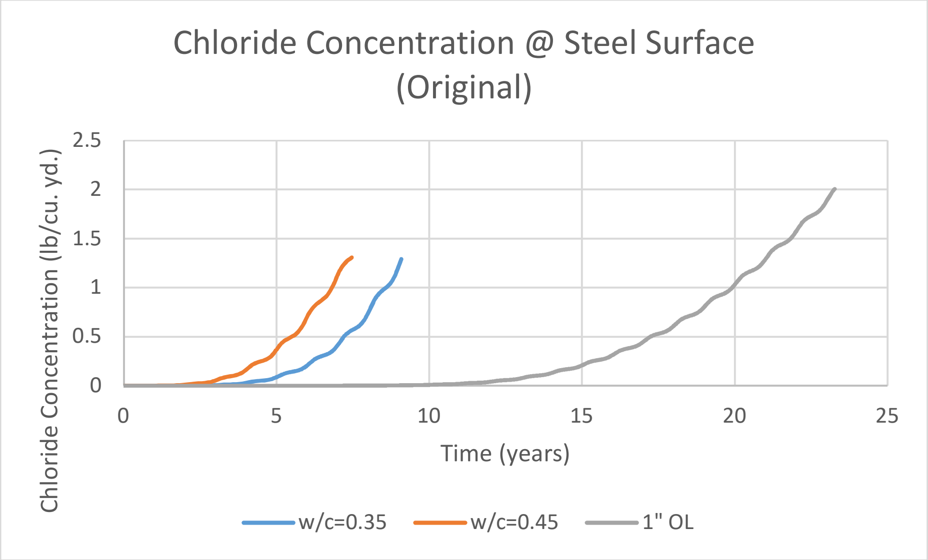

Figure 5-3 Chloride Concentration @ Steel Surface

From Figure 5-3, it can be seen that under severe exposure, the bridge deck has a very short expected service life. And due to the rapid accumulation of the surface concentration, preventive maintenance measures such as sealers are not effective, therefore, the overlay system is recommended.

However, the overlay system is not effective after the chloride concentration near the steel exceeds a certain value. The main reason is that the overlay can only remove the chloride ions in the top few inches of the bridge deck, and the chloride ions remaining in the original concrete will still tend to move to the steel and initiate the corrosion. After several cycles of iteration, a chloride concentration of 1.3 lb./yd^3 is determined as the threshold value to trigger the overlay application. For instance, the overlay system is reapplied whenever the chloride concentration of the steel surface reaches 1.3 lb./yd^3.

The overlay system used is 15% latex modified concrete and the diffusion characteristics are estimated using the proposed equation.

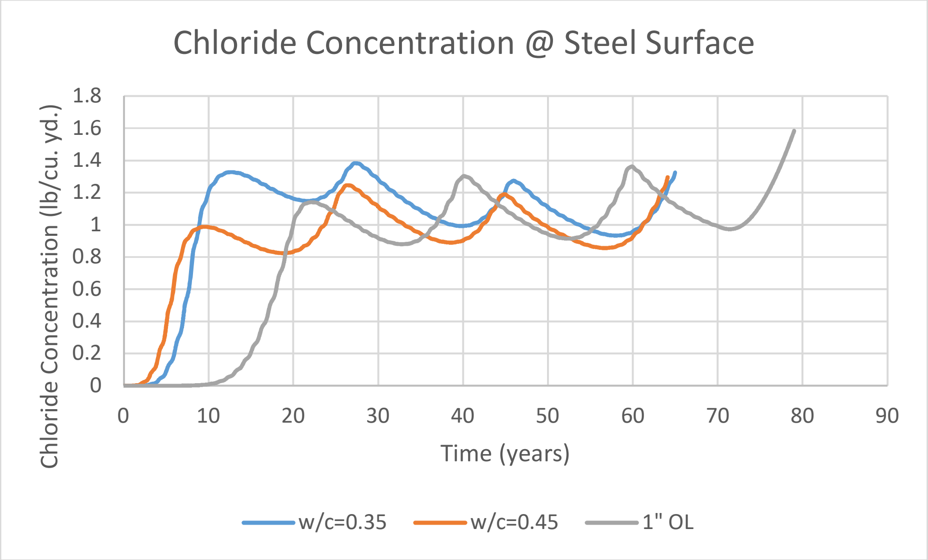

Figure 5-4 Chloride Concentration @ Steel Surface with Different Quality Concrete

The overlay applications are scheduled based on the following table.

Table 5-12 Overlay Schedule for Severe Exposure

No. of Application (LMC Overlay)	Time (year)		
	w/c=0.45	w/c=0.35	1" OL
1st	5	7	19
2nd	25	26	39
3rd	44	45	58
4th	62	63	

It can be seen that for severe exposure, the estimated service life for poor and normal concrete are relatively short and the concrete element needs overlay with in the first few years after construction. On the contrary, the concrete with 1” Latex modified overlay has a much longer service life of 22 years and the overlay can be postponed as late as 19 years.

The service life of the overlay system is approximately 20 years. However, reapplication of overlay may result in a decrease of the effectiveness of the application and needs more frequent treatment.

5.5.3 **Normal Exposure Condition**

The estimated service life for concrete bridge deck element under normal exposure condition is presented in Figure 5-5, and the expected service life for poor, normal and good quality concrete are 17 years, 18.5 years and 27 years respectively.

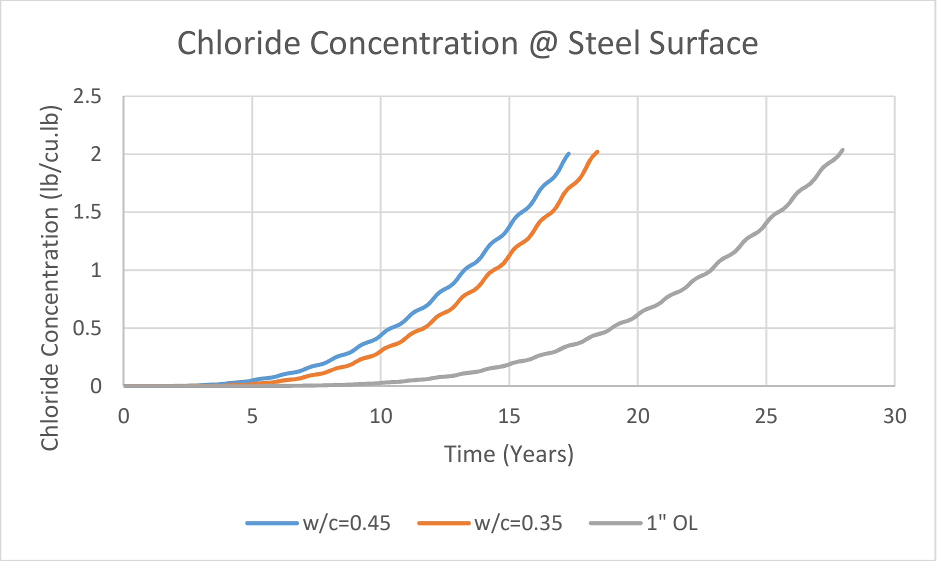

Figure 5-5 Chloride Concentration @ Steel Surface

Table 5-13 Overlay Schedule for Normal Exposure and w/c=0.45

No. of Application (overlay)	**Time (year)**
	w/c=0.45
1st	14
2nd	35
3rd	55

Due to the difference of the exposure condition, a chloride concentration of 1.5 lb./yd^3 is determined as the trigger to invoice the overlay application. For instance, the overlay system is reapplied whenever the chloride concentration of the steel surface reaches 1.5 lb./yd^3.

The overlay system used is 7% Silica Fume high performance concrete and the diffusion characteristics are estimated using the proposed equation.

For Poor quality concrete, the chloride concentration at the steel surface is shown in Figure 5-6 with the overlay schedule listed in Table 5-13.

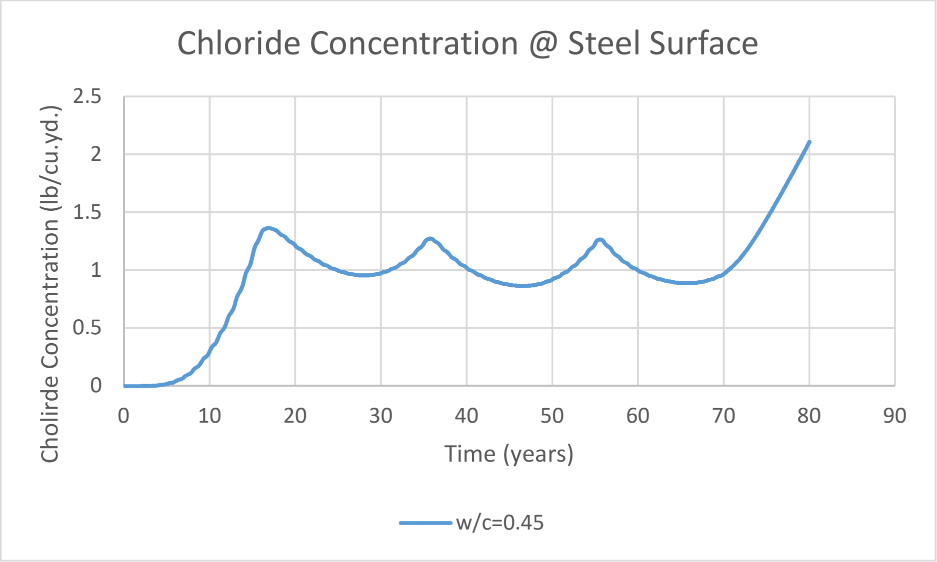

Figure 5-6 Chloride Concentration @ Steel Surface

For Normal quality concrete with a water cement ratio of 0.35, the expected service life is 18.4 years. However, two different maintenance strategies are considered. The first option is using overlay system only and the alternative is using the combination of overlay and sealer. The sealer is applied every 5 years with an initial effectiveness of 90%. The chloride concentration for different application is shown in figure 5-7.

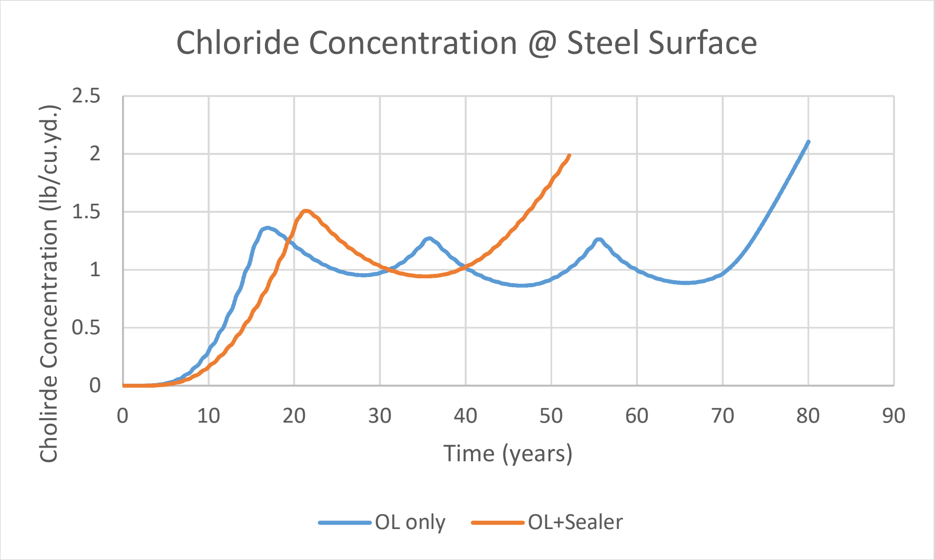

Figure 5-7 Chloride Concentration for Different Maintenance Strategy

The required preventive maintenance schedule is shown in Table 5-14 and 5-15.

Table 5-14 Overlay Schedule for Normal Exposure and w/c=0.35

No. of Application (overlay)	**Time (year)**
	w/c=0.45
1st	15
2nd	35
3rd	55

Table 5-15 Overlay and Sealing Schedule for Normal Exposure and w/c=0.35

Schedule for Sealing				**Schedule for Overlay**	
No. of Application	**Time (Year)**	**No. of Application**	**Time (Year)**	**No. of Application**	**Time (Year)**
1st	0	9th	40	1st	20
2nd	5	10th	45	2nd	47
3rd	10	11th	47		
4th	15	12th	52		
5th	20	13th	57		
6th	25	14th	62		
7th	30	15th	67		
8th	35	16th	72		

For good quality concrete with a water cement ratio of 0.35 and 1” cover of high performance concrete, the scheduled preventive maintenance is shown in Figure 5-8.

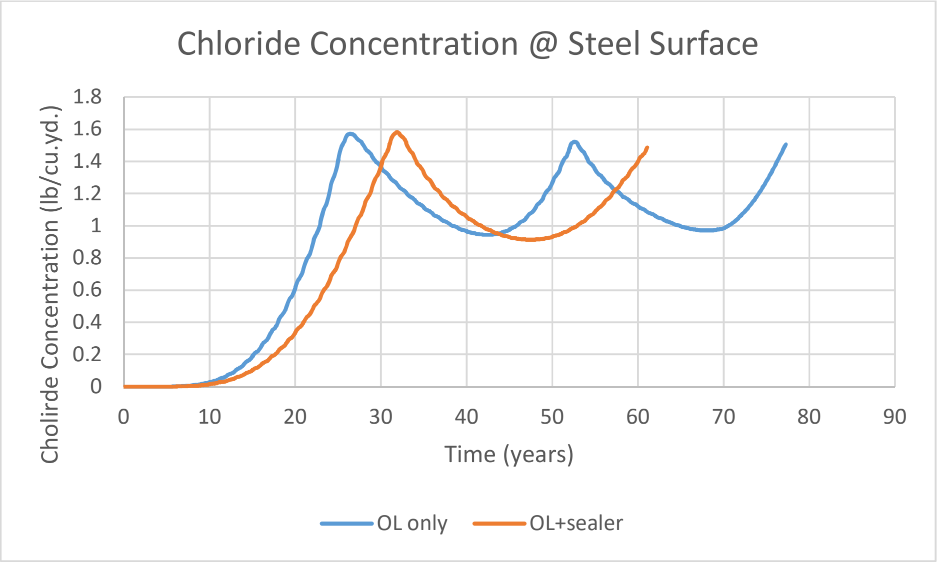

Figure 5-8 Chloride Concentration for Different Maintenance Strategy

Figure 5-8 indicates the required time to apply sealer or overlay treatment. If the overlay is selected as the only preventive maintenance measure, then the schedule should be applied based on Table 5-16.

Table 5-16 Overlay Schedule for Normal Exposure and Good Quality Concrete

No. of Application	**Time (year)**
	w/c=0.45
1st	25
2nd	52

If both overlay and sealer are selected as the potential preventive maintenance treatment, then the optimized schedule for sealing and overlay is shown in Table 5-17.

Table 5-17 Overlay and Sealing Schedule for Normal Exposure and Good Quality Concrete

Schedule for Sealing				**Schedule for Overlay**	
No. of Application	**Time (Year)**	**No. of Application**	**Time (Year)**	**No. of Application**	**Time (Year)**
1st	0	9th	41	1st	31
2nd	5	10th	46	2nd	61
3rd	10	11th	51		
4th	15	12th	56		
5th	20	13th	61		
6th	25	14th	66		
7th	31	15th	71		
8th	36				

5.5.4 **Mild Exposure Condition**

The estimated service life under mild exposure condition is presented in Figure 5-9, for poor, normal quality concrete.

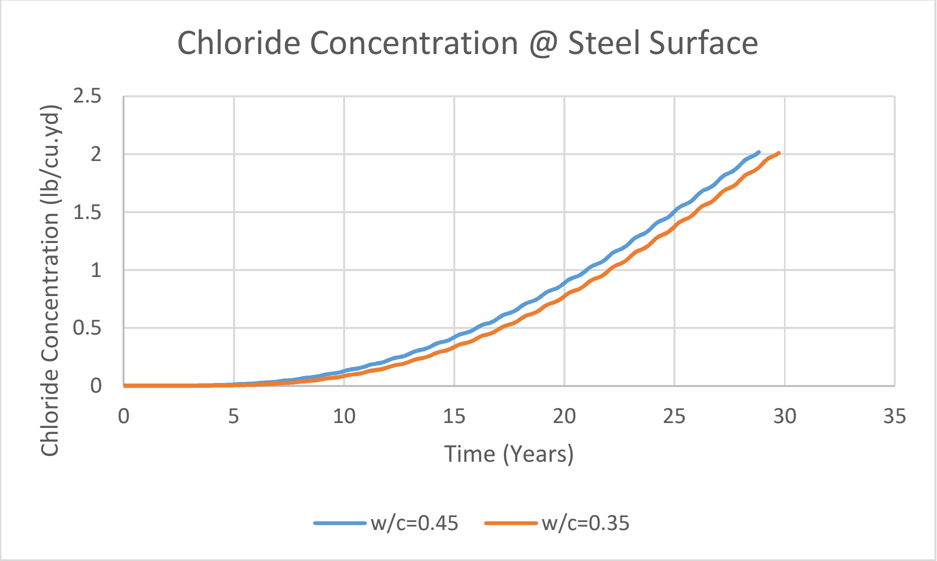

Figure 5-9 Chloride Concentration @ Steel Surface

From Figure 5-9, it can be seen that with the mild exposure, the expected service life is very close for both scenarios.

According to the trend, the sealer system combined with overlay are the best solution for mild exposure condition. If the overlay is the only used preventive maintenance method, it should be applied on at 26 years. If combined with sealer, the overlay application should be postponed to 35 years.

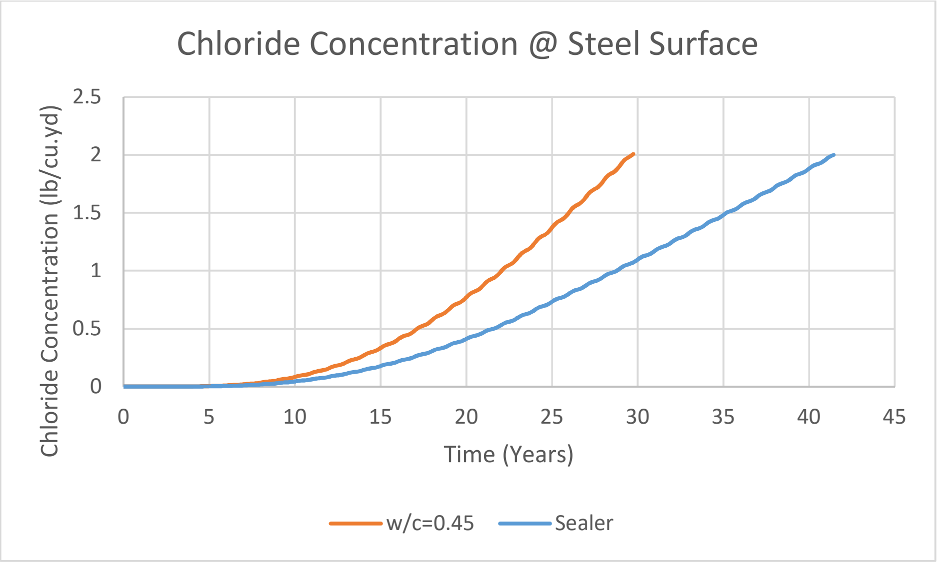

Figure 5-10 Chloride Concentration for Different Maintenance Strategies

However, due to the fact corrosion is not the only deterioration mechanisms on bridge decks, the service life for a concrete bridge deck is no longer governed by the chloride induced corrosion. Therefore, the overlay should be applied cyclically as a preventive maintenance method not only to prolong the service life of the bridge deck, but also to make sure the bridge deck can provide good riding quality for the drivers.

5.5.5 **Life-cycle Cost Comparison**

5.5.5.1 Introduction

In order to conduct this simplified life cycle cost analysis, a 75-year analysis period is selected. The 75-year period is determined by the average design service life reported from the questionnaire answers given by state DOTs. Also, the bridge may be functionally obsolete due to the increase of transportation demands.

Based on the literature reviewed, a 3% discount rate is assumed for the life-cycle analysis. For preventive maintenance actions conducted in year n, the equivalent present value can be derived from Equation 7-1:

$$(P/F, i, n) = F \times \frac{1}{(1+i)^n} \tag{7-1}$$

where, F is the future cost of the preventive maintenance, i is the discount rate and n is the year that the maintenance is applied.

All the strategies are compared based on the planning starts from the current year. Some single action's costs are not included in this analysis, such as rehabilitation of a small portion of an element in poor condition before applying treatment to the entire bridge component.

5.5.5.2 Service life Cost Comparison for Normal Exposure

In order to conduct the life cycle cost analysis, a set of assumptions have to be made. The integrated surface of the 1" overlay for the good quality concrete does not come with additional charge. The active preventive maintenance strategies are derived from the previous analysis.

However, for the reactive and delayed maintenance, the deterioration curve based on the condition state of the bridge deck has to be used, as shown in Figure 5-11.

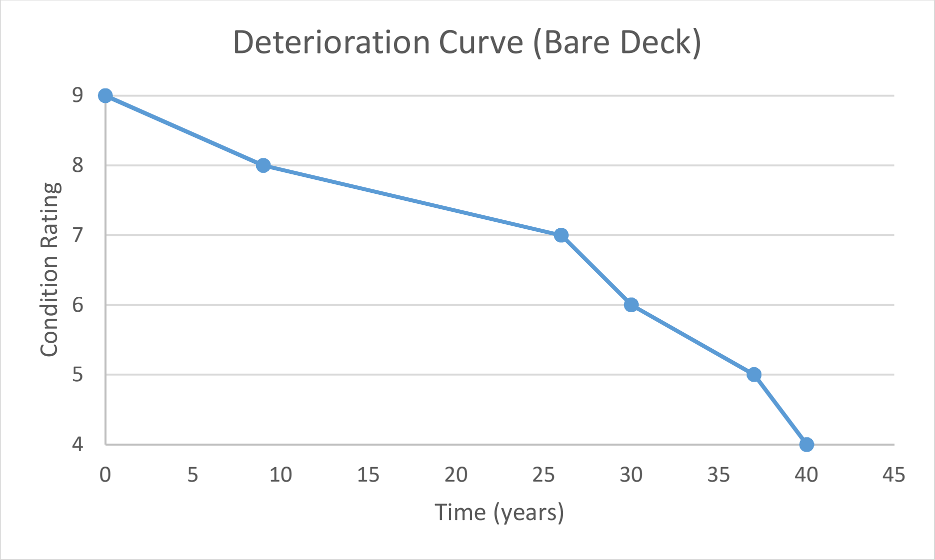

Figure 5-11 Deterioration Curve for Bare Concrete Bridge Deck (Johnston, 2014)

In this comparison, the active preventive maintenance costs are calculated for Poor, Normal and Good quality concrete.

The cathodic protection systems are also analyzed as one of the options. However, since the installation of the cathodic protection systems often requires the application of new overlay, the first cathodic protection application is applied as a reactive maintenance measures which happens at year 25. Another reapplication is needed at year 55 since the expected service life of the cathodic protection system is 30 years.

Three other different reactive maintenance methods are considered. The first one is performing the overlay systems periodically without knowing the effectiveness and the remaining service life of the overlay system. The seconded one is patching and replacement. In this case, patching is only performed after corrosion initiation and once it started, it has to be reapplied every six years for 10% of the total area of the bridge deck surface until the replacement of the bridge deck. The third option is doing nothing until the end of its service life and then do replacement.

Table 5-18 Life Cycle Cost Comparison

VA Life Cycle Cost (unit Cost=$/sq.ft.)		
Active Preventive Maintenance Cost		
	Overlay Only	Overlay +Sealer
Poor Concrete	21.21	27.95
Normal Concrete	21.02	25.76
Good Concrete	15.98	20.34
Cathodic Protection	26.97	
Reactive Maintenance Methods		
Replacement Only	27.59	
Patching & Replacement	33.24	
Overlay	28.01	

5.6. Summary and Conclusion

It can be concluded that active preventive maintenance provides advantages over the other alternatives. Especially for good quality concrete which comes with an integrated High performance concrete cover. Since it was cast during the construction stage, the extra cost will be much lower than rehabilitation works in which the bridge has to be closed.

Sealer seems not to be a good choice for such exposure environment. However, due to its nature of multiple times of reapplication, the additional cost is very sensitive to the unit price of the application. If the unit price drops down to one half of its current price, the difference between the two active preventive maintenance strategies will be negligible, which makes the sealer application an economical option.

Cathodic protection is not favorable in this case, however, under severe exposure conditions, it might be the only option to delay or even stop corrosion, especially on old structures.

Even though the do noting option has the lowest life cycle cost among reactive maintenance methods, it is still not favorable due to the drop of the condition state and quality of service.

After all, the use of alternative reinforcing material could also be a good reasonable alternative since it will eventually yield to a low life cycle cost despite of the fact that it requires more initial investment during construction.

6. RECOMMENDATIONS ON FUTURE INSPECTION AND MAINTENANCE PROGRAM

Current bridge design service life ranges from 75 years to 100 years. Extensive maintenance work is needed throughout the whole service life of the concrete bridges, the cost of which is commonly 4 or 5 time of the construction cost. If a cost effective preventive maintenance program is adopted, the maintenance cost will decrease drastically. The key to success of preventive maintenance program depends on preventing physical deterioration of concrete members, which could be done through preventing/ delaying harmful chemical reactions. Assessing the chemical condition of a bridge would allow preventive actions before physical deterioration starts.

Chemical NDTs are essential for estimating the deterioration process and predict the service condition state for concrete bridge elements. The test should be applied on all elements, including those elements that are still in good or fair condition. Carbonation tests, chloride content tests, chloride diffusion tests and ASR test should be performed in order to quantify the parameters for numerical deterioration equations. The following tests should be performed:

- Carbonation Test: The carbonation depth can be used to evaluate the cause of corrosion; to estimate service life where penetration of the carbonation frontier is critical; to monitor the effectiveness of applications for re-alkalization.
- Chloride Content Test: The chloride content test can be used to evaluate the cause of corrosion; to estimate the apparent diffusion coefficient by curve fitting using the chloride diffusion equations; to monitor the effectiveness of preventive maintenance measures such as sealers and membranes by comparing the chloride concentration.

- Chloride Diffusion Test: The chloride diffusion test can be used to test the resistance of concrete for chloride ingression under exposure; to estimate the diffusion coefficient and the remaining service life of the specimen; to check and verify the effectiveness of preventive maintenance applications such as sealers and membranes.
- ASR Test: The ASR test can be used to determine if the concrete structure is prone to ASR deterioration mechanism.

In addition to the tests listed above, the properties of the concrete should be tested and recorded. The compressive strength, porosity and permeability can be tested and used as a reference to get a value for the water cement ratio for the existing bridge if no historical data is available. The dynamic modulus of elasticity should also be tested for all new structures.

The NDT can be also used as a tool for selection of preventive maintenance alternatives. Combining the results of carbonation test, chloride diffusion test and chloride content tests with numerical deterioration models, the effectiveness of the preventive maintenance measures can be evaluated. Taking the advantage offered by NDTs and preventive maintenance approaches, the inspectors can identify possible deterioration before excessive physical damage has occurred, and then recommend a proper maintenance treatment based on the root cause of the deterioration. The reapplication of the cost-effective preventive maintenance measures such as the use of sealers and corrosion inhibitors can be determined by evaluating the chemical condition of concrete element. If deterioration reaches a critical threshold value, more aggressive methods, such as overlays could be applied to the structure. If the deterioration rate is high after years of service and corrosion is the main concern for further deterioration, then cathodic protection systems could be considered as an alternative treatment.

A flowchart (Figure 6-1) has been constructed to better illustrate the usage of Chemical NDE, followed by preventive maintenance activities.

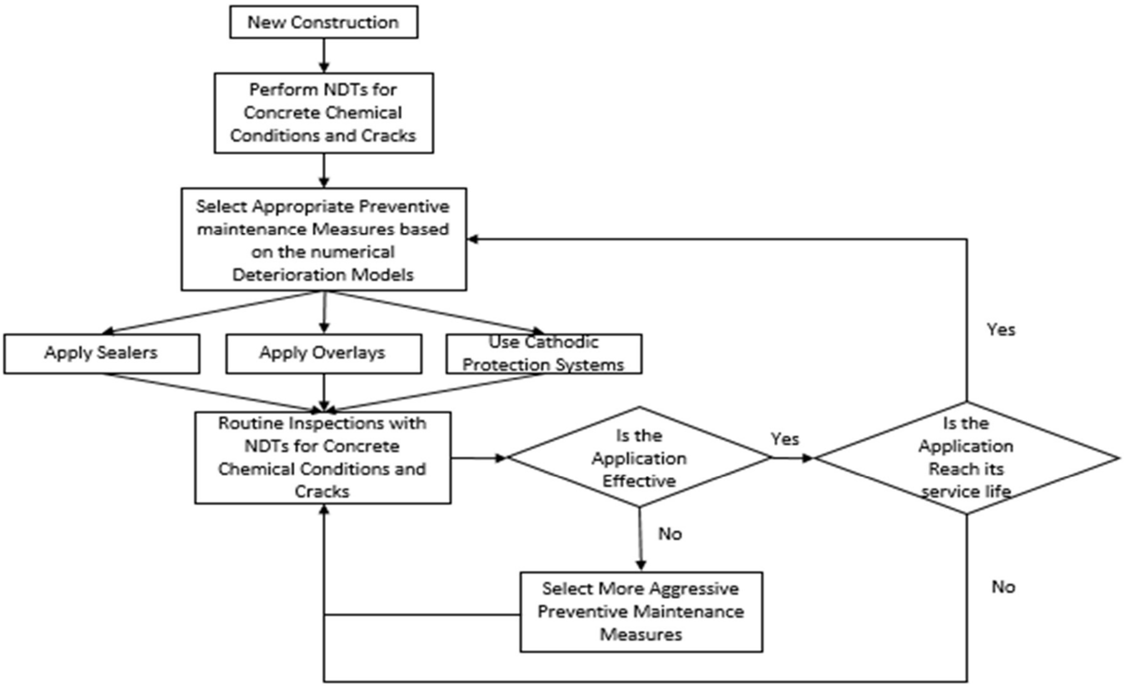

Figure 6-1 Flowchart for Chemical NDT Based Inspection and Preventive Maintenance Strategies

Therefore, the NDTs are not only a method for inspection. They should also be adopted as part of decision making process, as well as monitoring and evaluation system for a preventive maintenance plan. By performing a real active preventive maintenance plan, the overall life cycle cost of the concrete bridge system will decrease.

7. SUMMARY AND CONCLUSIONS

7.1. Summary

The current practice for physical evaluation and delayed maintenance of deteriorated concrete bridge is fundamentally wrong. A cost-effective bridge maintenance program is a program using preventive maintenance based on the chemical conditions of the concrete bridge elements. In order to conduct active preventive maintenance, a chemical based, nondestructive inspection program was proposed. A more refined equation for estimating the chloride diffusion coefficient that accounts for the effects of latex, cement replacement materials, exposure conditions, stress, curing, aging, and erosion was proposed. Based on which, an FEA model that can predict the future chloride profile and the remaining service life was constructed. The FEM was verified against experimental/field data and other commercial software. The FEM was then used to show its ability to evaluate the effectiveness of preventive maintenance measures and guide the active preventive maintenance practice. Furthermore, a life cycle cost analysis of a typical concrete bridge deck element is conducted in order to demonstrate that the preventive maintenance plan is economical.

7.2. General Conclusions

This dissertation presents the economy of preventive maintenance for concrete bridge elements due to corrosion. It presents an in-depth chemical evaluation and preventive maintenance of existing highway concrete bridges. Based on this study, the following general conclusions could be drawn:

1. Cost-effective maintenance of concrete bridges starts with the use of high quality concrete and durable materials. The quality of initial construction and workmanship needs to be guaranteed.
2. As the corrosion of steel bars is the primary cause of deterioration of concrete bridges, it is recommended to reinforce new concrete bridge decks with FRP bars, or stainless steel bars, or regular bars along with corrosion protection systems.
3. Preventive maintenance of concrete bridges starts on day one, right after the construction has been completed.
4. Bridge inspection should be based on the chemical condition more than on the physical condition of the bridge. There should be a systematic bridge inspection and evaluation of the chemical condition of bridges. Such new approaches would allow detecting deterioration mechanism (using preventive maintenance approach) before they start, long before deterioration of concrete and corrosion of steel bars have started.
5. Preventive maintenance approach may not eliminate the need for replacement of bridge decks during the service life of the bridge. Shrinkage, direct traffic wearing, fatigue stresses will continue to produce cracking in bridge decks. These cracks will reduce the service life of bridge decks, and require more aggressive maintenance measures.
6. There is no one preventive maintenance solution for all concrete bridges/bridge elements. The effectiveness of preventive maintenance is very much site dependent, as it is affected by the quality of concrete, type of traffic, age of bridge, severity of surrounding environment, accurate measurement of the effectiveness of preventive

maintenance measures, and the chemical condition of the bridge with and without maintenance measures.

7. Deterioration of concrete bridges is a two-step process; (1) harmful chemical reactions followed by (2) physical deterioration. The cost of freezing or delaying the harmful chemical reactions is much lower than the cost of fixing the physical damage.
8. The effective approach to freeze and/or delay the harmful chemical reactions starts with successful assessment of the chemical condition of the bridge through non-destructive testing
9. There is a need to conduct field tests to verify the effectiveness of maintenance actions. Lab test are insufficient to assess the effectiveness of these actions.

7.3. Specific Conclusions

Besides the general conclusions, some specific conclusions could be drawn based on the analytical models, the finite element modeling and the cost analysis examples.

1. The diffusion coefficient of the concrete element can be achieved by three different means. The first one is obtained by curve fitting to a chloride profile, which is suitable for old marine structures. The second one is obtained by using NDT methods such as the RCP tests. The third one is obtained by using the proposed refined estimation equation.
2. The chloride diffusion coefficient is dominated by numerous factors. The water cement ratio, the type and proportion of cementitious materials, and the curing process have a great impact on the initial chloride diffusion coefficient. In addition, aging of the concrete, presence and development of the cracks, the exposure

environment including temperature and humidity, also play a significant role on the chloride diffusion coefficient.

3. The impact of the cracks on the chloride diffusion coefficient is quantified by using the damage index, which is the ratio between the initial and the tested dynamic modulus of elasticity. The damage index could also be used to represent the impact of freeze and thaw effect and the ASR reaction on increasing the chloride induced corrosion process.
4. For concrete bridge deck elements, abrasion is also a vital parameter. In the analysis, it is modeled by moving the exposed surface. The abrasion rate is associated with the average daily traffic and the traffic type.
5. Based on the analysis, overlay is the most economical preventive method. It has a relatively low unit cost, when applied on bridge elements while they are still in good or fair conditions. The estimated service life of the overlay is around 20 years and varies depending on the overlay materials and the exposure conditions.
6. Sealer applications will postpone the corrosion initiation while increasing the life cycle cost of the bridge element. However, the life cycle cost of sealer treatment is very sensitive to the unit cost for each application due to its relatively short service life (3-5 years). If the unit cost is decreased and the durability of the sealer increased, the use of sealer along with periodic overlay could be an economical solution.
7. Cathodic protection systems are suitable for elements under extreme corrosive environments. Also, it is suitable for old structural elements that do not need major rehabilitation work but have ongoing corrosion.

7.4. Limitations and Recommendations for Future Study

1- Due to the limited availability of experimental/field data, it is recommended that further validation goes through other concrete bridge components.

2- Some of the chemical NDTs are partially destructive to the structural elements. The development of imbedded monitoring equipment could be helpful and possibly cost effective.

3- The chloride induced corrosion is considered as the primary deterioration mechanism and other deterioration mechanism impacts are only reflected through the change of diffusion coefficient. A more comprehensive deterioration model that accounts for the interrelations between different deterioration mechanisms should be investigated.

4- The effectiveness and the cost for preventive maintenance measures are selected based on the mean values from literature review. If sufficient data is available, sensitivity analysis should be performed for life cycle cost analysis.

8. APPENDIX

Appendix A. Approved Sealers by State DOTs

State	Product Name	Manufacturer	Active Ingredient	Concentration	Solvent	Reported Test results			Penetration (in)
						Water weight gain reduction	Absorbed chloride (series II)	Moisture vapor permeability (series II)	
California	Sil-Act ATS 100-LV	Advanced Chemical Technologies	Saline	100%	None	82%	84%		
California	Xiameter OFS 6341*	Dow Corning	Saline	98%					
California	Protectosil Chem-Trete BSM 400-BA	Evonik Industries	Saline	100%	None	85%	86%	100%	
California	SL 100 Water Repellent	Prosoco, Inc	Saline						
California	Loxon 40% Saline Low VOC Water Repellent, A31T00840	Sherwin Williams	Saline	40%			95%		
Maine	Sikagard 7670W Clear	Sika Corporation	acrylic	100%					
Maine	Sealate T70 MX-30	Transpo Industries	HMWM						
Maine	Aquanil Plus 100	ChemMasters	Saline	95%	None	85%	88%	92%	
Maine	Aquanil Plus 40A	ChemMasters	Saline	40%	Acetone/Isopropyl	85%	88%	92%	

Maine	Weather worker 40% J29WB	Dayton Superior	Saline	40%		86%		100%	
Maine	Weather Worker S-100 J29A	Dayton Superior	Saline	90%	Alcohol	87%		100%	
Maine	Baracade Saline 100	Euclid Chemical	Saline	100%	None	89%	91%		0.20
Maine	Sikagard 705 L	Sika Corporation	Saline	100%	None		88%		0.39
Maine	Sikaguad 740 W	Sika Corporation	Saline	40%	Water	85%	96%		
Maine	Certivex Powerseal 40%	Vexcon	Saline	40%	Water	87%	95%	95%	0.15
Maine	Sikagard 701W	Sika Corporation	Saline modified siloxane	20%		91%	90%	100%	
Maine	Protectosil AQUA-TRETE 20	Evonik Degussa	Saline/siloxane	20%	Water	80%	84%	93%	
Maine	Sil-Act ATS-100 LV	Advanced Chemical Technologies		100%	None	82%	84%		
Maine	Aridox 40 M	Anti Hydro							
Maine	Certi-Ven Penseal 244-40% AIM	Vexcon		40%		93.20%	94.60%	95%	0.15
Maine	Certi-vex Penseal 244 100	Vexcon				93.20%	94.60%	95%	0.15
Maine	Powerseal 20	Vexcon			Water	80%		90%	0.15
Massachusetts	SIL-ACT ATS-100LV	Advanced Chemical Technologies	Saline	100%	None	82%	84%		
Massachusetts	Enviroseal 40	BASF	Saline	40%	Water	85%	87%		
Massachusetts	Weather Worker J29A	Dayton Superior	Saline	90%	Alcohol	87%		100%	

Massachusetts	Baracade WB 244	Euclid Chemical	Saline		Water	85%	82%		0.38
Massachusetts	Dynasylan BH-N	Evonik Degussa	Saline	98%	None	86%	87%		0.38
Massachusetts	Protectosil Chem-Trete BSM 40 VOC	Evonik Degussa	Saline	40%	alcohol	86%	87%	100%	
Massachusetts	Powerseal 40	Vexcon	Saline	40%	Water	87%	95%	95%	0.15
Massachusetts	Weatherguard P40 Sealer		Saline	40%					
Massachusetts	SLX100	PROSOCO		93%					
New Hampshire	Sil-Act ATS-100 LV	Advanced Chemical Technologies	Saline	100%	None	82%	84%		
New Hampshire	Powerseal 40	Vexcon	Saline	40%	Water	87%	95%	95%	0.15
New Hampshire	Certi-Vex Penseal 244 100%	Vexcon				93.20%	94.60%	95%	0.15
New Hampshire	Certi-Vex Penseal 244 40% AIM	Vexcon				93.20%	94.60%	95%	0.15
New York	SIL-ACT ATS-100	Advanced Chemical Technologies	Saline	100%	None	88%	89%	100%	
New York	SIL-ACT ATS-100 LV	Advanced Chemical Technologies	Saline	100%	None	82%	84%		
New York	Enviroseal 40	BASF	Saline	40%	Water	85%	87%		
New York	Hydrozo 100	BASF	Saline	100%	None	90%	96%		0.35
New York	Aquanil Plus 100	ChemMasters	Saline	95%	None	85%	88%	92%	
New York	Aquanil Plus 40A	ChemMasters	Saline	40%	Acetone/Isopropyl	85%	88%	92%	
New York	Aquanil Plus 55 IPA	ChemMasters	Saline	55%		85%	88%	92%	

New York	Weather Worker S-100 (J29A)	Dayton Superior	Saline	90%	Alcohol	87%		100%	
New York	Baracade Saline 100	Euclid Chemical	Saline	100%	None	89%	91%		0.20
New York	Protectosil BH-N	Evonik Degussa	Saline	98%	None	86%	87%		0.38
New York	Iso-Flex 618-100	LymTal	Saline	90%	None	89%	90%		0.35
New York	KlereSeal 9100-S	Pecora	Saline	100%	None	85%	99%	102%	0.43
New York	PowerSeal 40	Vexcon	Saline	40%	Water	87%	95%	95%	0.15
New York	Aridox 40	Anti Hydro		40%	Alcohol				
New York	Certi-Vex Penseal 244 BTS-100% (Fast Dry)	Vexcon		100%	None	84%			0.28
New York	Certi-Vex Penseal 244-100 AIM NY DOT	Vexcon		100%	None	93.20%	94.60%	95%	0.15
New York	Certi-Vex Penseal 244-400 AIM NY DOT	Vexcon		55%	Alcohol	93.20%	94.60%	95%	0.15
Ohio	Enviroseal 40	BASF	Saline	40%	Water	85%	87%		
Ohio	Masterprotect H 400	BASF	Saline	40%	Water	85%	87%		
Ohio	Aquanil Plus 40A	ChemMasters	Saline	40%	Acetone/Isopropyl	85%	88%	92%	

Appendix B. Chloride Threshold Values in the Literature

Threshold Values or Ranges			w/c	(Binding capacity)	Binder type (Governing pH)	Age	Moisture Content	Steel potential (surface condition)	Environment	pH	Reference
Total Cl^- (%wc)	Free Cl^- (% wc)	Cl^- /OH^-									
0.4			0.45		100% OPC		65% RH	smooth	laboratory		Richartz [1969]
3			0.6		100% OPC			smooth	laboratory, exposed to air		Gouda and Halaka [1970]
1			0.6		35% GGBS + 65% OPC			smooth	laboratory, exposed to air		Gouda and Halaka [1970]
2.4			-		100% OPC			smooth	laboratory, submerged, but aerated		Gouda and Halaka [1970]
1.2			-		35% GGBS + 65% OPC			smooth	Laboratory, submerged, but aerated		Gouda and Halaka [1970]
0.2 – 1.4			-		various			-	outdoor exposure, exposed to air		Stratfull et al. [1975]
0.4 – 0.8			0.4		100% OPC			cleaned, ribbed	laboratory, exposed to air		Locke and Siman [1980]
0.25 – 0.5			0.5		100% OPC		60% RH	sandblasted	laboratory, submerged		Elsener and Böhni [1986]
0.1 – 0.19			0.45		100% OPC			polished	laboratory, exposed to air		Hope and Ip [1987]

0.1 – 0.19			0.45		100% OPC			polished	outdoor exposure, exposed to air		Hope and Ip [1987]
0.4 – 1.37			0.4 – 0.6		OPC, FA, SRPC, SF, RHPC			cleaned, smooth	laboratory, submerged		Hansson and Sørensen [1990]
0.287			0.4		DK-OPC			cleaned, smooth			Hansson and Sørensen [1990]
0.258			0.45		DK-OPC			cleaned, smooth			Hansson and Sørensen [1990]
0.212			0.5		DK-OPC			Cleaned			Hansson and Sørensen [1990]
0.26			0.5		DK-OPC			As received			Hansson and Sørensen [1990]
0.391			0.5		DK-OPC			Rusted			Hansson and Sørensen [1990]
0.257			0.6		DK-OPC			cleaned, smooth			Hansson and Sørensen [1990]
0.212	71(% of total)		0.5		DK-SRPC(low alkali sulphate resistance portland cement)			cleaned, smooth		12.75	Hansson and Sørensen [1990]
0.237	30(% of total)		0.5		DK-RHPC(Rapid Hardening)			cleaned, smooth		12.38	Hansson and Sørensen [1990]
0.14	28(% of total)		0.5		DK-STD(standard flyash)			cleaned, smooth		12.62	Hansson and Sørensen [1990]
0.099	33(% of total)		0.5		S-SIO2(Swedish OPC+10% microsilica)			cleaned, smooth		12.56	Hansson and Sørensen [1990]
0.5			0.4 – 0.6					-	laboratory, exposed to air		Schiessel and Raupach [1990]

0.5 – 2.0			0.4 – 0.6					-	laboratory, exposed to air		Schiessel and Raupach [1990]
1.5 – 2.5		3 – 20	0.5		OPC, SRPC			cleaned, smooth	laboratory, exposed to air		Lambert et al. [1991]
0.125			-		70% OPC + 30% SF			-	laboratory, submerged		Takagi et al. [1991]
0.5 – 1.8	0.36 – 3.22 mole/l		0.4 – 0.6		OPC, SF, FA			cleaned	laboratory, exposed to air		Pettersson [1992]
0.5 – 1.0			0.5 – 0.7		100% OPC			ribbed	laboratory, exposed to air		Schiessl and Breit [1996]
1.0 – 1.5			0.5 – 0.7		OPC with GGBS or FA			ribbed	laboratory, exposed to air		Schiessl and Breit [1996]
0.7			0.32 – 0.68		OPC with Fly ash content = 0			ribbed	outdoor exposure, tidal zone (marine exposure)		Thomas et al. [1996]
0.65			0.32 – 0.68		OPC with Fly ash content = 15%				outdoor exposure, tidal zone (marine exposure)		Thomas et al. [1996]
0.5			0.32 – 0.68		OPC with Fly ash content = 30%				outdoor exposure, tidal zone (marine exposure)		Thomas et al. [1996]
0.2			0.32 – 0.68		OPC with Fly ash content = 50%				outdoor exposure, tidal zone (marine exposure)		Thomas et al. [1996]
	0.44 – 0.65 mole/l		0.75		100% OPC			not reported	laboratory, submerged		Elsener et al. [1997]
	0.056 mole/l	0.26	-		-			cleaned	laboratory, submerged		Breit [1998]

0.25 – 0.75			0.5 – 0.6		100% OPC, 100% SRPC and OPC with SF, FA or GGBS.			smooth	laboratory, submerged		Breit [1998]
0.4 – 1.5			0.3 – 0.75		100% SRPC or SRPC with FA, SF and GGBS			ribbed, as recieved	outdoor exposure (seawater)		Sandberg [1998]
1.24 – 3.08	0.39 – 1.16 % cem wt	1.17 – 3.98	0.5		100% OPC		100% RH	ribbed and smooth	laboratory		Alonso et al. [2000]
		0.7 – 1.7	-		-			sandblasted, cleaned	laboratory, oxygen supply		Zimmermann et al. [2000]
0.25 – 1.25	0.045 – 0.55 mole/l		0.6		100% OPC			sandblasted, cleaned	laboratory, exposed to air		Zimmermann et al. [2000]
0.2 – 0.4			-		100% OPC			-	outdoor exposure		Zimmermann [2000]
		0.01 – 2.5	-		-			as received, sandblasted, pre-rusted	laboratory, submerged		Li and Sagüés [2001]
0.73	0.50 % cem wt	1.76±0.3	0.5		OPC, SRPC, FA			ribbed, millscaled	laboratory submerged		Alonso et al. [2002]
0.23	0.36 mole/l	1.5	0.37		100% SRPC			ribbed	laboratory, exposed to air		Castellote et al. [2002]
0.15	0.33 mole/l	2	0.37		100% SRPC				laboratory, exposed to air		Castellote et al. [2002]
0.4			0.4 – 0.6		100% OPC (~7 and ~12% C_3A)		(23C, 50% RH)		laboratory, exposed to air		Whiting et al. [2002]
0.4			0.4 – 0.6		75% OPC + 25% FA (Class C and F)		(23C, 50% RH)		laboratory, exposed to air		Whiting et al. [2002]
0.02 – 0.24		0.05 – 0.62	0.5		100% OPC				laboratory, submerged		Trejo and Pillai [2003]

0.68 – 0.97	0.07 – 0.13 % cem wt	0.16 – 0.26	0.35 – 0.55		OPC with 15 to 30% FA or 30% GGBS				laboratory, exposed to air		Oh et al. [2003]
0.45	0.10 % cem wt	0.27	0.35 – 0.55		SRPC				laboratory, exposed to air		Oh et al. [2003]
0.52 – 0.75			0.45		100% OPC		exposed to air (22% RH and 30˚C for 60 days) then submerged		laboratory		Nygaard and Geiker [2005]
	0.4 – 0.8 % cem wt		0.5		100% OPC				laboratory, exposed to air		Mohammed and Hamada [2006]
1.1 – 2.0			0.6		100% OPC				laboratory, exposed to air		Manera et al. [2007]
0.6 – 1.2			0.6		90% OPC + 10% SF				laboratory, exposed to air		Manera et al. [2007]
1.1-2.0			0.6		OPC				laboratory, exposed to air		Manera et al. [2007]
1-1.5					High alkali OPC						Fagerlund et al. [2011]
0.7-0.9					Low alkali OPC						Fagerlund et al. [2011]
0.35			0.45	Cb=7.2C/(1+4.3C)	OPC with 2.43% of C3A						Glass et al. [1997]
0.62			0.45	Cb=7.2C/(1+3.2C)	OPC with 7.59% of C3A						Glass et al. [1997]
1			0.45	Cb=1.8C/(1+1.9C)	OPC with 14% of C3A						Glass et al. [1997]

Appendix C. Chloride Diffusion Coefficient Published in Literature

D_c (*10^{-9} cm^2/s)	w/c	Binder type	Permeability coefficient (*10^{-13} m/s)	Compressive Strength (MPA)	Air content	Density (kg/m3)	Oxygen Diffusion Coefficient (*10^{-8} cm^2/s)	Test Performed	Test Duration	Reference
10.6	0.4	OPC		42.4	7	2298		ACPT	12-14 weeks	(Sugiyama, 1996)
23.1	0.4	OPC		25.7	6.5	1837		ACPT	12-14 weeks	(Sugiyama, 1996)
11.8	0.6	OPC		27	7	2314		ACPT	12-14 weeks	(Sugiyama, 1996)
25.3	0.6	OPC		24.7	6	1934		ACPT	12-14 weeks	(Sugiyama, 1996)
11.9-19.4	0.5	OPC		59.5	1.2			AASHTO T 277-83		(Zhang, 1994)
28.6-36.5	0.5	OPC Mortar		38	3.9			AASHTO T 277-83		(Zhang, 1994)
67	0.38	OPC				2010				(Liu, 2011)
60	0.38	OPC	0.9	71		2360				(Liu, 2011)
NA	0.54	OPC	14.7	49		2290				(Liu, 2011)
53	0.38	OPC	1.1	50		1900				(Liu, 2011)
59	0.38	OPC	1.9	47		1860				(Liu, 2011)
64	0.38	OPC	1.6	42		1740				(Liu, 2011)
NA	0.38	OPC	1.2	38		1610				(Liu, 2011)

90	0.38	OPC	4	34		1620				(Liu, 2011)
31.2	0.5	OPC						Spray Zone		(Costa, 1999)
53.2	0.5	OPC						Tidal Zone		(Costa, 1999)
1.21	0.5	OPC						Atmospheric Zone		(Costa, 1999)
30.4	0.5	OPC						Dockyard		(Costa, 1999)
16	0.3	OPC with superplasticiser						Spray Zone		(Costa, 1999)
å7.7	0.3	OPC with superplasticiser						Atmospheric Zone		(Costa, 1999)
13.1	0.3	OPC with superplasticiser						Dockyard		(Costa, 1999)
13.8	0.35							Spray Zone		(Costa, 1999)
6.7	0.35							Atmospheric Zone		(Costa, 1999)
9	0.35							Dockyard		(Costa, 1999)
39.5	0.4	OPC					9.3		10 weeks	(Ngala, 1995)
78	0.5	OPC					10.4		11 weeks	(Ngala, 1995)
126	0.6	OPC					13.64		12 weeks	(Ngala, 1995)

214.6	0.7	OPC					21.75		13 weeks	(Ngala, 1995)
3.9	0.4	OPC with 30%FA					5.79		14 weeks	(Ngala, 1995)
4.3	0.5	OPC with 30%FA					6.67		15 weeks	(Ngala, 1995)
9	0.6	OPC with 30%FA					7.51		16 weeks	(Ngala, 1995)
10.3	0.7	OPC with 30%FA					8.88		17 weeks	(Ngala, 1995)
32	0.3	OPC	1	100	3.5			NT BUILD 443	35 days	(Elahi, 2010)
9	0.3	7.5%SF	1.018	117.3	3			NT BUILD 444	36 days	(Elahi, 2010)
7.5	0.3	15%SF	0.979	120.8	2.5			NT BUILD 445	37 days	(Elahi, 2010)
9.5	0.3	50% blast-furnace slag	0.969	98.6	2.75			NT BUILD 446	38 days	(Elahi, 2010)
8	0.3	70% blast-furnace slag	1.038	74.3	2.5			NT BUILD 447	39 days	(Elahi, 2010)
12.5	0.3	20% Fly ash	0.733	79.5	3			NT BUILD 448	40 days	(Elahi, 2010)
16	0.3	40% Fly ash	1.16	58	2.5			NT BUILD 449	41 days	(Elahi, 2010)

7	0.3	20% Fly ash+SF	0.92	94.3	2.5			NT BUILD 450	42 days	(Elahi, 2010)
5	0.3	40% FA+SF	1.297	76	2.5			NT BUILD 451	43 days	(Elahi, 2010)
9.13	0.32	CPA-CEMI 52 5 PMES		72				NFP18305		(Truc, 2000)
28.53	0.32	CPA-CEMI 52 5R 425		92				NFP18306		(Truc, 2000)
1.3	0.55	CPA-CEMI 52 5 PMES		33.5				NFP18307		(Truc, 2000)
23.2	0.55	CPA-CEMI 52 5R 425		34.5				NFP18308		(Truc, 2000)
44.7	0.5	OPC								(Page, 1981)
14.7	0.5	OPC with 30%FA								(Page, 1981)
4.1	0.5	OPC with 30% BFS								(Page, 1981)
100	0.5	SRPC								(Page, 1981)
87	0.4	OPC							150 tidal cycle	(Mangat, 1987)
67.7	0.4	OPC with steel fiber							150 tidal cycle	(Mangat, 1987)
20	0.67	OPC		26				Fickian Law	775 days	(Vedalakshmi ,2009)

16	0.54	OPC		36				Fickian Law	775 days	(Vedalakshmi ,2009)
19	0.42	OPC		47				Fickian Law	775 days	(Vedalakshmi ,2009)
48.4	0.67	OPC		26				Warburg diffusion coefficient	775 days	(Vedalakshmi ,2009)
36.7	0.54	OPC		36				Warburg diffusion coefficient	775 days	(Vedalakshmi ,2009)
22.3	0.42	OPC		47				Warburg diffusion coefficient	775 days	(Vedalakshmi ,2009)
35.2-46.6		OPC						Tidal/ Splash Zone	16 years	(Funahashi, 1990)
21.3-33.9	0.5	OPC						Tidal/ Splash Zone	24 years	(Liam, 1992)
35		OPC						Tidal/ Splash Zone	20 years	(Kudoh, 1991)
44.1-4.91	0.5	OPC						Tidal/ Splash Zone	30 years	(Mustafa and Yusof, 1994)
120	0.4	OPC						Aerated	1 year	(Bentz, 1996)

13	0.4	OPC with 30%FA						submerged specimen	1 year	(Bamforth and Price, 1982)
65.3	0.66	OPC						submerged specimen	1 year	(Bamforth and Price, 1982)
8.9	0.54	OPC with 30%FA						Tidal Zone	3 years	(Bamforth and Price, 1982)
7.6	0.48	OPC with 70%FFBS						Tidal Zone	3 years	(Bamforth and Price, 1982)
39.8	0.72	OPC with 8% SF						Tidal Zone	3 years	(Bamforth and Price, 1982)
21.42	0.45	OPC						Submerged specimen	15 years	(Mohammed, 2002)
4.86	0.45	GGBS						Submerged specimen	15 years	(Mohammed, 2002)
5.52	0.45	PFA						Submerged specimen	15 years	(Mohammed, 2002)
0.42	0.44-0.6	OPC						Tidal/ Splash Zone	33 years	(Troconis de Rinco'n, 2004)
6.48	0.44-0.7	OPC						Tidal/ Splash Zone	38 years	(Troconis de Rinco'n, 2004)
0.27	0.44-0.8	OPC						Tidal/ Splash Zone	60 years	(Troconis de Rinco'n, 2004)

1.36	0.44-0.9	OPC						Tidal/ Splash Zone	64 years	(Troconis de Rinco'n, 2004)
9.7	0.45	OPC						Freeze and Thaw 0 Cycles		(Gérard,2000)
24.48	0.45	OPC						Freeze and Thaw 31 Cycles		(Gérard,2000)
41.64	0.45	OPC						Freeze and Thaw 61 Cycles		(Gérard,2000)
76.52	0.45	OPC						Freeze and Thaw 95 Cycles		(Gérard,2000)

9. REFERENCES

1) AASHTO, “The AASHTO LRFD Bridge Construction Specifications,” American Association of State Highway and Transportation Officials, ISBN: 978-1-56051-452-7, 2010.
2) AASHTO, “Manual for Bridge Element Inspection,” American Association of State Highway and Transportation Officials, ISBN: 978-1-56051-591-3, 2013.
3) Aboutaha, Riyad, “Guide for Maintenance and Rehabilitation of Concrete Bridge Components with FRP Composites – Research into Practice,” Research Report, Syracuse University, Syracuse, NY, USA, 2004.
4) Alizadeh, R., “Effect of Curing Conditions on the Service Life Design of RC Structures in the Persian Gulf Region”, DOI: 10.1061/(ASCE)0899-1561,20:1(2), 2008
5) Angst, U., “Critical chloride content in reinforced concrete — A review”, Cement and Concrete Research, 39 1122–1138. 2009).
6) Ann, K.Y., “Chloride Threshold Level for Corrosion of Steel in Concrete”, Corrosion Science 49 4113–4133. 2007.
7) Ann, K.Y., “The importance of chloride content at the concrete surface in assessing the time to corrosion of steel in concrete structures”. Construction and Building Materials 23 2009.
8) Bangert, F., “Chemo-hygro-mechanical modeling and numerical simulation of concrete deterioration caused by alkali–silica reaction”, International Journal for Numerical and Analytical Methods in Geomechanics. 2004.

9) BASHAM, K., “Choices in corrosion resistant Rebar”. Publication #C99J027, The Aberdeen Group, a division of Hanley-Wood, Inc.1999.

10) Bennett, J., “Electrochemical Chloride Removal and Protection of Concrete Bridge Components: Field Trials”. SHRP-S-669, Strategic Highway Research Program, 1993.

11) Bertolini, L., “Effects of cathodic prevention on the chloride threshold for steel corrosion in concrete”, Electrochimica Acta 54 (5) 1452-1463. 2009.

12) Boulfiza, M., “Prediction of chloride ions ingress in uncracked and cracked concrete”. ACI Mater J; 100(1): 38–48, 2003.

13) Clemeña, G., “Trial Application of Electrochemical Chloride Extraction On Concrete Bridge Components in Virginia,” VTRC 00-R18, Virginia Transportation Research Council, 2000.

14) Collepardi, M., et al, “Penetration of chloride ions into cement pastes and concrete”. American Ceramic Society, Vol. 55. USA. 1972.

15) Costa, A., “Chloride penetration into concrete in marine environment - Part I1: Prediction of long term chloride penetration”. Materials and Structures/Matriaux et Constructions, Vol. 32, pp 354-359, 1999.

16) Erlin, B., Hime, W., “Some chemical and physical aspects of phenomena associated with chloride-induced corrosion”. Corrosion, Concrete and Chlorides, ACI SP-102, pp. 1-12, 1987.

17) Etcheverry, L., “Evaluation of Cathodic Protection Systems for Marine Bridge Substructures,” TX-00/2945-1, Center for Transportation Research the University of Texas at Austin. 1998.

18) Fagerlund G., “The Threshold Chloride Level for Initiation of Reinforcement Corrosion in Concrete: Some Theoretical Considerations”, Report TVBM-3159, 2011.

19) Ferreira, R.M., “Optimization of RC structure performance in marine environment”. Eng. Structure, 32(5), pp. 1489-1494. 2010

20) Ferreira, RM., “Optimization of RC structure performance in marine environment”. Eng. Structure, 32(5): 1489–94. 2010.

21) Frederiksen, J.M., “Method for Determination of Chloride Threshold Values for Steel in Concrete”, NORDTEST project number: 1441-99. 2002.

22) Frederiksen, J.M., “HETEK, A system for estimation of chloride ingress into concrete, Theoretical background”, The Danish Road Directorate, Report No. 83. 1997.

23) Gao, J.M., “Experimental study on properties of polymer-modified cement mortars with silica fume”. Cement and Concrete Research 32, 41–45. 2002.

24) Gerard, B., “Influence of cracking on the diffusion properties of cement-based materials”. Cement and Concrete Research 30, 37–43. 2000.

25) Gergely, J., “Concrete Diffusion Coefficients and Existing Chloride Exposure in North Carolina”, FHW A/NC/2006-26, 2006.

26) Hausmann, D.A., “Steel corrosion in concrete. How does it occur?” Materials Protection 6,19-23.1967.

27) Hobbs, D.W., “Alkali-Silica Reaction in Concrete”, Thomas Telford, London, 1988.

28) Hong K., Hooton R.D., “Effects of Cyclic Chloride Exposure On Penetration of Concrete Cover”, Cement and Concrete Research, V. 29, pp.1379-1386. 1999.

29) Hurley, M., “Chloride Threshold Levels in Clad 316L and Solid 316LN Stainless Steel Rebar”, Center for Electrochemical Science and Engineering Department of Materials Science and Engineering University of Virginia Charlottesville, VA. 2008.

30) Jang, S.Y., “Effect of crack width on chloride diffusion coefficients of concrete by steady-state migration tests”, Cement and Concrete Research 41,9-19. 2011.

31) Jin, L.B., “Likeness of multiple environment time reaches his to apply medium in wear of coastal concrete structure theoretically”, Zhejiang University, Zhejiang, China. 2008.

32) JSCE, “JSCE standard specification for concrete structures (construction)”, Japan Society of Civil Engineering, Tokyo; 2002.

33) Johnston, D., “Handbook for Practical Bridge Preservation Actions and Investment Strategies,” NCHRP 14-23, National Center for Pavement Preservation. 2014.

34) Kepler, J., “Evaluation of Corrosion Protection Methods for Reinforced Concrete Highway Structures”, Structural Engineering and Engineering Materials SM Report No. 58, University of Kansas Center for Research, Inc. Lawrence, Kansas. 2000.

35) Krauss, P., “Guidelines for Selection of Bridge Deck Overlays, Sealers and Treatments”, NCHRP Project 20-07, Task 234, National Cooperative Highway Research Program, Transportation Research Board. 2009.

36) Latah Bridge Rehabilitation Study, “Latah Bridge Rehabilitation Study”. City of Spokane, Washington. 2012.

37) Lee, H., “Effectiveness of Electrochemical Chloride Extraction for The Iowa Avenue Pedestrian Bridge”. Iowa Department Transportation Iowa Highway Research Board Project # TR-499. 2005.

38) Lee, H., “Effectiveness of Electrochemical Chloride Extraction for The Iowa Avenue Pedestrian Bridge,” Iowa Department Transportation Iowa Highway Research Board Project # TR-499. 2005.

39) Life-365, “Life-365 Service Life Prediction Model and Computer Program for Prediction the Service Life and Life-Cycle Cost of Reinforced Concrete Exposed to Chlorides”. Life-365 user’s manual. 2014.

40) Mohammed, T.U., “Relationship between Free Chloride and Total Chloride Contents in Concrete”, Cement and Concrete Research 33, 1487–1490. 2003.

41) Moradllo, M., “Time-dependent performance of concrete surface coatings in tidal zone of marine environment”. Construction and Building Materials 30, 198-205. 2012.

42) NCHRP Report 14-20, “Consequences of Delayed Maintenance.” Cambridge Systematics, Inc. Rep. no. Washington, DC: Transportation Research Board, 2012.

43) Nilsson, L.O., “Chloride penetration into concrete, State-of-the-Art”, HETEK Report No. 53, 1996, 1-151. 1996.

44) NRMCA, “Resistance of Pervious Concrete”. National Ready Mixed Concrete Association, 2004.

45) Oman, M., “Concrete Bridge Deck Crack Sealant Evaluation and Implementation”. Report No. MN/RC 2014-34. 2014.

46) Pettersson, K., “Corrosion threshold value and corrosion rate in reinforced concrete”. CBI report 2:92., Swedish Cement and Concrete Research Institute, 1-43. 1992.

47) Pettersson, K., “Corrosion of steel in high performance Concrete”. Proceedings of 3rd International Symposium on Utilization of High Strength Concrete, Lillehammer, Norway, 1993.

48) Pettersson, K., “Chloride induced reinforcement corrosion”, status report. Högpresterande Betongkon- struktioner, CBI, Report M1:5, 1994.

49) Pettersson, K., “Criteria for cracks in connection with corrosion in high performance concrete”. In: Proceedings of CANMET/ACI International Symposium on Utilization of High Strength/High Performance Concrete, Paris, France, 1996.

50) Poulsen, S., “Chloride Threshold Values – State of the art”, Danish Expert Centre for Infrastructure Constructions, Danish Expert Centre for Infrastructure Constructions. 2012.

51) Rahman, K., “Simulation of Chloride Migration in Compression-Induced Damage in Concrete”. DOI: 10.1061/(ASCE)MT.1943-5533.0000458. 2012.

52) Ronning, T., “Freeze-Thaw Resistance of Concrete Effect of: Curing Conditions, Moisture Exchange and Materials”, Doctoral thesis, The Norwegian Institute of Technology, 2001.

53) Saetta, A.V., “Analysis of chloride diffusion into partially saturated concrete”. ACI Mater J; 90(5): 441–51. 1993.

54) Saetta, A.V., Scotta, R., Vitaliani, R., “Analysis of chloride diffusion into partially saturated concrete”. ACI Materials Journal, 90, pp. 441–451. 1993.

55) Schiessel, P., Breit. W., “Time to depassivation depending on concrete composition and environmental conditions”, Proceedings of the RILEM Workshop on “Chloride Pnetration in Concrete”, Saint-Rémylès-Chevreuse, France, 1995.

56) Sharp, S. “Field Comparison of the Installation and Cost of Placement of Epoxy-Coated and MMFX 2 Steel Deck Reinforcement: Establishing a Baseline for Future Deck, 2009.

57) SHRP 2, “Field validation testing of NDT technologies on a concrete bridge deck 02”, University of Illinois, The National Academics, http://vimeo.com/26123878. 2011.

58) So, H.S., “The Properties of Chloride Ion Diffusion of Concrete Under High Temperature Conditions, with Implications for the Storage of Spent Nuclear Fuel in Concrete Casks”. KSCE Journal of Civil Engineering, 18(7):2227-2233. 2014.

59) Song, G., “Corrosion of steel in Concrete: Causes, Detection and Prediction”, Review Report 4, ARRB Transport Research Ltd. 1998.

60) Song, H., “Factors influencing chloride transport in concrete structures exposed to marine environments”. Cement & Concrete Composites 30,113-121. 2008.

61) Song, L., “Time Dependent Chloride Diffusion Coefficient in Concrete”, DOI 10.1007/s11595-013-0685-6, 2013

62) Song, L., “Time Dependent Chloride Diffusion Coefficient in Concrete”. Journal of Wuhan University of Technology-Mater. Sci. Ed. Vol.28 No.2. 2013.

63) Soriano, A., “Alternative Sealants for Bridge Decks,” SD2001-04-D, AEC Engineering, Inc. 2001

64) Stanish, K.D., “Testing the chloride penetration resistance of concrete: a literature review”, FHWA contract DTFH61 1997, Department of Civil Engineering, University of Toronto, Canada. 1997.

65) Sugiyama, T., “Determination of Chloride Diffusion Coefficient and Gas Permeability of Concrete and Their Relationship”. Cement and Concrete Research, Vol. 26, No. 5, pp. 781-790, 1996.

66) Suprenant, B., “Testing for chloride permeability of concrete- the rapid chloride permeability test (RCPT) is an alternative to ponding tests”, Concrete Construction, July 1991, pp. 8-12. 1991.

67) Thomas, MDA, “Modelling chloride diffusion in concrete Effect of fly ash and slag”, Cement and Concrete Research 29 (1999) 487–495. 1999.

68) Ward-Waller, E., “Corrosion Resistance of Concrete Reinforcement”, Master thesis, Sc.B. Civil Engineering, Brown University. 2004.

69) Won, J., “Evaluation of Diffusion Property of Latex Modified Concrete”. DOI: 10.5389/KSAE.2008.50.4.027. 2008.

70) Xu, J., “Effectiveness of inhibitors in increasing chloride threshold value for steel corrosion”, Water Science and Engineering, 2013, 6(3): 354-363. 2013.

71) Yang, Z., “Effect of styrene – butadiene rubber latex on the chloride permeability and microstructure of Portland cement mortar”. Construction and Building Materials 23, 2283-2290. 2009.

72) Zhang, S., “Experimental determination of chloride penetration in cracked concrete beams”. Procedia Engineering 24, 380-384. 2011.

73) Zhao, J., Cai, G., Gao, D., Zhao, S., “Influences of freeze–thaw cycle and curing time on chloride ion penetration resistance of Sulphoaluminate cement concrete”. Construction and Building Materials 53, pp. 305–311. 2014.

74) Zhao, X., “Durability Study of concrete Structures Based on Chloride Ingress”, College of Civil Engineering of Chongqing University, Chongqing, China. 2011.

75) Zhao, Y., “I-345 Bridge Repair”. 2010 Structures Congress. 2010.

10. VITA

NAME OF AUTHOR	Haotian Zhang
PLACE OF BIRTH	Xi’an, China
DATE OF BIRTH	February 16, 1988

EDUCATION

September 2016	Ph.D. in Civil Engineering, College of Engineering and Computer Science, Syracuse University, Syracuse, NY, USA
JULY 2013	M.S. in Civil Engineering, College of Engineering and Computer Science, Syracuse University, Syracuse, NY, USA
July 2010	B.S. in Engineering Mechanics, School of Mechanical Engineering, Tianjin University, Tianjin, China

EXPERIENCE

Aug. 2013-May 2016	Graduate Research Assistant, Department of Civil and Environmental Engineering, Syracuse University, Syracuse, NY, USA